Section-III

IA-LIPOSOMAL DRUG DELIVERY

1. Introduction

1.1 Liposomes

A liposome is defined as a structure consisting of one or more concentric spheres of lipid bilayers separated by water or aqueous buffer compartment as shown in **Fig. 1.1.**[1-2] A liposome is an artificially prepared vesicle composed of a lipid bilayer, formed spontaneously when the lipids are dispersed in aqueous media giving rise to population of vesicles, which may range in size from tens of nanometers to tens of microns in diameter.[3]

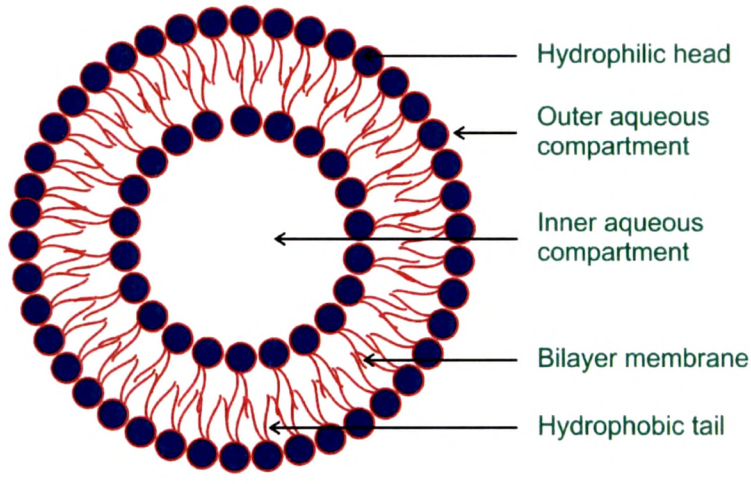

Fig. 1.1: General structure of liposome

Liposomes were brought in attention to the scientific world by A.D. Bangham in 1960's.[4] From 1969 to 1979, various method for preparation of liposome were developed to study biological process of membranes and membrane bound proteins. By 1979, liposomes were proposed as drug carriers to modify the therapeutic index of a drug by reducing toxicity or increasing efficacy of the parent drug. The potential use of liposome as a biodegradable or biocompatible drug carrier to enhance the potency and reduce the toxicity of the therapeutic agent was recognized only in late 80's and early 90's. Only then series of liposome-based therapeutics were approved for human use by U.S. Food and Drug Administration (FDA).

The modern era of liposomes is characterized by scale-up of liposomal production and a better selection of lipid raw materials for liposome preparation. Many sophisticated lipids, allowing control over the physicochemical and biological fate of liposomes became available. This includes lipids that change the integrity of liposomes in response to change

in temperature and *p*H, polymerizable lipids and lipids that reduce or prevent the uptake of liposomes by mononuclear phagocytes system (MPS) etc.

1.2 Classification of liposomes

Liposomes are mainly classified on the basis of their structural properties, method of preparation or their composition and applications as shown in **Table 1.1-1.3**[5-6]

Table 1.1: Liposome classification based on structure (size and lamellarity).

No	Type of liposome	Abbreviation	Size range (Diameter)	No of lipid bilayers
1	Unilamellar vesicle	UV	All size range	one
2	Small unilamellar vesicle	SUV	20-100 nm	one
3	Medium unilamellar vesicle	MUV	>100 nm	one
4	Large unilamellar vesicle	LUV	>100 nm	one
5	Giant unilamellar vesicle	GUV	>1 μm	one
6	Oligo lamellar vesicle	OLV	0.1-1 μm	Approx. 5
7	Multi lamellar vesicle	MLV	>0.5 μm	5-25
8	Multi vesicular vesicle	MV	>1 μm	multicompartmental

Table 1.2: Liposome classification based on method of preparation

No	Abbreviation	Type
1	REV	Single or OLV made by the reverse phase evaporation method.
2	MLV-REV	MLV made by the reverse phase evaporation method
3	SPLV	Stable plurilamellar vesicles
4	FATMLV	Frozen and thawed MLV
5	VET	Vesicles prepared by extrusion methods
6	FUV	Vesicles prepared by fusion
7	DRV	Dehydration rehydration vesicles

Table 1.3: Liposome classification based on Composition and Application

No	Type of liposome	Composition	Abbreviation
1	Conventional liposome	Phospholipid and cholesterol	CL
2	Fusogenic liposome	Reconstituted sendai virus envelops	RSVE
3	*p*H Sensitive liposomes	Phospholipid such as PER or DOPE	-
4	Cationic liposome	Cationic lipid with DOPE	-
5	Long circulating liposome	Cholesterol, 5-10% PEG, DSP	LCL
6	Immunoliposome	CL or LCL with attached monoclonal antibody	IL

1.3. Components of liposomes

Liposome are generally composed of the following classes of materials[5,7]

1.3.1. Phospholipids

1.3.2. Sphingolipids and steroids

1.3.3. Other substances

1.3.1 Phospholipids

Phospholipids are one of the major components of liposomes. Four groups of phospholipids that can be used for liposome preparation have been described. These include phospholipids from natural sources [e.g. egg phoshatidylcholine (PC), egg phosphatidylethanolamine], modified natural semi synthetic phospholipids (e.g. phospholipids obtained from the natural sources whose acyl chains are removed and chemically replaced by defined acyl chains), fully synthetic phospholipids (e.g. phospholipids made by complete synthetic pathway) and phospholipids with non-natural head groups (e.g. polyethylene glycol-phosphatidyl ethanolamine).

1.3.2 Sphingolipids and steroids

Important member of sphingolipids group include sphingomyelin and gangliosides and sterols such as cholesterol and derivatives included as components of liposomal membranes.[1] Cholesterol is a major component of natural membrane and its incorporation into lipid bilayer causes major changes in the property of vesicles. Cholesterol itself does not form bilayer structure but can be incorporated into phospholipid membrane in high concentrations. These lipids tend to increase vesicle stability on shelf and increase the fluidity or micro viscosity of the bilayer, decrease the permeability of the membrane to water soluble molecules and stabilize the membrane in the presence of biological fluids[8-10]

1.3.3 Other substances

A variety of other lipids and surfactants can be used to form liposomes such as single chain surfactants in combination with cholesterol, non-ionic lipids such as a variety of polyglycerol and polyethoxylated mono and dialkyl amphiphiles for topical pharmaceutical preparations. Some recently prepared single and double chain lipids having fluorocarbon chains which can form very stable liposomes, stearylamine and dicetyl phosphate which impart either a positive or a negative surface charge to liposomes and number of other compounds having a single long-chain hydrocarbon and an ionic head such as quaternary ammonium salt and dialkyl phosphate have been found to be capable of forming vesicles.[1-2] Antioxidants such as α-tocopherol or BHT are often included as components of liposomal membranes to minimize lipid degradation by oxidation. [3] A chelating agent (EDTA) is also included to sequester heavy metals which act as catalysts for the oxidation-reduction processes.[3]

1.4 Preparation of liposomes[11]

Formation of liposomes is not a spontaneous process. Lipid vesicles are formed when phospholipids are placed in water and consequently form one bilayer or a series of bilayers, each separated by water molecules, once enough energy is supplied. Liposomes can be created by sonicating phospholipids in water. In different preparation procedures, a general pattern is involved as follows:

- Dissolution of lipid and formation of film
- Hydration of the lipid or film
- Sizing of the liposomes
- Removal of the non-encapsulated drug

Commonly used methods for preparation of liposomes are as given below:

1.4.1 Thin film hydration

1.4.2 Reverse phase evaporation

1.4.3 *p*H induced vesiculation

1.4.4 Injection of water miscible solvents

1.4.5 Injection of water immiscible solvents

1.4.6. Detergent dialysis method

1.4.1 Thin film hydration

In the laboratory, a mixture of lipids in volatile organic solvent is deposited on the surface of a round bottom flask as the solvent is removed by rotary evaporation under reduced pressure. MLVs ranging in tens of micrometers to several tenths of a micrometer form spontaneously when an excess volume of aqueous buffer is added to the dry lipid and the flask are agitated.

1.4.2 Reverse phase evaporation

LUVs can be prepared by forming water in oil emulsion of phospholipids and a buffer in excess organic phase followed by removal of the organic phase under reduced pressure. Removal of the organic phase under the vaccum causes the phospholipid coated droplets of water to coalesce and eventually form a viscous gel.

1.4.3 *p*H induced vesiculation

SUVs can be prepared from mixed depression of PC and phosphatidic acid (PA) provided that the molar proportion of PC is 70 % or less. These liposomes are formed when the phospholipid mixtures are dispersed directly in sodium hydroxide at *p*H 10 or in water the *p*H of which is rapidly increased. However, the technique is limited to charged phospholipids and their mixtures with neutral phospholipids.

1.4.4 Injection of water miscible solvents

Water miscible solvents like ethanol, glycerin and polyglycols have been employed in preparation of liposomes. The solvent containing the lipid is diluted by an excess amount of the aqueous phase rather than being vaporized. As the solvent concentration is reduced by diafiltration or ultrafiltration liposomes are formed.

1.4.5 Injection of water immiscible solvents

The lipid mixture is injected into an aqueous solution of the material to be encapsulated at reduced pressure. Vaporization of the solvents leads to formation of single layer vesicles

1.4.6 Detergent dialysis method

Removal of detergent molecules from aqueous dispersion of phospholipid-detergent mixture is another approach to produce liposomes. As the detergent is removed, the micelles become progressively richer in the phospholipid contents and coalesce to form closed single bilayer vesicles.

1.5 Separation of un-entrapped drug from liposomal suspension

Many lipophilic drugs exhibit a high affinity to the lipid bilayer and are associated with liposomes completely. However, for other compounds encapsulation efficiency is less than 100 % so un-entrapped material has to be removed using various techniques such as dialysis and ultrafiltration[5], ultracentrifugation[3,5], gel permeation chromatography[3,5], ion-exchange resins[13], protamine aggregation[3] etc.

1.6 Mechanism of liposome formation

The exact mechanism involved in liposome formation is still not fully understood. It has been suggested that the large free energy change between water and hydrophobic environment is responsible for the preference of a typical lipid to assemble in bilayer structure excluding water as much as possible from the hydrophobic core in order to achieve the lowest free energy level and hence the highest stability for the aggregate structure (thermodynamic basis of bilayer assembly or the hydrophobic effect).

1.7 Basic properties of liposomes

Variations in liposome size, charge, surface hydration, membrane fluidity and clearance of lipid-associated drug are responsible for liposomal stability and for various cellular interactions.

1.7.1 Surface charge

Based on the head group composition of the lipid and *p*H, liposomes bear a negative, neutral or positive charge on the surface. The nature and density of charge on the surface of the liposomes influence stability, kinetics and extent of biodistribution, as well as interaction with and uptake of liposomes by target cells. Liposomes with a neutral surface charge have a lower tendency to be cleared by cells of the reticuloendothelial system (RES) after systemic administration and the highest tendency to aggregate. Although negatively charged liposomes reduce aggregation and have increased stability in suspension, their non-specific cellular uptake is increased *in vivo*. Negatively charged liposomes containing phosphatidylserine (PS) or phosphatidylglycerol (PG) were observed to be endocytosed at a faster rate and to a greater extent than neutral liposomes.[14-15]

Negative surface charge is recognized by receptors located on a variety of cells, including macrophages.[16] Inclusion of some glycolipids, such as the ganglioside GM1 or phosphatidyl inositol (PI), inhibit uptake of such liposomes by macrophages and RES cells and result in longer circulation times. It has been suggested that a small amount of

negatively charged lipid stabilizes neutral liposomes against an aggregation-dependent uptake mechanisms. [17] High doses of positively charged liposomes have been shown to produce varying degrees of tissue inflammation.[18]

1.7.2 Surface hydration or steric effect

The surface of the liposome membrane can be modified to reduce aggregation and avoid recognition by RES using hydrophilic polymers. This strategy is often referred to as surface hydration or steric modification. Surface modification is often done by incorporating gangliosides, such as GM1 or lipids that are chemically conjugated to hygroscopic or hydrophilic polymers, usually polyethylene glycol (PEG); this technology is similar to protein PEGylation.

1.7.3 Fluidity of lipid bilayer

Lipid bilayers and liposome membranes exhibit a well ordered or gel phase below the lipid phase transition temperature (Tc) and a disordered or fluid phase above the Tc. The lipid phase transition is measured and expressed as Tc, the temperature at which equal proportion of the two phases coexist. At temperature corresponding to Tc, a maximum leakiness is observed in liposomes.[20]

1.7.4 Liposome size

Early research has demonstrated that liposome size affects vesicle distribution and clearance after systemic administration. The rate of liposome uptake by RES increases with the size of the vesicles.[10] Whereas *in vivo* RES uptake can be saturated at high doses of liposomes or by pre-dosing with large quantities of control liposomes, this strategy may not be practical for human use because of the adverse effects related to the impairment of physiological functions of RES. The general observation for liposomes of similar composition is that increasing size results in rapid uptake by RES.[20] Most recent investigations have used unilamellar vesicles, 50-100 nm in size, for systemic drug delivery applications.

1.8. Characterization of liposomes

Once liposomes are prepared by suitable method it is important to determine physical and chemical characteristics of the prepared liposomes which influence their behavior *in vivo* and *in vitro*. Several examples demonstrating the importance of proper selection of liposomal structure to obtain optimum and reproducible therapeutic effects have been published.[20-22] The types of the characterization of liposomes can be divided into three broad categories as summarized below:[23]

- Physical characterization
- Chemical characterization
- Biological characterization

Physical, chemical and biological characterization of liposomes includes evaluation of the parameters as given in **Tables 1.4-1.6**

Table 1.4: Physical characterization methods of liposomes

No	Parameter	Instrumental method for analysis
1	Vesicle shape and surface morphology	TEM, SEM
2	Vesicle size and size distribution	TEM, Dynamic light scattering
3	Surface charge	Free flow electrophoresis
4	Electrical surface potential	Zeta potential measurement
5	Lamellarity	P^{31}-NMR
6	Phase behavior	DSC, Freeze fracture electron microscopy
7	Drug entrapment	HPLC
8	Drug release	Diffusion cell/dialysis

Table 1.5: Chemical characterization of liposomes

No	Parameter	Instrumental method for analysis
1	Phospholipid concentration	HPLC/Barrlet assay
2	Cholesterol concentration	HPLC/cholesterol oxide assay
3	Drug concentration	Assay
4	Anti-oxidant degradation	HPLC/TLC
5	*p*H	*p*H meter
6	Osmolarity	Osmometer

Table 1.6: Biological characterization of liposomes

No	Parameter	Method for analysis
1	Sterility	Aerobic/anaerobic culture
2	Pyrogenicity	Rabbit fever response
3	Animal toxicity	Monitoring of survival of rats

1.9 Stability of liposomes

The stability of liposomes should meet the same standard as conventional pharmaceutical formulations and can be discussed under the following headings:

1.9.1 Physical Stability

Changes in the size of the liposomes can take place over a period of time. These changes can be a result of aggregation and sedimentation or fusion (irreversible formation of new colloidal structures). The methods used to characterize the size of liposomes can be used to follow these changes in size. However, to differentiate between aggregation and fusion, fluorescent markers such as terbium citrate, sodium dipicolinate, calcein cobalt complex in association with EDTA etc. are used. Liposome membrane fusion may also be detected through fluorescence resonance energy transfer between two lipids originally present in different sets of liposomes.[24]

1.9.2 Chemical stability

As phospholipids usually form the backbone of the bilayer, their chemical stability is important. Two types of chemical degradation reactions can affect the performance of phospholipid bilayers which include hydrolysis of the ester bonds and peroxidation of the unsaturated acyl chains (if present). Oxidation of cholesterol can be monitored through gas liquid chromatography using a silica capillary column to separate cholesterol from its oxidation products.[3]

1.10 Approaches to improve liposomal stability[6]

To be commercially feasible, liposomes should have a satisfactory shelf life. Various approaches to improve the physical and chemical stability of liposomes are discussed below.

A) Selection of bilayer components

Stability of liposome can be improved by minimum use of unsaturated phospholipids. If unsaturated lipids are used, addition of antioxidants such as α-tocopherol (<15 mg/day, adult) or butylated hydroxyltoluene (0.02 %) and use of argon or nitrogen to minimize exposure of oxygen are recommended. Oxidation of unsaturated phospholipids, catalyzed by heavy metals may be inhibited by addition of metal chelators such as EDTA (<2 %) and use of light resistance containers. Processing and storage of liposomes at low temperature can add stability to the liposomes. With aqueous liposome dispersion, the selection of a proper *p*H range (*p*H 6-7) will reduce hydrolysis and lipid peroxidation-mediated damage.

Addition of substantial fraction of cholesterol decreases the rate of leakage during storage by rendering the bilayer structure more rigid. Use of saturated phospholipids is a useful technique to improve the stability. To reduce the probability for liposome aggregation or fusion, a charge inducing agent is often included in the bilayer. Conversion of small vesicles to large structures as a result of fusion process can be markedly reduced by the presence of trace amount of the phospholipid 1,3-diacyl-2-phosphatidyl choline[6]

B. Freeze drying of liposomes

Freeze drying of liposomes is an excellent method to increase the shelf life of liposomes. Cryoprotectants such as sucrose, maltose, trehalose, lactose, proteins, amino acids, and polyalcohols have been used as additives.[6]

C. Proliposome approach

Lipids dissolved in organic solvents and deposited on finely powdered sodium chloride or sorbitol, upon hydration form liposome dispersion. This approach can only be used for those compounds that are fully liposome associated upon hydration and when a wide particle size distribution is acceptable in the clinical situation.

1.11 Applications of liposomes[6]

The literature concerning the applications of liposomes is so vast that a detailed review in this thesis is not possible. An idea of the varied applications of liposomes can be obtained from **Table 1.7.** which shows the developed liposomal products or products under development.

Table 1.7: Liposomal formulations commercially available or under development

No	Drug/Application	Liposome Utility	Trade Name/Company	Disease States Treated
1	Amphotericin-B	Solublization	Ambisone/Gilead Sciences	Fungal infections
2	Doxorubicin	Site avoidance	Myocet/Zeneus	Metastatic breast Cancer
3	Morphine	Prolonged action	DepoDur/Skyepharma	Postsurgical analgesia
4	Estradiol	--	Estrasorb/Novavx	Menopausal therapy
5	Corticosteroids, Drug depot	Sustained Release	--	Cancer, Biotherapeutics
6	Cytosine arabinoside, IL	Drug Protection	--	Cancer etc.
7	Immunomodulators, Vaccines	RES Targeting	--	Cancer, Tropical Parasites

References

1. Lasic D., Weiner N., Riaz M. and Martin F., Liposomes in pharmaceutical dosage forms: Disperse systems. Lieberman H.A., Rieger M.M., and Banker G.S. Eds. Vol 3, Marcel Dekker Inc. New York. **1998**, 43-86
2. Lasic D.D., The mechanism of vesicle formation. *Biochim. J.* **1998**, 256, 1-11
3. New RRC., "Introduction, Preparation and Characterization of liposomes: A practical Approach, New RCC ed. Oxford University Press, Oxford, **1990**,1-161
4. Bangham A.D., Standish M. M. and Watkins J. C., Diffusion of univalent ions across the lamellae of swollen phospholipids. *J. Mol. Biol.* **1965**, 13, 238-52
5. Crommelin D.J.A. and Schreir H., Liposomes in colloidal Drug delivery systems. Kreuter J. Ed. Marcel Dekker Inc. New York, **1994**, 73-190
6. Lasic D.D., Chapter-10, Applications of Liposomes. Handbook of Biological Physics. Elsevier Science BV Ltd. **1995**, 1, 494
7. Bangham Y. and Crommelin D.J.A., "Liposomes as pharmaceutical dosage forms to microencapsulation "in Encyclopedia of pharmaceutical Technology, Marcel Dekker Inc. New York, **1994**, 9, 1-39
8. Gabizon A.A. and Barenholz Y., liposomes as Drug Carriers. Gregoriadis G Ed. John Wiley and Sons, New York, **1988**, 365-79
9. Gabizon A.A. and Papahadjopoulous D., Liposomes formulations with prolonged circulation time in blood and enhanced uptake by tumors. *Proc. Natl. Acad. Sci.* USA, **1988**, 85, 6949-53
10. Hwang K.J., In liposomes: From biophysics to Therapeutics. Ostro MJ (Ed.) Marcel Dekker Inc. New York, **1987**, 109-156
11. Kathleen M. M., Efstathios K., Ananth V. A. and Ravi V. B., Masking and triggered unmasking of targeting ligands on nanocarriers to improve drug delivery to brain tumors. *Biomaterials,* **2009**, 30, 3986–95
12. Shinitzky M. and Barcnholz Y., Fluidity parameters of lipid regions determined by fluorescence polarization. *Biochim. Biophys. Acta.* **1978**, 515, 367-94
13. Storm G., Van-Bloois L., Brouwer M. and Crommelin D.J.A., The interaction of cytosatic drugs with adsorbents in aqueous media. The potential implications for liposome preparation. *Biochim. Biophys. Acta.,* **1985**, 818, 343-51
14. Allen T.M., Hansen C., Martin F., Redemann C. and Yau-young A., Liposome containing synthetic lipid derivatives of poly (ethylene glycol) show prolonged circulation half-life *in vivo. Biochim. Biophys.*, **1991**, 1066, 29-36

15. Lee R.J. and Low P.S., Folate mediated tumor cell targeting of liposomes entrapped doxorubicin in vitro. *Biochim. Biophys. Acta.,* **1995**, 1233, 134-44
16. Lee R.J. and Low P.S., Delivery of liposomes into cultured KB cells via folate receptor mediated endocytosis. *J. Bio. Chem.,* **1994**, 269, 3198-04
17. Israelachvili J., Marcelja S. and Horn R.G., Physical principles of membrane organization. Q. *Rev. Biophys.* **1980**, 13, 121-200
18. Scheule R.K., St. George J.A., Bagley R.G., Marshall J., Kaplan J.M., Akita G.Y., Wang K.X., Lee E.R., Harris D.J., Jiang C., Yew N.S., Smith A.E. and Cheng S.H., Basis of pulmonary toxicity associated with cationic lipid-mediated gene transfer to the mammalian lung. *Hum. Gene. Ther.* **1997**, 8, 689-707
19. Nassander U.K., Strom G., Peeters PAM. and Crommelin D.J.A. Liposomes in Bio-degradable polymers as Drug Delivery Systems, Mchasin, Langer R ed. Macel Dekker Inc. New York, **1990**, 261-3338
20. Senior J., Crawley J.C. and Gregoriadis G., Tissue distribution of liposome exhibiting long half lives in the circulation after the intravenous injection. *Biochim. Biophys. Acta.,* **1985**, 839, 1-8
21. Goren D., Gabizon A. and Barenholz Y., The influence of physical characteristics of liposomes on their pharmacological behavior. *Biochim. Biophys. Acta.*, **1990**, 1029, 285-94
22. Storm G., Van Bloois L., Steerenberg P.A., Van Etten E., Degroot G. and Crommelin D.J.A. Liposome encapsulation of doxorubicin: Pharmaceutical and Therapeutic aspects. *J. Control. Rel.*, **1989**, 9, 215-229
23. Samad A., Sulatana Y. and Aqil M., Liposomal drug delivery systems: An Update Review, *Curr. Drug. Deliv.* **2007**, 4, 297-305.
24. Jones G.R. and Cossins A.R., Physical methods of study in Liposomes: A Practical Approach. New RRC ed. Oxford University press, Oxford, **1990**, 183-220

2. Aims and Objectives

Liposomes have long been proposed as ideal carriers for the delivery of drugs and to improve their therapeutic effect.[1] Liposomal physicochemical properties can be changed as per the requirements from therapeutic point of view to get maximum benefits, such as passage through biological barriers, retention at the target site, avoiding toxicity to non-target sites and to prevent premature degradation.[2-3] These formulations can be applied locally or systemically. As the present work is concerned about arthritis so it was planned to use liposome formulations to deliver the drug locally.

From the study of intra-articularly (IA) administered cationic chemical delivery systems (CDS) in previous section and literature survey it was concluded that introduction of positive charge on drug carrier system improves the residence time of drugs within the joint cavity. The NSAID diclofenac sodium in particular has attracted more attention due to quick onset of analgesic effects and anti-inflammatory properties.[4] However diclofenac has very short plasma half life (1.2-2 h), undergoes enterohepatic circulation (35 %), lacks affinity towards joints (synovial disappearance half life 1.5h), shows non-selectivity towards cycloxygenase enzymes (COX) and can evoke adverse gastrointestinal side effects.[5]

The aim of the present work was to develop cationic liposomal formulations of NSAIDs with long half life, selectivity towards COX-II enzyme and affinity towards joint cavity producing less gastrointestinal side effects (ideally without undergoing enterohepatic circulation). The encapsulation of NSAIDs possessing all these ideal features in to liposomes with further modifications of liposomal properties such as size, lammelarity, charge etc. was expected to improve the overall therapeutic efficacy of these agents after IA injection in patients with OA.

The specific aims of the present work were as follows:

1. **Syntheses of NSAIDs:** It was planned to prepare liposomes of 6-methoxy-2- naphthyl acetic acid (6-MNA) **(1)** and biphenylacetic acid (BPA) **(2)**, as these molecules fulfill

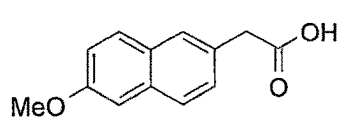

(1)

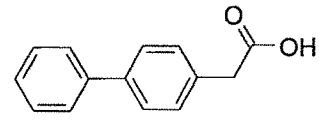

(2)

the above criteria required for ideal NSAIDs. 6-MNA and BPA are the active metabolites of nabumetone[6] and fenbufen[7] with half lives of 23-33 h and 10-12 h

respectively. So, it was planned to synthesize both these molecules in the laboratory as these are not available commercially.

2. **Preparation of cationic liposomes:** Cationic liposomes may increase the retention time of the drug delivery system within joint cavity. Further, multilammellar liposomes also provide lubricating effect which is beneficial during this diseased condition.
3. **Characterization of liposomes:** It was planned to characterize the prepared liposomes for their size, charge, lamellarity, entrapment efficiency, stability etc.
4. **Release study:** It was planned to study release of the drug from liposomes. Sustained release of active medicament is an essential criterion for the development of long acting drug delivery systems which could be injected IA.
5. ***In vivo* efficacy in animal model:** It was planned to evaluate efficacy of these drug delivery systems using Freunds adjuvant induced arthritis model.[6]

References

1. Van den Hoven J.M., Van Tomme S.R., Metselaar J.M., Nuijen B., Beijnen J.H. and Storm G., Liposomal Drug Formulations in the Treatment of Rheumatoid Arthritis *Mol. Pharm.* **2011**, 8, 1002-15.
2. De Silva M., Page Thomas D. P., Hazleman B. L. and Wraight P., Liposomes in arthritis: a new approach. *Lancet* **1979**, 313, 1320–22.
3. Fendler J.H. and Romero A. Liposomes as drug carriers. *Life Sci.* **1977**, 20, 1109.
4. Saravanan M., Bhaskar K., Maharajan G. and Pillai K.S., Development of gelatin microspheres loaded with diclofenac sodium for intra-articular administration. *J Drug Target.* **2011**, 19, 96-103.
5. Larsen C., Ostergaard J., Larsen S.W., Jensen H., Jacobsen S., Lindegaard C. and Andersen P.H., Intra-Articular Depot Formulation Principles. *J. Pharm. Sci.* **2008**, 97, 4622-54.
6. Nobilis M., Kopecký J., Kvetina J., Svoboda Z., Pour M., Kunes J., Holcapek M. and Kolárová L., Comparative biotransformation and disposition studies of nabumetone in humans using HPLC. *J. Pharm. Biomed. Anal.* **2003**, 32, 641-56.
7. Chiccarelli F.S., Eisner H.J. and Van Lear G.E., Metabolic and pharmacokinetic studies with fenbufen in man. *Arzneimittelforschung.* **1980**, 30, 728-35.

3. Results and Discussion

The work carried out towards achieving the proposed plan has been discussed under the following four main headings:

3.1. Syntheses of the selected NSAIDs

3.2. Salt formation and characterization

3.3. Formulation of liposomes

3.4. Characterization of liposomes

3.5. Stability testing of liposomes

3.6. Biodistribution and gamma imaging studies

3.7. *In vivo* studies in arthritis model

3.1 Syntheses of NSAIDs

The primary aim of this drug delivery approach was to improve the residence time of the drug within the joint cavity after IA administration. The half life of the drug contributes equally for long duration of action along with the nature and type of drug delivery system. As majority of the clinically used NSAIDs have short half lives (<2-4 h) it was planned to synthesize active metabolites of nabumetone and fenbufen i.e. 6-MNA **(1)** and BPA **(2)** respectively which have long half lives (21-27 and 10-12 h respectively) and other favorable properties such as affinity towards joint, COX-II selectivity etc.

3.1.1 Synthesis of 6-MNA (1)

Nabumetone **(3)** was synthesized in the laboratories of Beecham Pharmaceuticals in 1978 and is a non-acidic NSAID devoid of local gastric irritation side effect. But as such this is not active biologically, it undergoes rapid and extensive first-pass biotransformation in the liver to form the principal active compound 6-MNA **(1)**, which acts as an anti-inflammatory agent.[1]

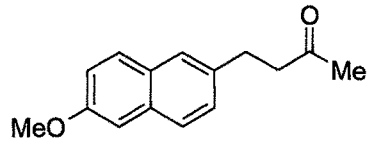

(3)

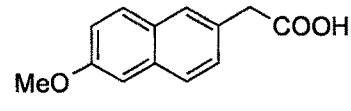

(1)

6-MNA is more than 99 % bound to plasma proteins[2], with the volume of distribution being small (7.5 L) after intravenous administration[2]. 6-MNA penetrates well into the synovial fluid, and does not undergo enterohepatic circulation.[3] The average terminal phase elimination half-life of 6-MNA is approximately 21-27 h. The mode of

action of 6-MNA consists of potent and relatively selective inhibition of cyclooxygenase-2 (COX 2). The biotransformation pathway of nabumetone **(3)** is shown in **Fig. 3.1.**

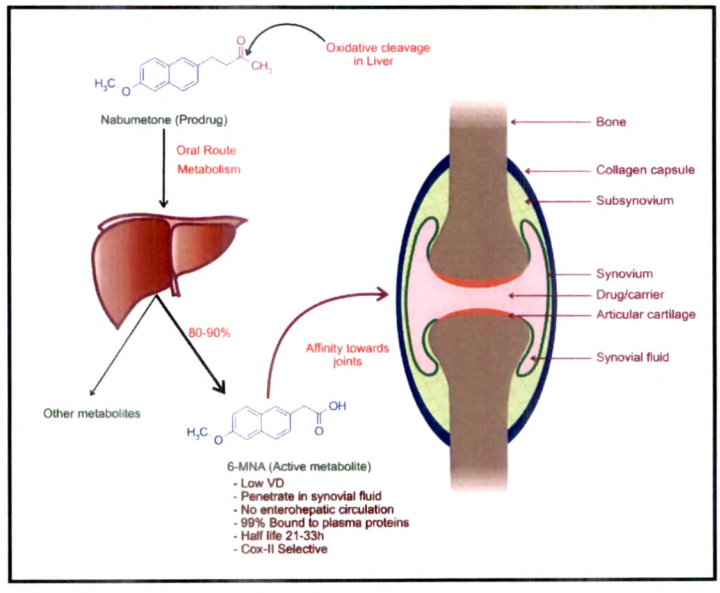

Fig. 3.1: Biotransformation pathway of nabumetone **(3)** and ideal features of the active metabolite 6-MNA **(1)**

It was planned to synthesize 6-MNA by the reported procedure as shown in **Scheme-1**. β-Naphthol **(4)** was methylated to naroline[4] **(5)** using dimethyl sulphate under basic conditions. Naroline **(5)** was acetylated with acetyl chloride under controlled conditions to offer 6-acetyl-2-methoxynaphthalene **(6)** as per the reported method.[5]

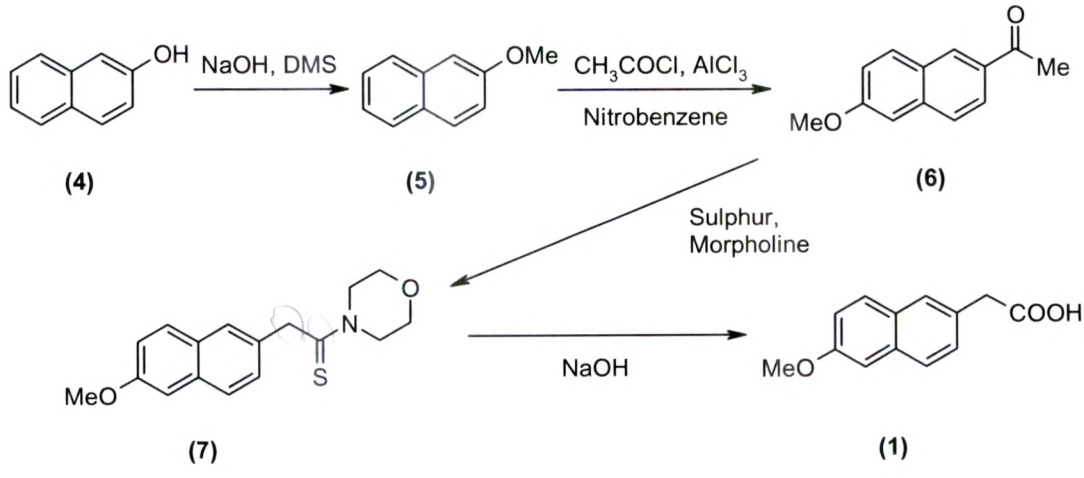

Scheme 3.1: Synthesis of 6-MNA **(1)**

The acetylated product **(6)** was subjected to Kindler-modified Wilgerodt reaction by refluxing it in morpholine containing sulphur. The thiomorpholide **(7)** so formed was isolated and hydrolysed under basic conditions. Hydrolysis of the thioamide **(7)** was performed by refluxing it in aqueous solution of sodium hydroxide to get acid **(1)** which was isolated and recrystallized to get pure acid[6] **(1)** as white powder.

6-MNA **(1)** gave a broad band at 3003 cm^{-1} (O-H*str*) and a strong characteristic peak at 1693 cm^{-1} (C=O*str*) in its IR spectrum. In the NMR spectrum (**Fig. 3.2. A**) aromatic protons appeared at δ 7.70-7.08, It yielded singlets at δ 3.87 (3H; OCH_3) and 3.68 (2H; $-CH_2$) in the PMR spectrum. Mass spectrum showed a molecular ion peak at 215.91 (M^+) which was also the base peak **(Fig. 3.2.B)**. The compound also showed high chromatographic purity by HPLC **(Fig. 3.2.C)**

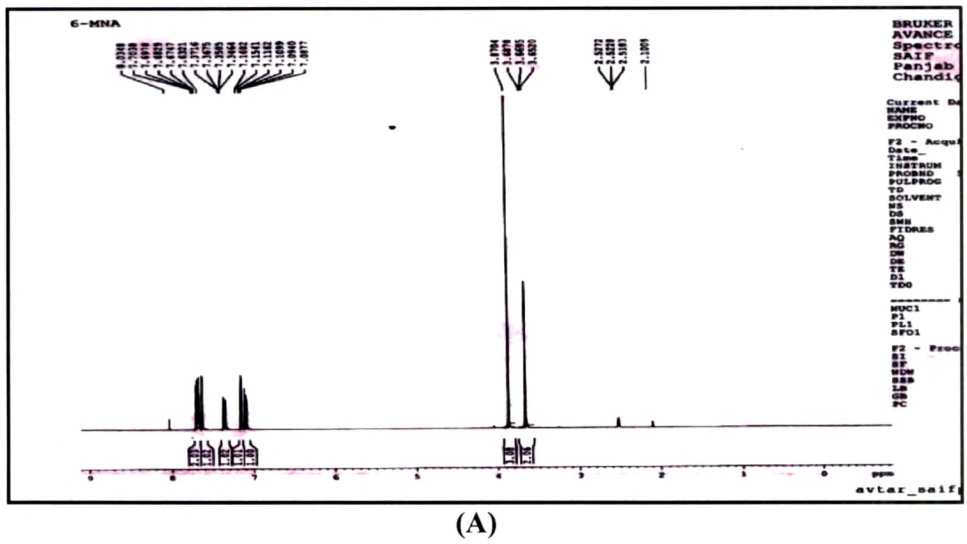

(A)

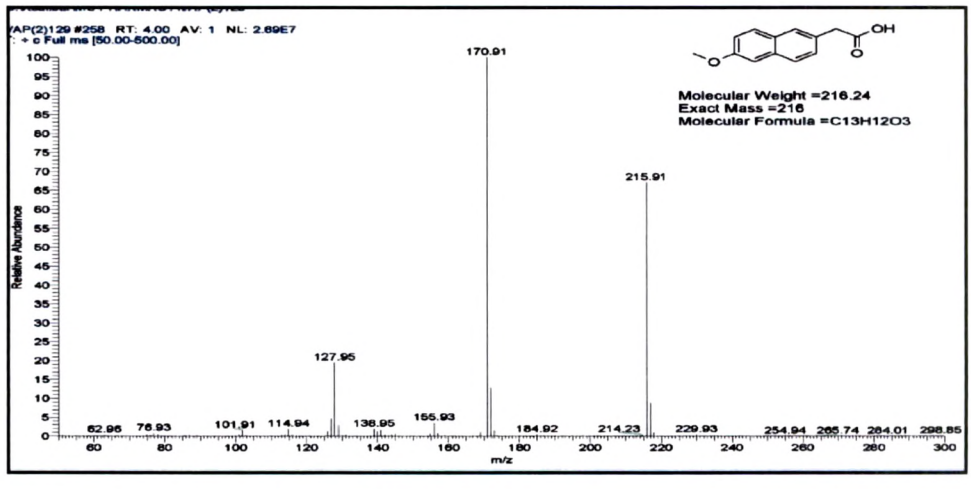

(B)

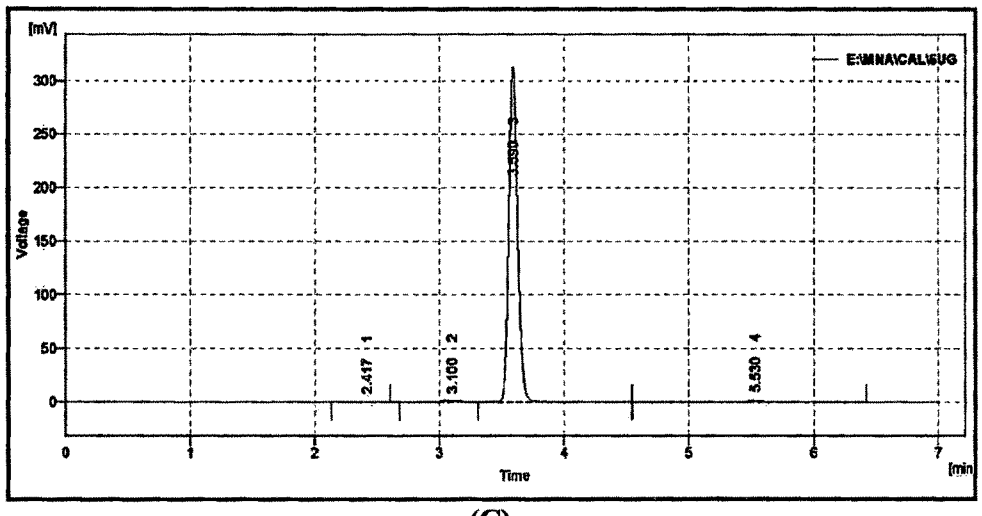

(C)

Fig. 3.2. A: PMR spectrum of 6-MNA **(1)**, **B:** Mass spectrum of 6-MNA **(1)**, **C:** Chromatogram of 6-MNA **(1)**

3.1.2 Synthesis of BPA (2)

Fenbufen **(8)** is a potent anti-inflammatory agent that is metabolized into 4'-hydroxy-4-biphenylbutanoic acid and 4-biphenylacetic acid **(2)**. 4-Biphenylacetic acid **(2)** is an active metabolite of fenbufen **(8)** with three times more activity than the parent drug and has a long half life.[7-9]

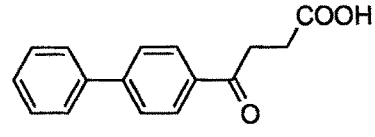

(8)

The NSAID 4-biphenylacetic acid **(2)** required for the preparation of liposomes was synthesized starting from biphenyl[9] **(9)** as shown in **Scheme-3.2.**

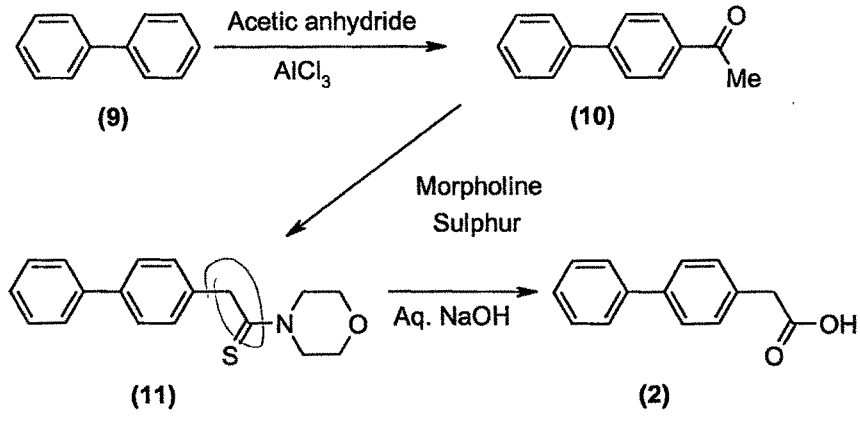

Scheme 3.2: Synthesis of BPA

Biphenyl **(9)** was reacted with acetic anhydride in the presence of anhydrous aluminium trichloride to yield 4-phenylacetophenone **(10)**. The compound **(10)** showed an intense peak at 1677cm^{-1} for the carbonyl (C=O) stretching in the IR spectrum. The ketone **(10)** was converted to 4-biphenylacetic acid **(2)** by the modified Willgerodt reaction which was carried out in two steps. The first step involved the conversion of ketone **(10)** to thiomorpholide **(11)** by reacting the ketone **(10)** with sulfur in presence of morpholine. In the second step, the thiomorpholide **(11)** was hydrolysed under basic conditions to obtain the required acid **(2)**.

Compound **(2)** showed the carbonyl stretching band at 1685 cm^{-1} and a broad peak for hydroxyl stretching at 3400 cm^{-1}in IR spectrum. The PMR spectrum **(Fig. 3.3. A)** showed broad signal at δ 8.84 due to carboxylic acid proton. A sharp singlet for the methylene protons (Ar-CH_2) appeared at δ 3.65 and signal for the aromatic protons appeared as multiplet at δ 7.88-7.28.

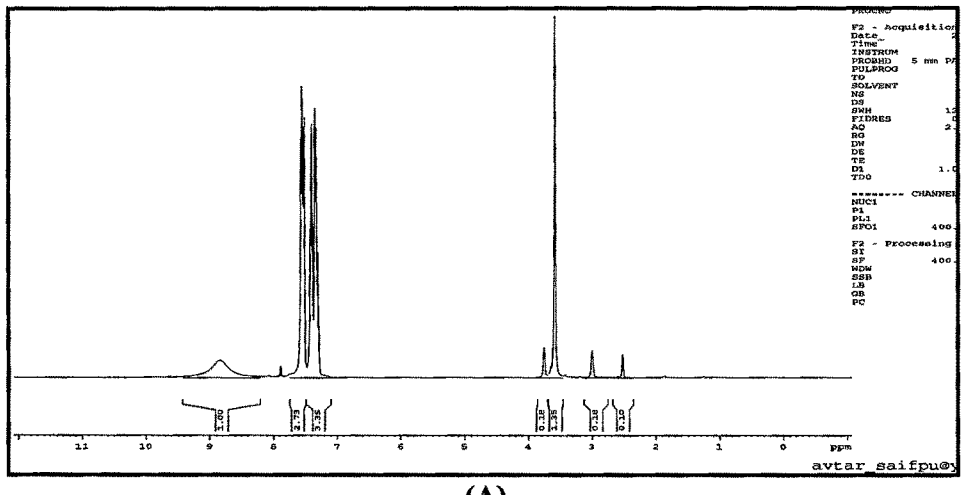

(A)

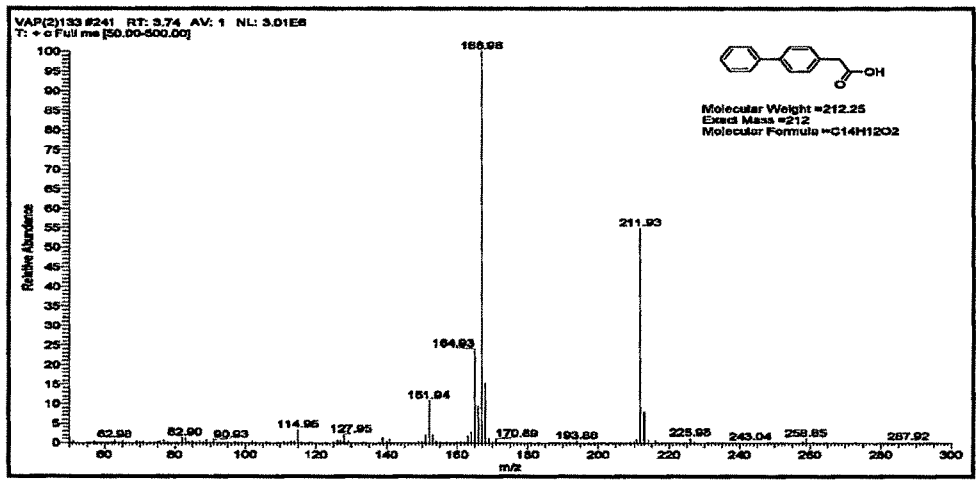

(B)

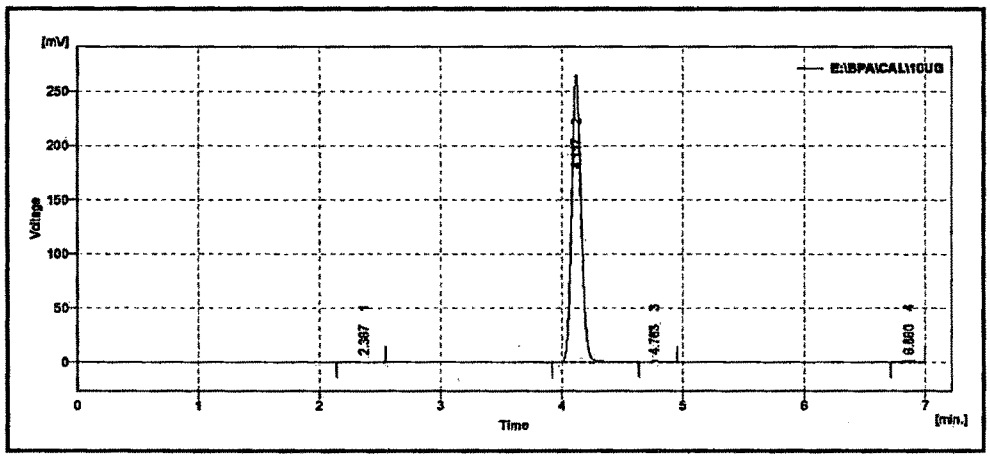

(C)

Fig. 3.3. A: PMR spectrum of BPA **(2), B:** Mass spectrum of BPA **(2)**
C: Chromatogram of BPA **(2)**

Mass spectrum showed molecular ion peak at 211.93 (M^+) which was also the base peak **(Fig. 3.3. B)**. The compound also showed high chromatographic purity by HPLC **(Fig. 3.3. C)**

3.2 Preparation of salts and their characterization

3.2.2 Syntheses and characterization of NSAID-DSPE salts

Since the present work aims to prepare liposomes of NSAIDs mainly 6-MNA and BPA, literature survey was performed with respect to liposomal formulations of various NSAIDs. From the search it was revealed that liposomal formulations of naproxen, indomethacin and ketorolac tromethamine[10-12] have been developed to avoid side effects and control the *in vitro* release of the drugs. From the literature survey is was concluded that liposomal formulations of NSAIDs showed sustained release effect in comparison to the free drug and the said effect lasted for about 6-8 h. But for the IA drug delivery the requirement is that the drug should be released over a longer duration of time, ideally over a time period of >24 h. In order to achieve sustained and slow release of the active drug from liposomal formulation the NSAID must be physically entrapped in lipid membranes and also form ionic interactions with the lipids. So, it was achieved by salt formation with basic amino group containing lipids such as 1,2-distearoyl-*sn*-glycero-3-phosphoethanolamine (DSPE, **12**). Keeping this structure in mind and taking advantage of carboxylic acid functional group present in 6-MNA and BPA it was planned to prepare

salts of these NSAIDs with DSPE and then prepare their liposomal formulations which could result in slow release of the drug.

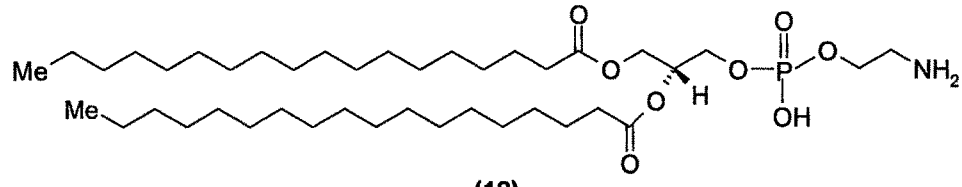

(12)

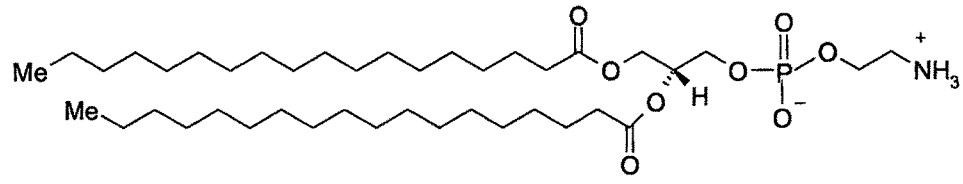

(13)

The required phospholipid was received as gift sample from lipoid GmbH (Germany) but we were not sure whether it was present as free base **(12)** or as a salt **(13)** due to intermolecular reaction. MSDS data disclosed structure **13** and showed its molecular formula as $C_{41}H_{82}NO_8P$ with molecular weight **748.07**. IR spectrum did not show broad peak for the presence of free amino group.

To solve this ambiguity it was planned to give it a base treatment to get sodium salt of DSPE **(14)** and generate free amino group which could further form salt with NSAIDs.

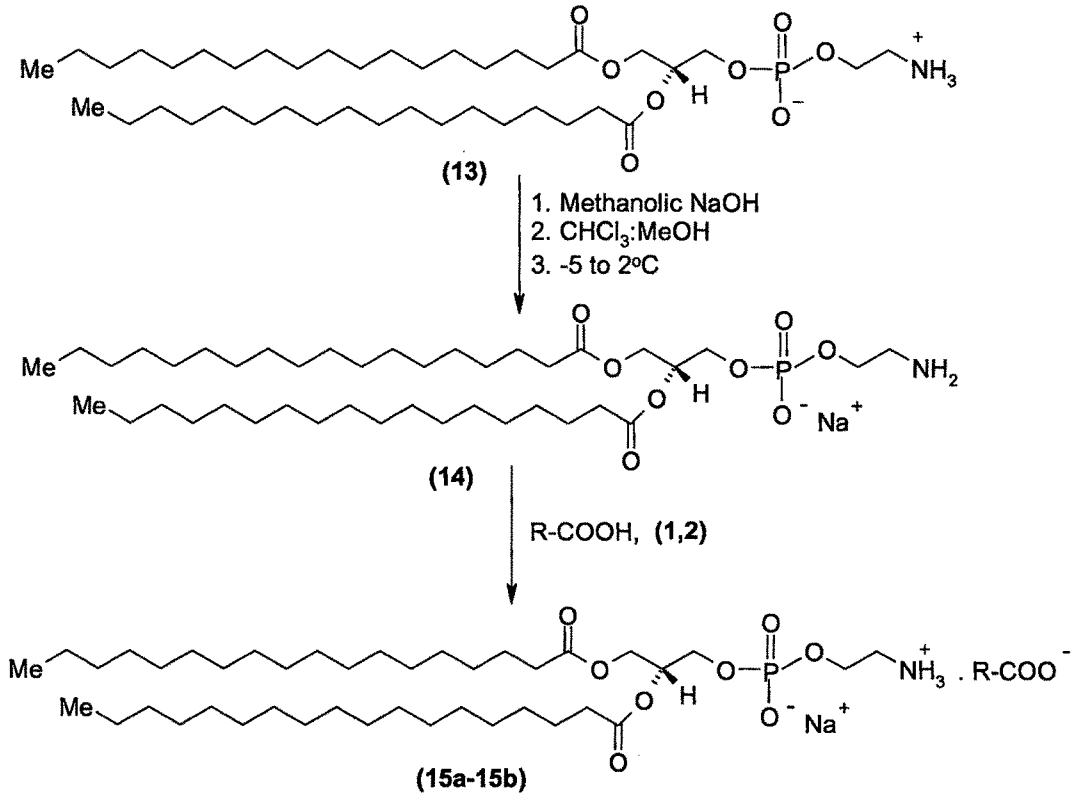

Scheme 3.3: Synthesis of salts of 6-MNA and BPA

The IR spectrum of DSPE-Na **(14)** showed carbonyl stretching due to presence of ester at 1741 cm^{-1} and N-H stretching of amine was observed at 3430 cm^{-1} **(Fig. 3.4)** which was absent in IR spectrum of DSPE **(Fig. 3.5)** From this it could be concluded that ester functional group remained intact after salt formation and free amino group got generated due to breakdown of the internal salt and formation of sodium salt. Along with IR, mass spectrum also showed peaks at m/z 747 (negative mode) and 771 (positive mode) equivalent to DSPE (MW: 748) and its sodium salt (MW: 771) respectively **(Fig. 3.8)**

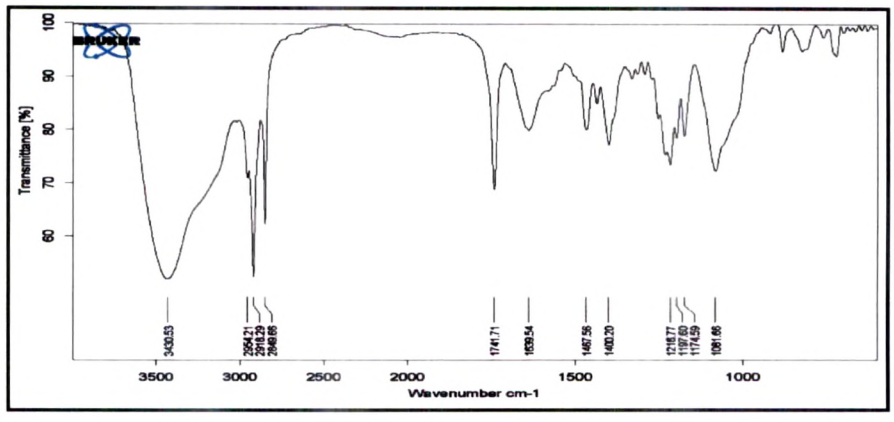

Fig. 3.4: IR Spectrum of DSPE-Na

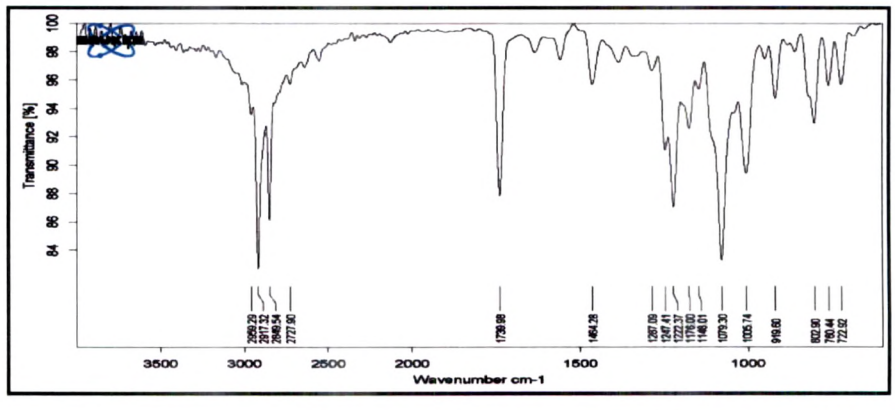

Fig. 3.5: IR Spectrum of DSPE

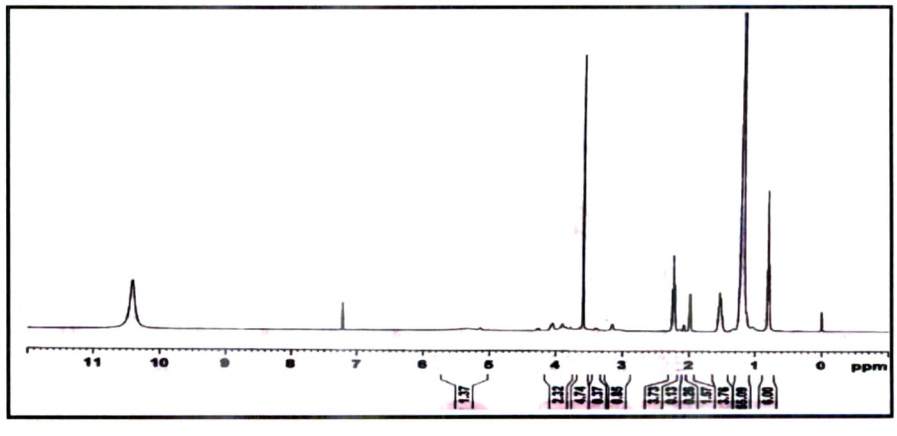

Fig. 3.6: PMR spectrum of DSPE-Na (Solvent-$CDCl_3$: acetic acid-d_4)

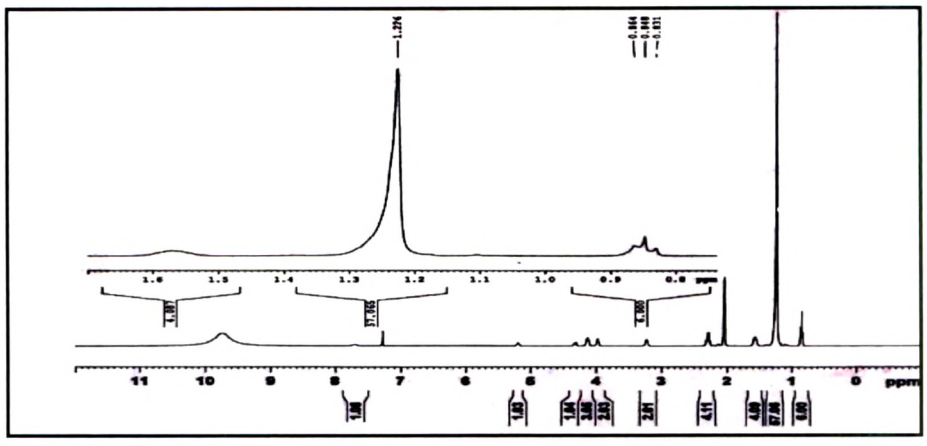

Fig. 3.7: PMR spectrum of DSPE (Solvent-$CDCl_3$: acetic acid-d_4)

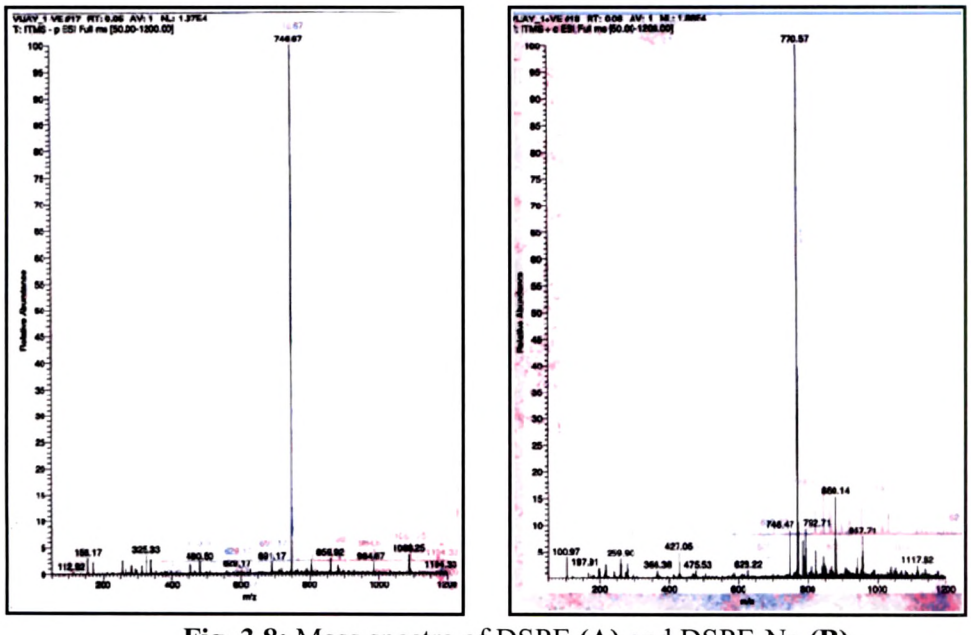

Fig. 3.8: Mass spectra of DSPE **(A)** and DSPE-Na **(B)**

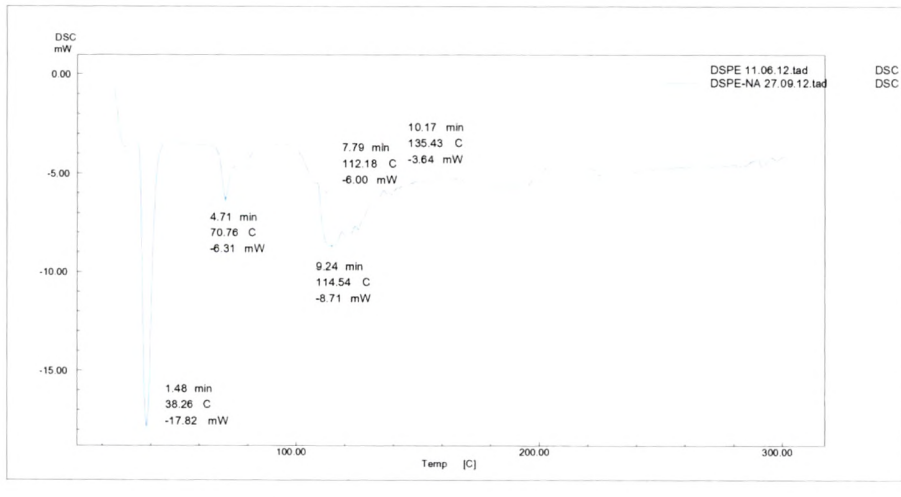

Fig. 3.9: DSC Thermogram of DSPE and DSPE-Na

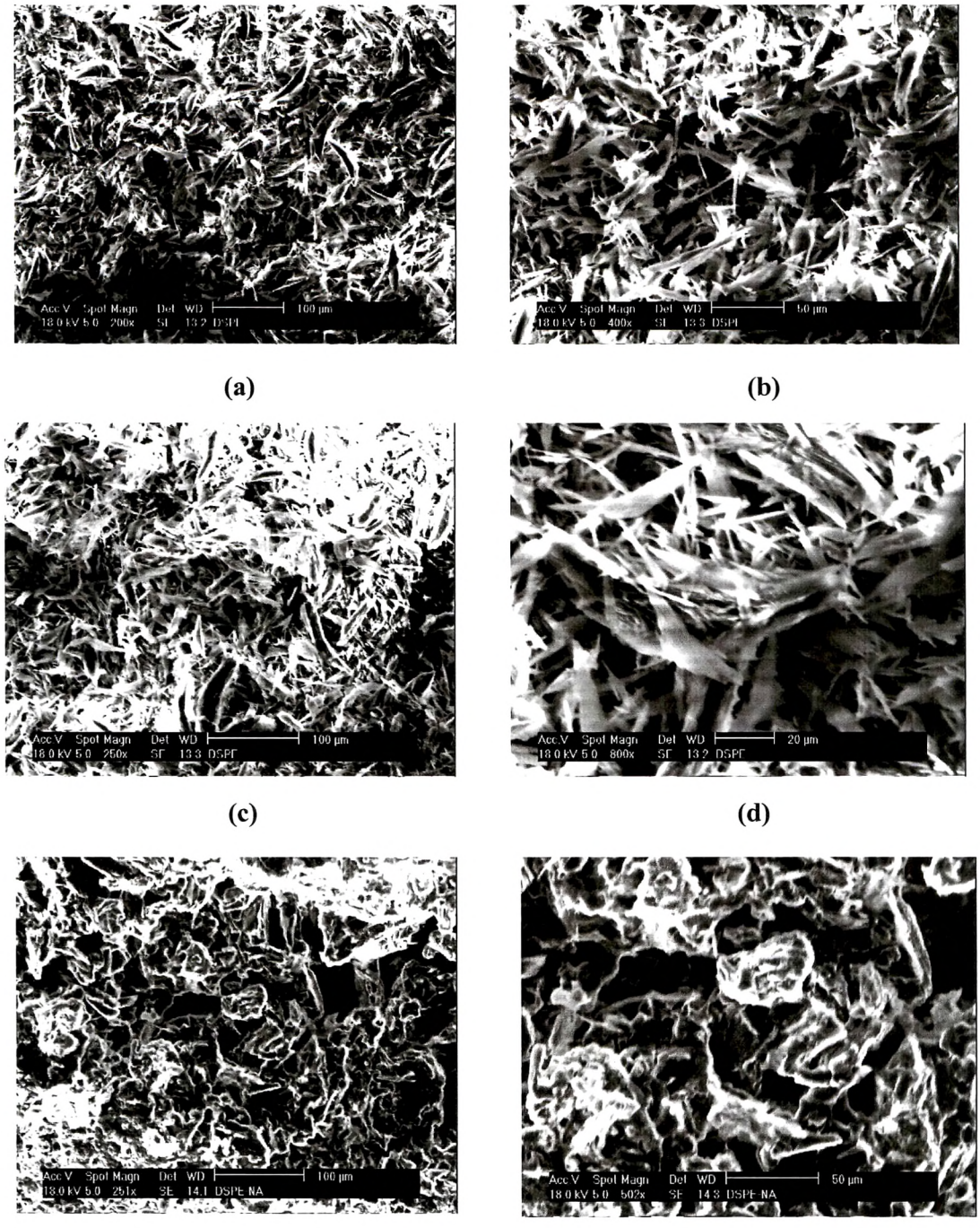

Fig. 3.10: Scanning electron microscope images of DSPE **(a-d)** and DSPE-Na **(e-f)**

Prepared DSPE-Na was characterized by using DSC. DSC showed endothermic peaks at 112.8 and 70.76°C for DSPE and DSPE-Na respectively **(Fig. 3.9)** and these values are in good agreement with their melting points. DSC thermogram of DSPE-Na shows new endothermic peak at 70.76°C which is absent in DSPE thermogram indicating

formation of sodium salt. Surface morphology was studied by SEM. SEM images also show changes in morphology when DSPE is converted to sodium salt (**Fig. 3.10**).

After successfully preparing sodium salt of DSPE containing free amine group, it was further treated with 6-MNA or BPA in chloroform and methanol mixture to get 6-MNA-DSPE or BPA-DSPE salts respectively. These salts were further characterized by various analytical techniques.

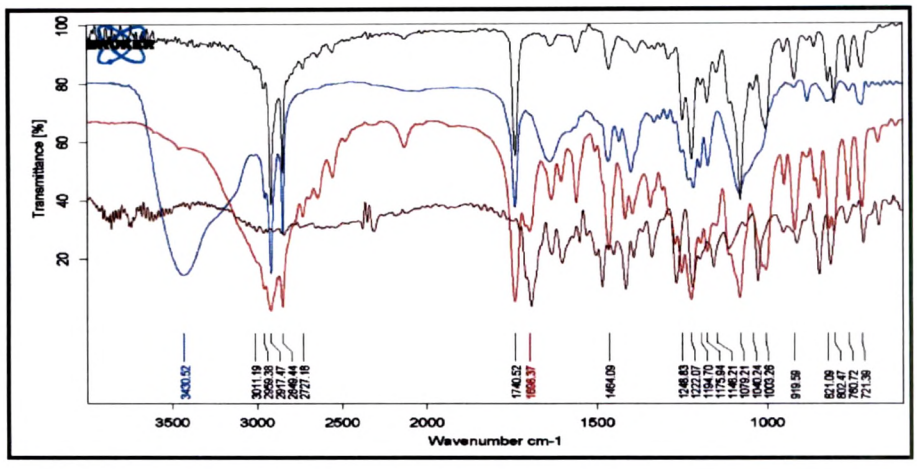

DSPE, DSPE-Na, 6-MNA-DSPE 6-MNA

Fig. 3.11: Overlaid FT-IR Spectra of 6-MNA **(1)**, DSPE and its salt

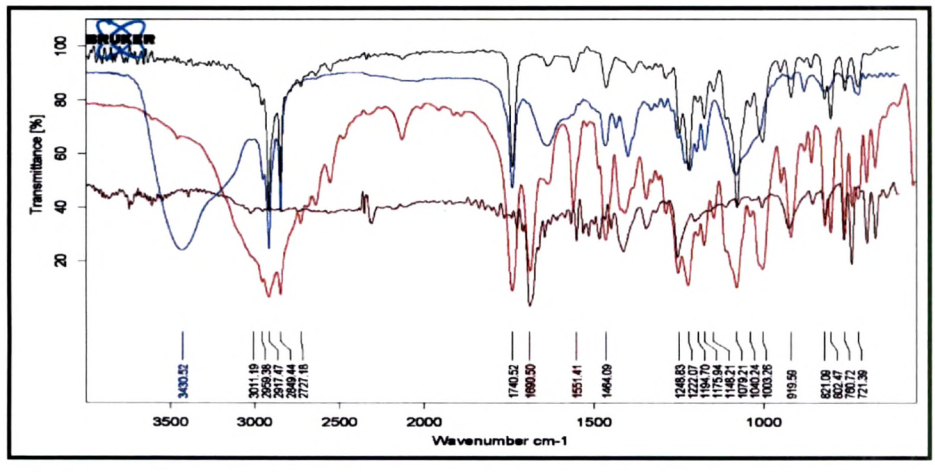

DSPE, DSPE-Na, BPA-DSPE BPA

Fig. 3.12: Overlaid FT-IR Spectra of BPA **(2)**, DSPE and its salt

IR spectra of both 6-MNA-DSPE and BPA-DSPE show disappearance of peak at 3430 cm^{-1} of free amino group indicating formation of salt. PMR and CMR spectra of both the salts show protons or carbons equivalent to both the moieties of the salt. Salt formation and subsequent presence of both the moieties were also confirmed by mass spectra. Mass

spectrum of 6-MNA-DSPE salt showed single peak at 216.05 for 6-MNA but did not show peak of DSPE-Na using electron impact (EI) as ionization source **(Fig. 3.17)**. Similar results were observed when performed on LC-MS system having electrospray ionization (ESI) as ionization source **(Fig. 3.18).**

Finally mass was performed on instrument having electrospray chemical ionization technique (ESCI=ESI+APCI). It showed peaks at 217.22 and 750.62 indicating presence of 6-MNA and DSPE-Na **(Fig. 3.19)**. Similar results were obtained with BPA and its salts. DSC thermograms also showed changes with respect to endothermic peaks when salt formation occurred **(Figs. 3.21-3.22)**.

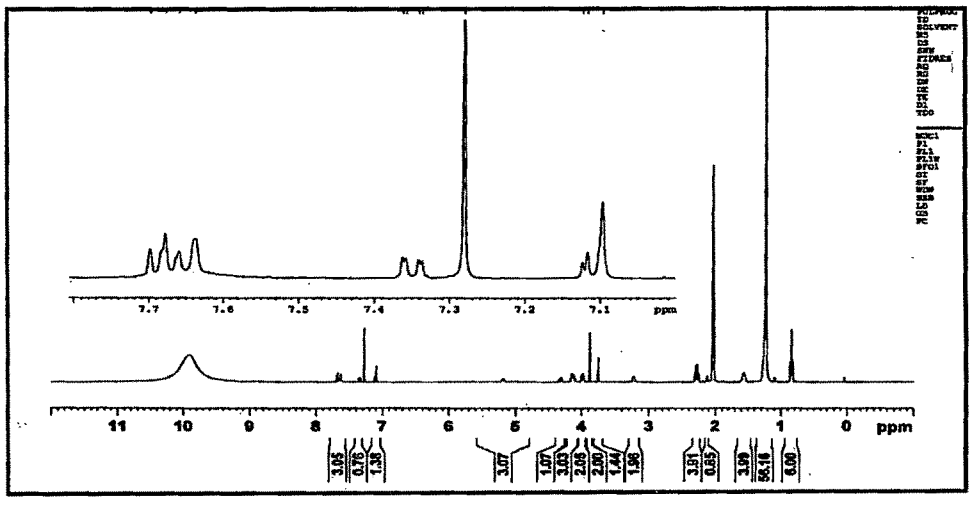

Fig. 3.13: PMR spectrum of 6-MNA-DSPE ($CDCl_3$: 1drop GAA-d_4)

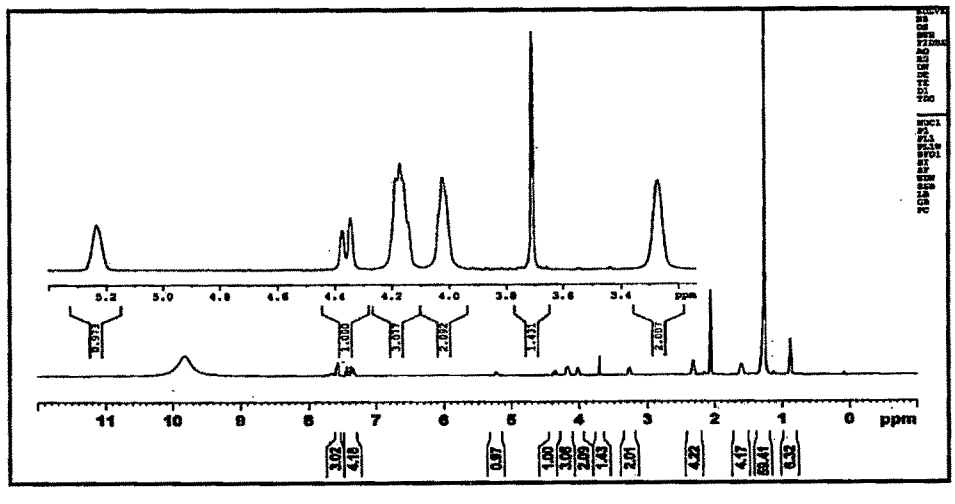

Fig. 3.14: PMR spectrum of BPA-DSPE ($CDCl_3$: 1drop GAA-d_4)

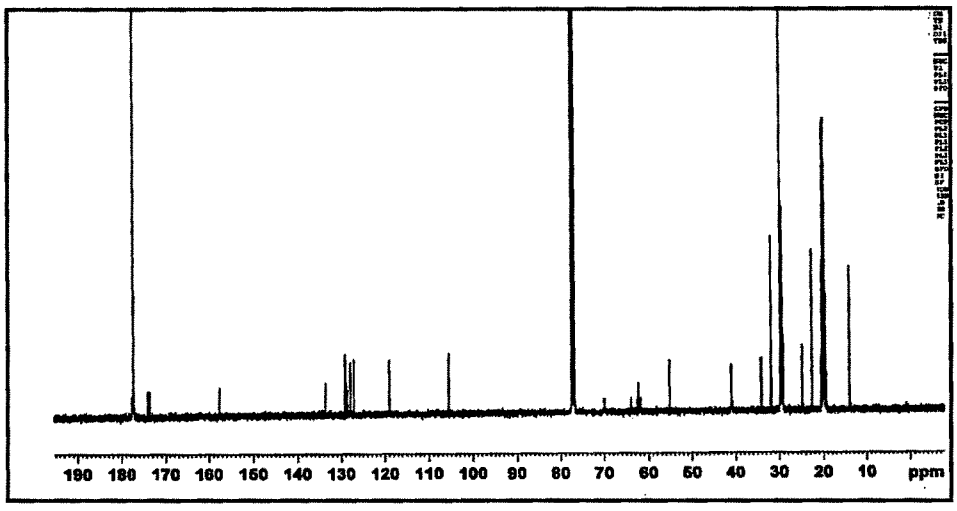

Fig. 3.15: ^{13}CMR spectrum of 6-MNA-DSPE ($CDCl_3$: 1drop GAA-d_4)

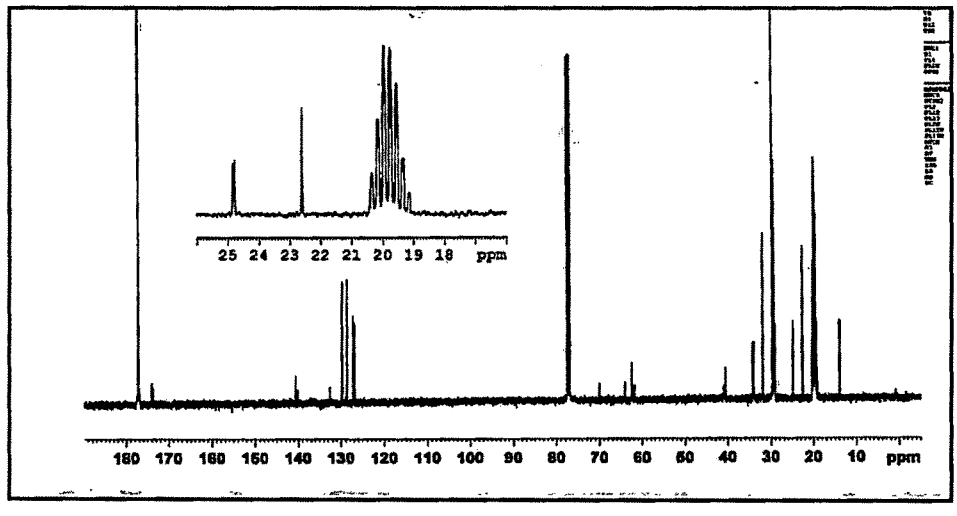

Fig. 3.16: ^{13}CMR spectrum of BPA-DSPE ($CDCl_3$: 1drop GAA-d_4)

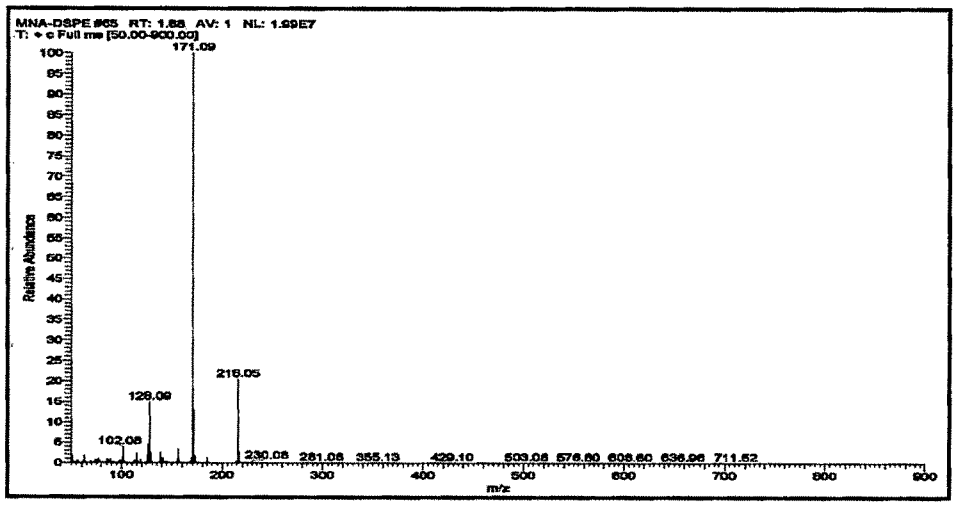

Fig. 3.17: Mass spectrum of 6-MNA-DSPE (Ionization: EI, DPI mode)

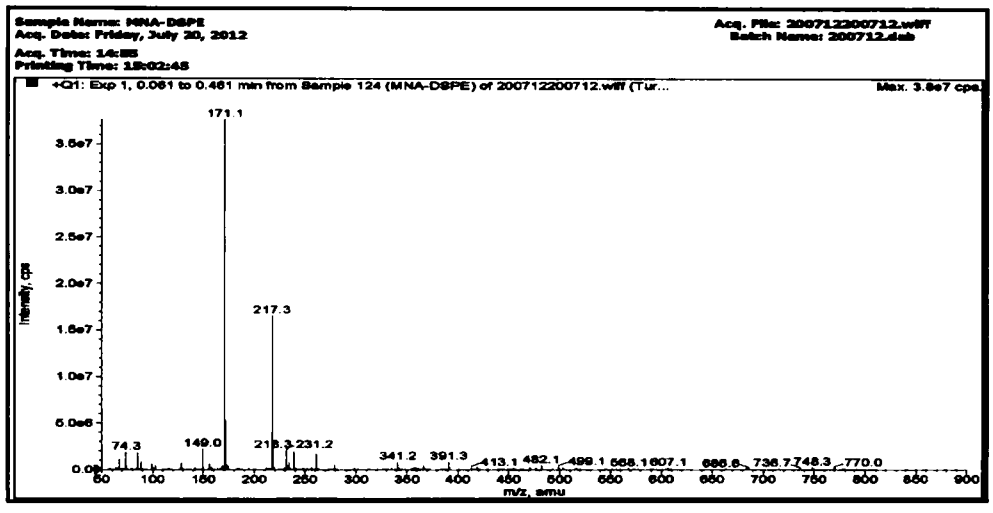

Fig. 3.18: Mass spectrum of 6-MNA-DSPE (Ionization: ESI)

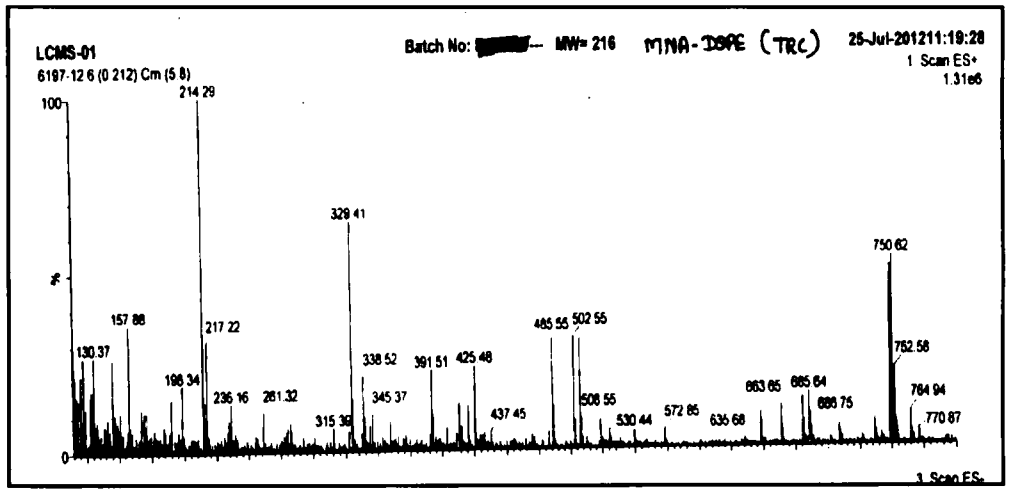

Fig. 3.19: Mass spectrum of 6-MNA-DSPE (Ionization: ESCI=ESI+APCI)

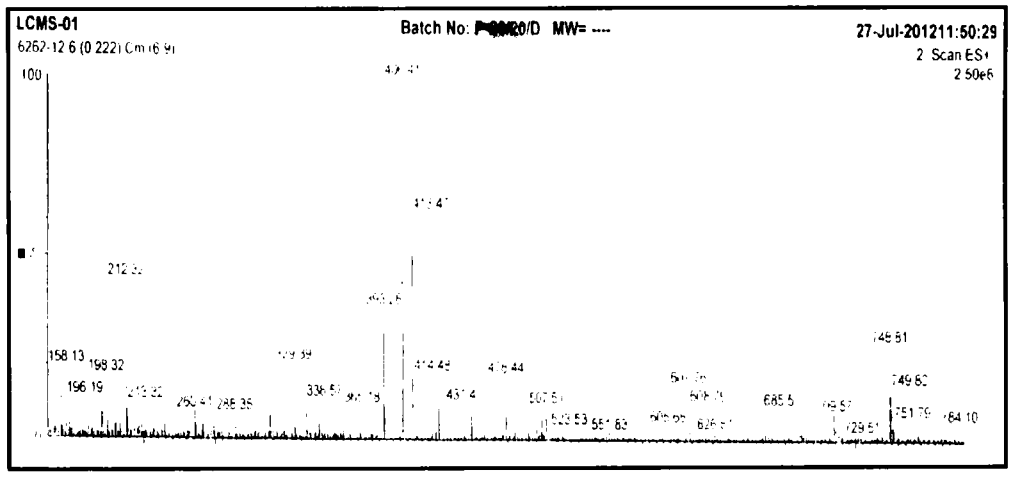

Fig. 3.20: Mass spectrum of BPA-DSPE (Ionization: ESCI=ESI+APCI)

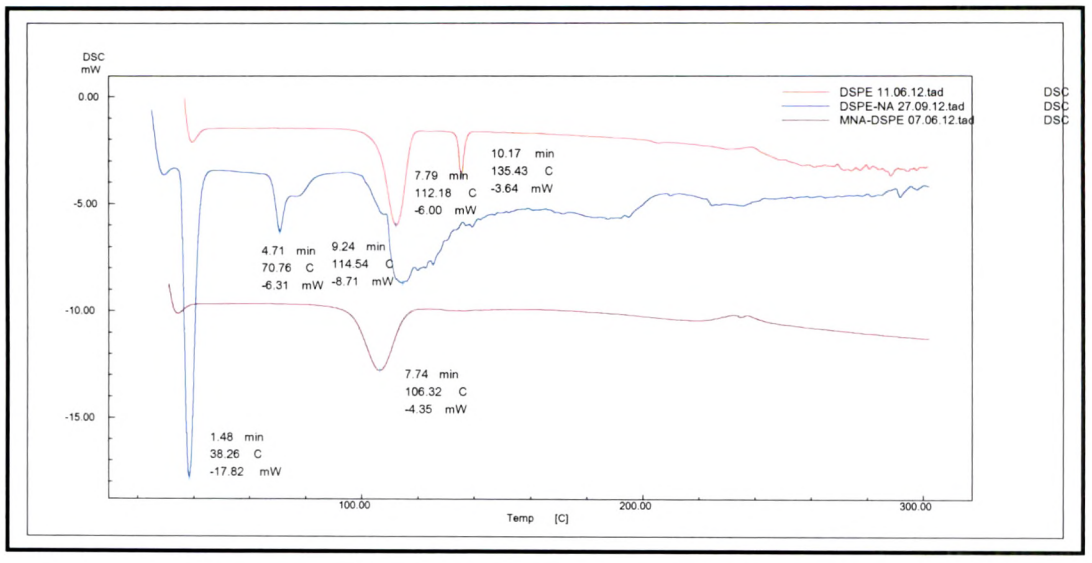

Fig. 3.21: DSC Thermograms of DSPE, DSPE-Na, 6-MNA-DSPE

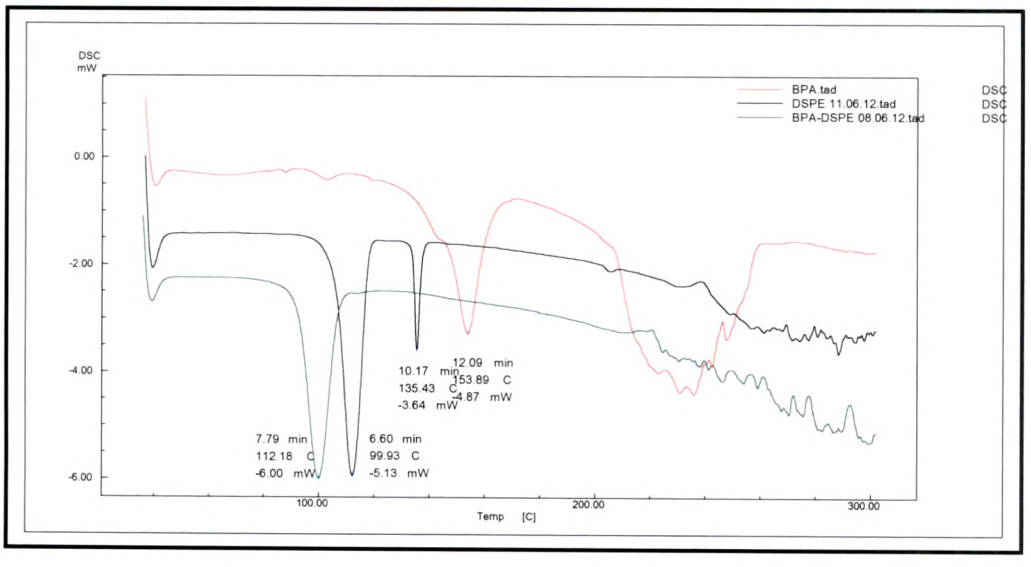

Fig. 3.22: DSC Thermograms of BPA, DSPE-Na, BPA-DSPE

3.3 Formulation of liposomes

3.3.1 Introduction

Liposomes are spherical lipid bilayers that serve as convenient delivery vehicles for biologically active compounds. The field of liposome research has expanded considerably over the last 35 years. It is now possible to engineer a wide range of liposomes varying in size, phospholipid composition and surface characteristics to suit the specific application for which they are intended. In comparison to other drug carriers, liposomes have some advantages like biological degradability and relative toxicological and immunological safety. It is not our intention to describe the details of such a vast field briefly and do injustice to all the relevant studies.

3.3.2 Preparation of liposomes

Liposomes containing NSAIDs were prepared by the lipid film hydration technique as it is simple and reproducible. Multilamellar vesicles (MLVs) were chosen for the entrapment of NSAIDs. Additional advantages of MLVs include ease of preparation and mechanical stability[13]. The requirement of mechanical stability and rigidity was further fulfilled by incorporating cholesterol, which is well documented to:

a) decrease the fluidity or micro viscosity of the bilayer by filling empty spaces among the phospholipid molecules.
b) reduce permeability of the membrane to water-soluble molecules due to the above effect and,
c) stabilize the membrane in the presence of biological fluids such as plasma.

A mixture of lipids, cholesterol and respective NSAID were dissolved in a mixture of chloroform and methanol (ratio 3:1) an RBF as the solubility of these lipids is higher in this solvent blend[13]. The flask was rotated in a rota evaporator at 65-75 rpm for 20 min in a thermostatically controlled water bath at 37 °C under vacuum (300 mm.Hg). The thin film so formed inside the RBF was further dried under vacuum for 6h. The thin dry lipid film was hydrated using purified water and the flask was rotated once again for 30 min at 50 °C. The liposomal suspension thus formed was then transferred to a suitable glass container for size measurement and it was found to be >1 μ. The liposomal suspension was incubated for 1-2 h at 75 °C (glass transition temperature of lipid) and the sample was sonicated for few seconds to reduce size and improve drug entrapment. The sonicated dispersion was then allowed to stand undisturbed for about 2h at room temperature for the annealing to be completed.

The next step in the preparation of the liposomes was the separation of unentrapped drug from the liposomes. Unentrapped drug was removed from the liposomal suspension by centrifugation at 4000-5000 rpm for 8-10 min at 0-5 °C temperature. The major process parameters were optimized using the percentage drug entrapment, size and zeta potential as the response parameters. The observations of the optimization processes are tabulated in **Table 3.1.**

3.3.3 Optimization of liposome formulation (Preliminary batches)

The following conditions were optimized for liposomes containing NSAIDs.

A. Composition of lipid mixture

Trials were initiated with a molar ratio of 1:4:0.15 (6-MNA: HSPC: Cholesterol, % EE=42.34±1.58 %, Table 3.1.). Increase in the proportion of HSPC, cholesterol in the lipid

mixture significantly enhanced the percentage of drug entrapped (Table 3.1). However further increase in HSPC, cholesterol proportion above 1:9 and 1:0.5 respectively did not lead to any significant improvement in the drug entrapment. This is probably due to saturation of the available space.

B. Hydration medium

Distilled water was used as the hydration medium for hydrating the dry lipid film. Trials using phosphate buffer or saline were not taken because solubility of 6-MNA/BPA in phosphate buffer might increase (due to salt formation) reducing drug entrapment, hence hydration medium was limited only to distilled water. The volume of distilled water was optimized to 8 ml for 6-MNA liposomes **(Batch: ML-7)**. Increase in the volume of water did not show any significant improvement in drug entrapment.

C) Hydration time

Increase in hydration time in the rotator flask from **15 min to 30 min** led to significant increase in drug entrapment. Further increase in hydration time did not lead to increase in drug entrapment. This indicated that the drug got incorporated in the lipid bilayer rather than aqueous compartment. A decrease in hydration time (<15 min) was associated with the incompletely formed liposomes when observed microscopically.

D) Sonication time

A sonication time of 15 sec was found to be sufficient for reduction in the particle size to around or less than 1μm without any significant change in the percent of drug entrapment. Sonication of liposomal suspension was optimized by altering time, cycle and amplitude according to the size requirements keeping in mind that sonication would not result in complete conversion of MLVs into LUVs and SUVs. Sonication was done at 60 % amplitude, 0.6 cycles for 15 sec to get mixture of MLVs, LUVs, and SUVs.

E) Zeta potential (DOTAP concentration)

Formation of liposome having positive zeta potential is important for this work hence cationic lipid DOTAP was used for this purpose and its concentration was optimized. DOTAP in low concentration (Drug: DOTAP=1:0.1) gave zeta potential in the range of 18-22 mV and it had no effect on liposome formation. To produce liposomes with zeta potential >25 mV higher concentrations of DOTAP (Drug: DOTAP=1:0.4 or 1:0.3) were used in formulation which resulted in increased zeta potential to >55.4 mV but the size of liposomes decreased significantly and initial size of liposomes without sonication was found to be <250 nm. This might be due to repulsion between charged lipids which leads to decreased drug entrapment. In order to get optimum zeta potential (25-35 mV)

and size of liposomes (>250 nm to <1.5 μm) with good entrapment efficiency (>70 %), DOTAP concentration was optimized to a ratio of 1:0.2 (Drug: DOTAP). It was found to be suitable to produce zeta potential in the range of 25-35 mV.

F) Entrapment efficiency

The percentage of drug entrapment of liposomes was calculated by estimating the drug in the liposomes. Liposomes were centrifuged at 6,000 RPM for 10-15 min at 2-8 °C the supernatant was removed off for estimating the entrapped drug in the liposome after lysis with methanol. Briefly, 0.1 mL of liposome was diluted upto 1.0 mL with methanol, sonicated for 5 min. and centrifuged at 3,000 RPM for 10 min at 2-8°C. Supernatant was analyzed for respective drug contents after suitable dilution with mobile phase using HPLC. For the estimation of 6-MNA and BPA HPLC method was developed and the chromatographic conditions used for the assay are given in **Table 3.1.** Percentage of entrapment was calculated using the formula given below:

Table 3.1: Chromatographic conditions for the estimation of 6-MNA and BPA

NSAIDs	Linearity range (μg)	Mobile phase composition	Flow rate (ml/min.)	Retention time (R_t Min.)	λ_{max}
6-MNA	500 ng-20 ug	ACN:PB 15 mM (3:1)	1.0	3.60 ± 0.2	230
BPA	500 ng-20 ug	ACN:PB 15 mM (3:1)	1.0	4.10 ± 0.2	253

PB=Phosphate buffer (15 mM, *p*H 5.0), ACN=Acetonitrile

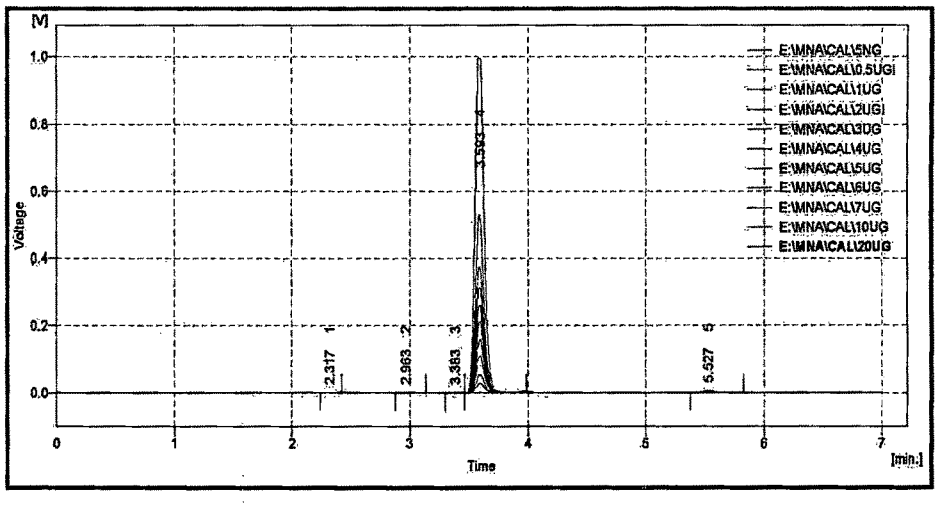

Fig. 3.23: Calibration and linearity chromatograms of 6-MNA **(1)**

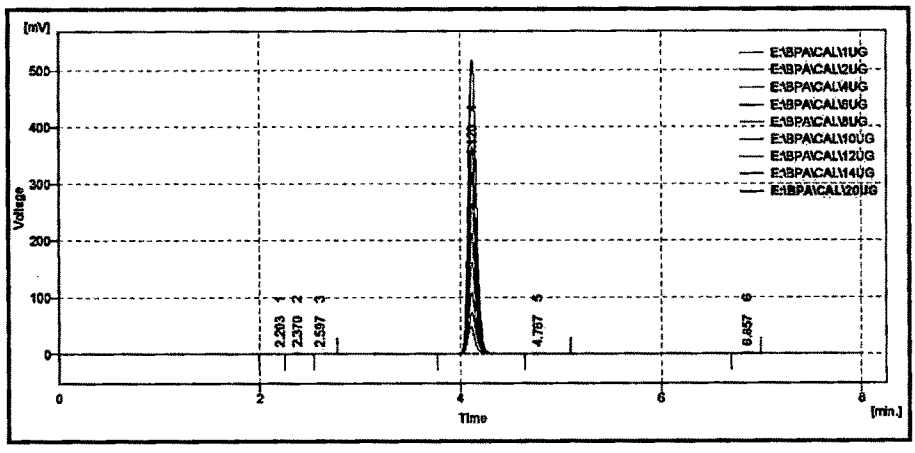

Fig.3.24: Calibration and linearity chromatograms of BPA **(2)**

$$\% \text{ Entrapment efficiency} = \frac{\text{Total drug added - Free drug}}{\text{Total drug added}} \times 100$$

$$= \frac{\text{Entrapped drug}}{\text{Total drug added}} \times 100$$

Table 3.2. shows preliminary batches used for optimization of liposomal formulation with their response parameters.

Table 3.2: Optimization of Drug: Lipid: DOTAP mixture ratio (6-MNA=10 mg)

Batch No.	MNA	HSPC	DOTAP	Volume†	% EE*	Size* (nm)	Zeta* (mV)
ML-1	1	4	0.1	6	42.34±1.58	1672±20.1	21.4±2.0
ML-2	1	6	0.1	6	56.12±2.04	1579±18.5	20.8±2.1
ML-3	1	8	0.1	8	67.96±2.56	1297±16.7	20.6±2.4
ML-4	1	8	0.3	8	62.89±1.98	239±12.6	65.3±4.3
ML-5	1	8	0.2	8	69.44±2.45	840±15.8	32.4±3.2
ML-6	1	10	0.2	8	71.66±3.04	914±17.4	31.8±2.3
ML-7	**1**	**9**	**0.2**	**8**	**74.23±3.22**	**722±18.9**	**29.8±2.4**
ML-8	1	9	0.2	9	74.56±3.41	761±14.8	38.44±3.1
ML-9	1	9	0.2	6	69.64±3.84	547±16.1	42.57±3.2
*=Mean±SD, n=3; †=Hydration volume (ml);							

3.3.4 Optimization of formulation variables by applying 3^2 factorial designs

Based on the results obtained in preliminary experiments, drug: lipid (HSPC) and drug: DOTAP ratio, were found to be the major variables affecting the percent drug content (PDC), zeta potential and mean particle size (MPS). To reduce the computational

complexities, the above mentioned components were eased to 2 independent variables namely lipid (HSPC) and cationic carrier (DOTAP) concentrations. Approximate levels of these independent variables were chosen from the data available from literature as well as from the initial experimentation.

It was assumed that the independent variables would affect responses in linear or quadratic manner and the possibility of interaction effect of the independent variables was also taken in to consideration. This assumption was necessary to develop a mathematical model which could be tested for significance of contribution of various independent variables. Hence, it became essential to use a factorial design with three levels to estimate curvature of response (i.e. 3^2 factorial with total no. of experiments= 9). To save time, single block design with zero (0) replication has been preferred. The experimental grid was coded for ease of representation in **Table 3.3.**

Nine batches of different combinations were prepared by taking values of selective variables X1 and X2 at different levels as shown in **Table 3.3**. All other formulation and process variables were kept invariant throughout the study (Cholesterol concentration 0.023 mM (9.0 mg); hydration time 45 min; annealing time 2 h; hydration temperature 65±2 ^{0}C). The prepared batches were evaluated for drug entrapment/content, particle size and zeta potential as dependent variables, and the results are recorded in **Table 3.5. Table 3.4** summarizes the experimental runs and the employed factor combinations.

Table 3.3: Translation of experimental conditions into physical units for liposome formulation optimization.

Variables	**Level**		
	-1	0	1
X1 (lipid concentration)	294	314	334
X2 (DOTAP concentration)	3	6	9

Table 3.4: Factor combination as per the experimental design for optimization

Level	Batch								
	F1	F2	F3	F4	F5	F6	F7	F8	F9
X1	-1	0	1	-1	0	1	-1	0	1
X2	-1	-1	-1	0	0	0	1	1	1

Following parameters were kept constant for liposome formulation optimization process:

a) Cholesterol concentration=0.023 mM (9 mg), b) Hydration volume= 8 ml

The results obtained are given in **Table 3.5**. the obtained data was subjected to statistical analysis.

Table 3.5: 3^2 Full factorial design consisting of experiments for the study of two experimental factors in coded and actual levels with experimental results

Formulation	Actual value variables		Respone value		
	X1	X2	% Drug entrapment	Mean Particle size (nm)	Zeta potential (mV)
FML-1	294	3	68±2.14	1244±20.1	21.4±1.5
FML-2	314	3	71±3.44	1454±19.8	22.5±2.2
FML-3	334	3	75±1.89	1596±22.4	22.2±2.5
FML-4	294	6	72±2.56	550±18.4	25.9±3.1
FML-5	**314**	**6**	**74±3.08**	**774±14.66**	**30.5±3.2**
FML-6	334	6	76±2.7	582±12.58	44.7±4.7
FML-7	294	9	58±1.94	258±10.89	55.4±4.6
FML-8	314	9	62±1.74	269±11.44	66.4±6.7
FML-9	334	9	64±3.40	465±13.78	65.3±5.0

Values are Mean±SD, n=3

The effect of lipid and DOTAP concentration was statistically analyzed using Stat-Ease software (Design-Expert® 8), ANOVA for response surface quadratic model gives results as given in **Table 3.6.**

Table 3.6: ANOVA results for optimization of entrapment efficiency.

Source	F value	p-value, Prob>F
Model	63.67	0.0044
A-HSPC	45.37	0.0095
B-DOTAP	150.0	0.0017
AB	0.19	
A^2	0.011	
B^2	95.35	

The model F value of 49.47 implies that the model is significant. There is only a 0.44 % chance that a model f-value this large could occur due to noise. Values of prob >F less than 0.0500 indicate model terms are significant. In this case A, B and B^2 are

significant model terms. The "Pred R-Squared" of 0.8556 is in reasonable agreement with the "Adj R-Squared" of 0.9680 "Adeq Precision, measures the signal to noise ratio, a ratio greater than 4 is desirable. Our ratio of 19.522 indicates an adequate signal, so this model can be used to navigate the design space.

Table 3.7: Statistical data for % entrapment

Parameter	Value	Parameter	Value
Std. Dev.	1.13	R-Squared	0.9880
Mean	68.94	Adj R-Squared	0.9680
C.V. %	1.65	Pred R-Sequared	0.8556
Press	46.54	Adeq Precision	19.522

Final equations in terms of coded factors is given below:

% Entrapment= $+74.22+2.75xA-5xB-0.25xAB-0.083xA^2-7.83B^2$

Where A= Conc. of HSPC, B=Conc. of DOTAP (ANOVA for response surface quadratic model p <0.0044)

Zeta potential=+39.37+4.92xA+20.17xB (ANOVA for response surface linear model p<0.0008)

Size= +799.11+98.50xA-550.33xB (ANOVA for response surface linear model p<0.0007)

When the relationship for the response is given as a function of two independent variables, it can be well represented by 3D plots. The surface responses show the 3D plot of two independent variables simultaneously. Graphically there are contour plots on which the axes represent the two independent variables; the counters represent a specific level of response and, we can select an optimum value. Graphically 3D surface response plot for % entrapment is shown in **Figure 3.25 A-C.**

Confirmatory report suggested batch-5 (FML-5) as the most appropriate batch with respect to % entrapment, size and zeta potential. This final batch was optimizd and evaluated thrice having composition of 6-MNA 0.046 mM (10 mg), HSPC 0.414 mM (314 mg), cholesterol 0.023 mM (9 mg), DOTAP 0.009 mM (6mg) and purified water 8 ml.

Another objective of the present work was to develop sustained release liposomal formulations of NSAIDs, hence salts of these two NSAIDs with DSPE were used in the formulation to sustain the release. So, in order to develop liposomal formulations containing Drug-DSPE salts the above optimized batch (**FML-5**) was used for further

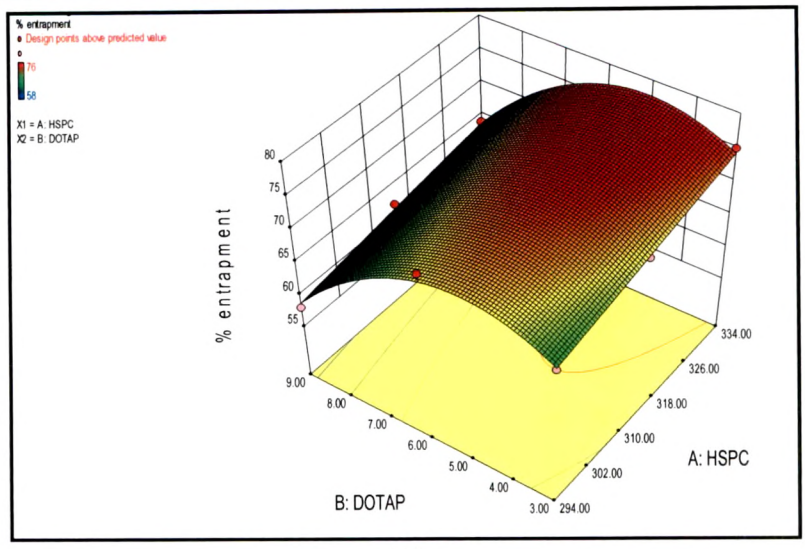

(A)

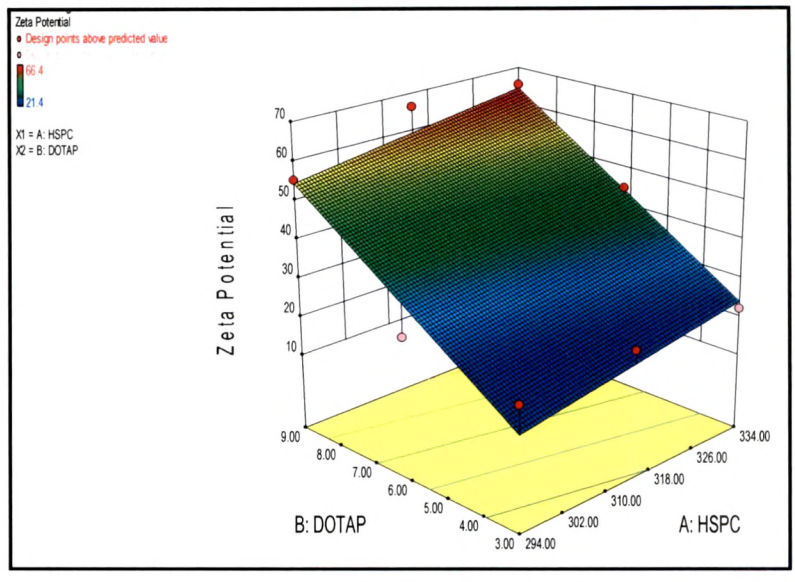

(B)

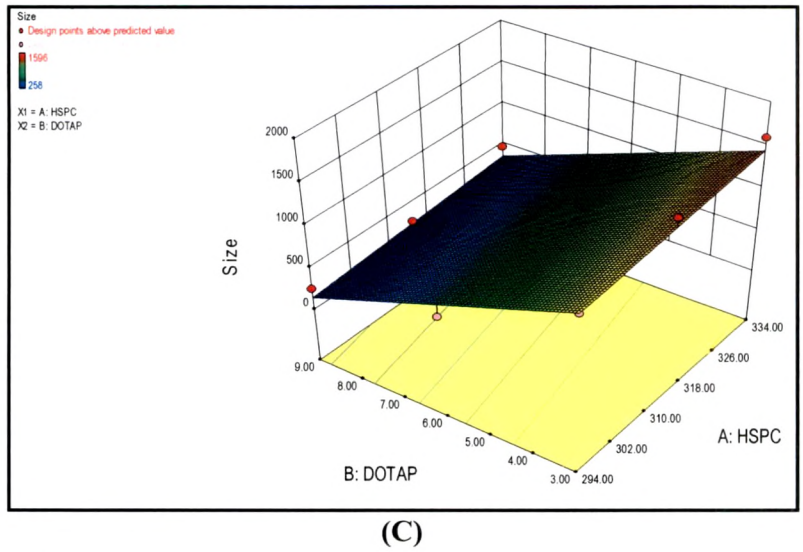

(C)

Fig. 3.25: 3D surface response plot for **A**: % entrapment, **B**: Zeta potential and **C**: Size

development with varying mole ratio of the parent drug and Drug-DSPE **(Table 3.8)**. Four batches with 6-MNA: 6-MNA-DSPE mole ratios of 9:1, 8:2, 7:3 and 6:4 were taken and evaluated.

From the results it can be concluded that increasing the ratio of 6-MNA-DSPE salt decreases the drug entrapment, and the optimum ratio was found to be 8:2. In order to maintain optimum entrapment efficiency and susteined release we have chosen batch **(CML-2)** which contains 6-MNA: 6-MNA-DSPE salt with mole ratio of 8:2. From the previous studies it was conclude that plain 6-MNA batches have maximum drug entrapment and it may be due to maximum space available in liposomes as shown in **Fig. 3.26A**. Incorporation of only 6-MNA-DSPE salt in liposome may result in very low entrapment of the drug in liposomes but a higher sustained release effect **(Fig. 3.26B).** Combining the advantages of both the approaches would give ideal drug delivery system having higher entrapement capacity and sustained release of drug **(Fig. 3.26C).**

Table 3.8: Optimization of the effect of ratios of 6-MNA: 6-MNA-DSPE on liposomes.

Formulation	**Mole Ratio#**	**Respone value**		
Formulation	6-MNA: 6-MNA-DSPE#	% Drug entepment	Mean Particle size (nm)	Zeta Potential (mV)
CML-1	9:1	73±2.10	864±12.78	31.5±4.2
CML-2	**8:2**	**72.55±4.25**	**695±10.89**	**33.4±5.3**
CML-3	7:3	64.88±5.17	680±11.33	28.7±3.8
CML-4	6:4	59.95±6.18	547±09.66	32.5±4.7

equivalent to 6-MNA

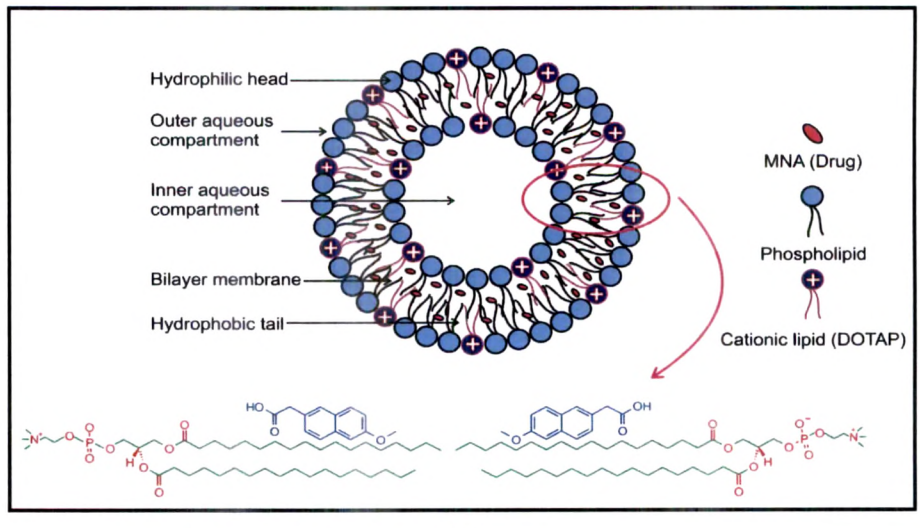

(A)

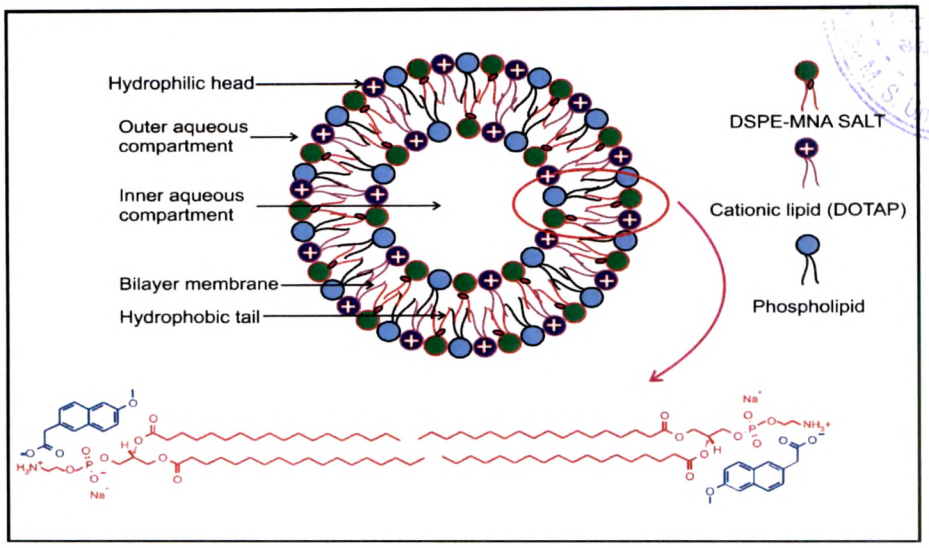

(B)

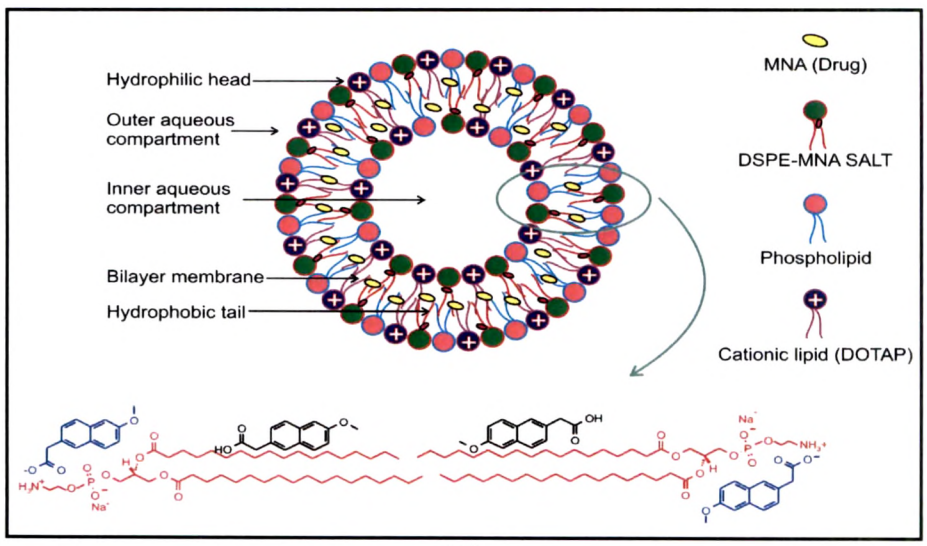

(C)

Fig. 3.26: A-C: Drug entrapment into liposomes

3.4 Characterization of liposomes

Both physical and chemical characterizations of liposomes influence their *in vivo* and *in vitro* behavior. Liposome characterization was performed immediately after preparation. The prepared liposomes were characterized for the following attributes:

A) Size

B) Morphology

C) Zeta (ς) potential

D) *In vitro* diffusion

A) Size

Size is an important parameter for IA drug delivery. Bonanomi *et al.* reported that increasing the size of liposomes, ranging from 160 nm to 750 nm in diameter, resulted in a 2.6-fold increase in retention to 48 h post-injection.[14-15] A similar observation was described for liposomes containing methotrexate, for which a mean diameter of 1.2 μm ensured a higher retention, and thus anti-inflammatory action, than the one with 100 nm size.[16-17] There is an upper limit (40-250 nm radius) to the size of particles that can escape freely from the joint cavity. So, >250 nm size of liposomes is an essential requirement of liposomal drug delivery.

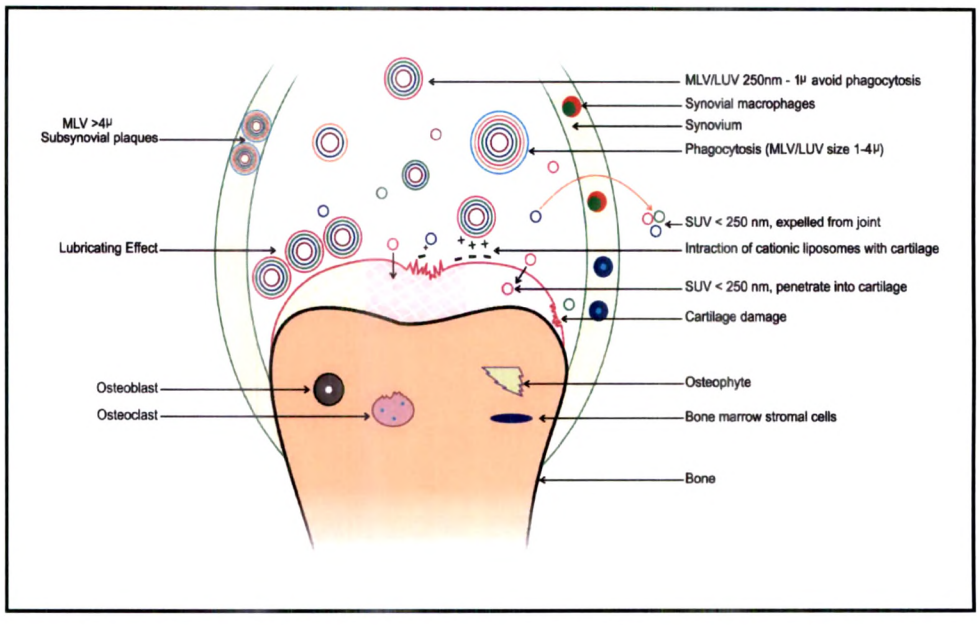

Fig. 3.27: Fate of IA administered liposomal drug delivery systems.

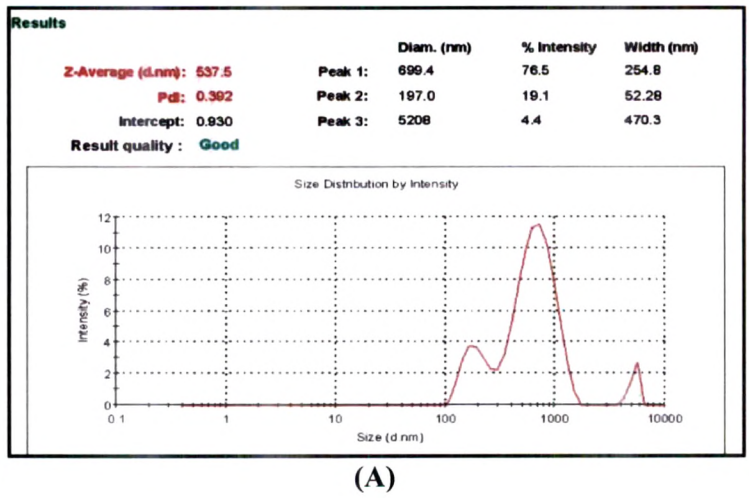

(A)

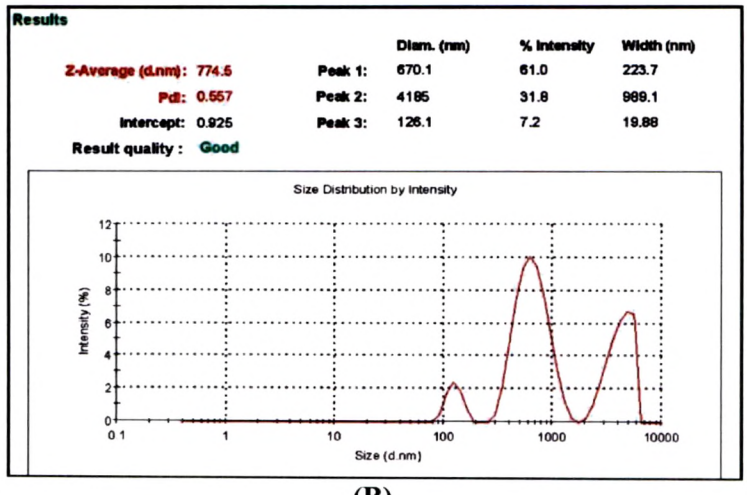

(B)

Fig. 3.28: Particle Size analysis of the optimized liposome batch, two readings **(A)** and **(B)**

Multilamellar as well as unilamellar liposomes with size range of 250-1000 nm will provide ideal drug delivery system. Small unilamellar vesicles would be expelled from the joint whereas large liposomes (>1 μ) would undergo phagocytosis as shown in **Fig. 3.27**. Considering all the above factors liposomes having size range of >250 nm but <1 μ have been prepared. The average particle size and PDI were calculated after performing the experiment in triplicate. PDI of 0.0 represents a homogenous particle population while 1.0 indicates a heterogeneous size distribution in the liposome. The particle size analysis results of liposomal formulation were shown in **Fig. 3.28A-B.**

Transmission electron microscopy (TEM)

The TEM images of the prepared liposomes are shown in **Fig. 3.29 A-D** below. Average size of the formed liposomes was found to be around 800 nm.

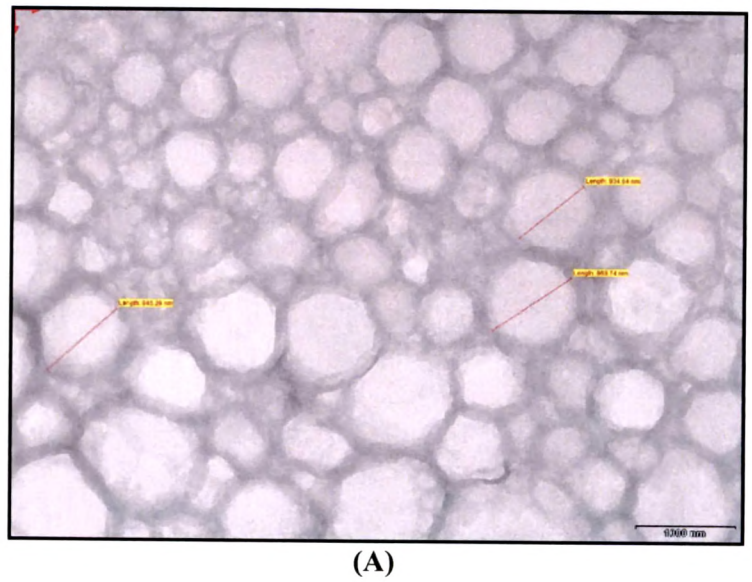

(A)

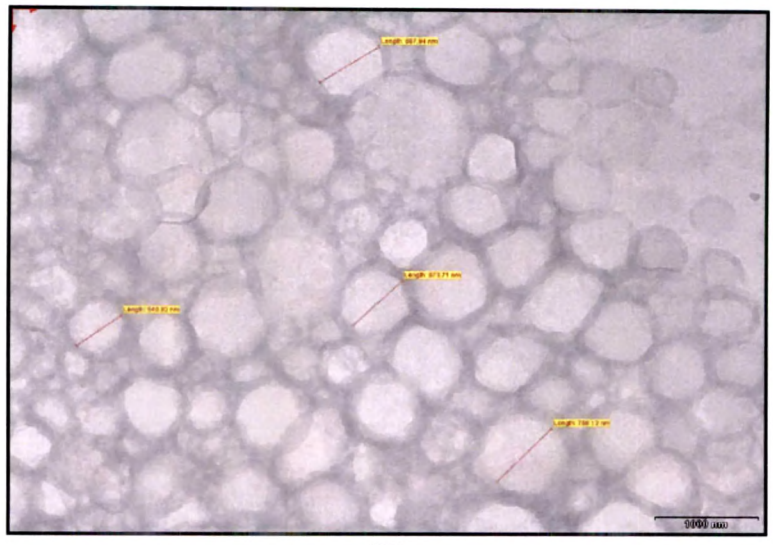

(B)

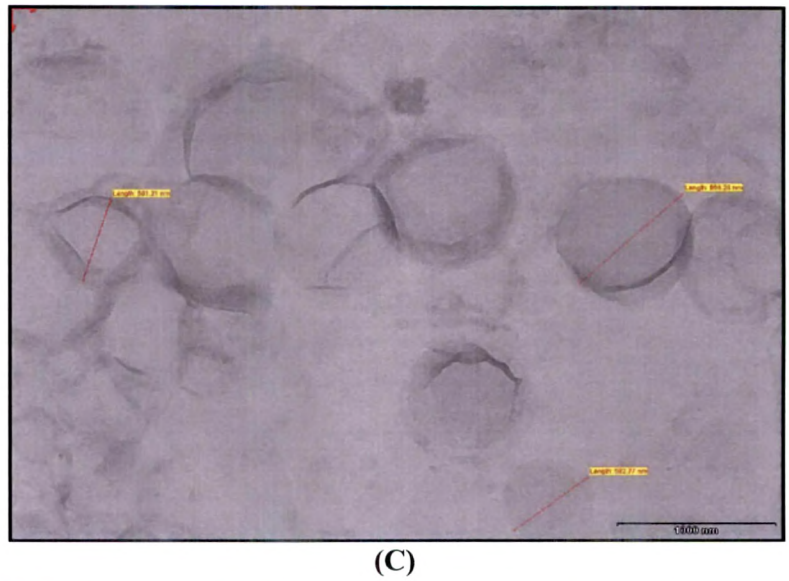

(C)

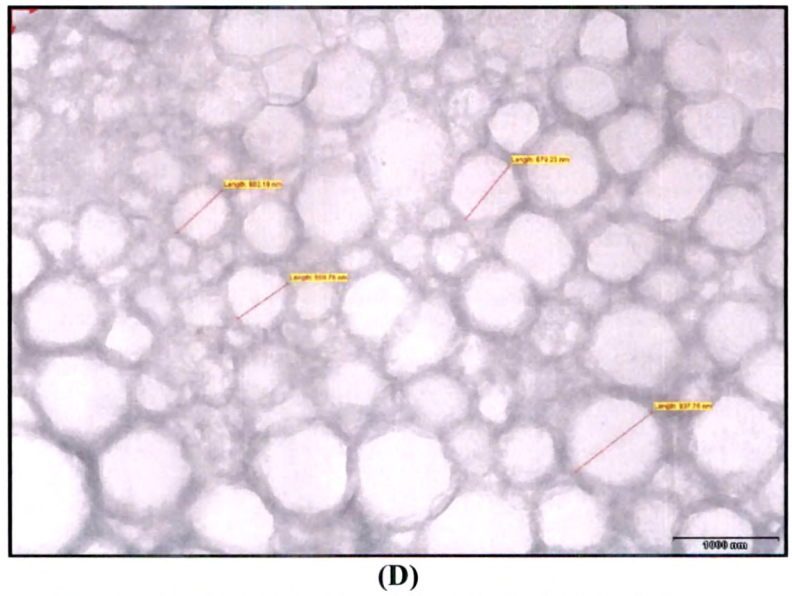

(D)

Figure 3.29: TEM of liposomes **A-D** (Scale 1000 nm)

Further, nature of the vesicles is also important as SUVs vesicles penetrate deep into cartilage whereas MLVs and LUVs are retained on cartilage surface and provide lubricating effect as well as adherence to cartilage via ionic interaction and slowly releases the drug over a long period of time as shown in **Fig 3.30.**

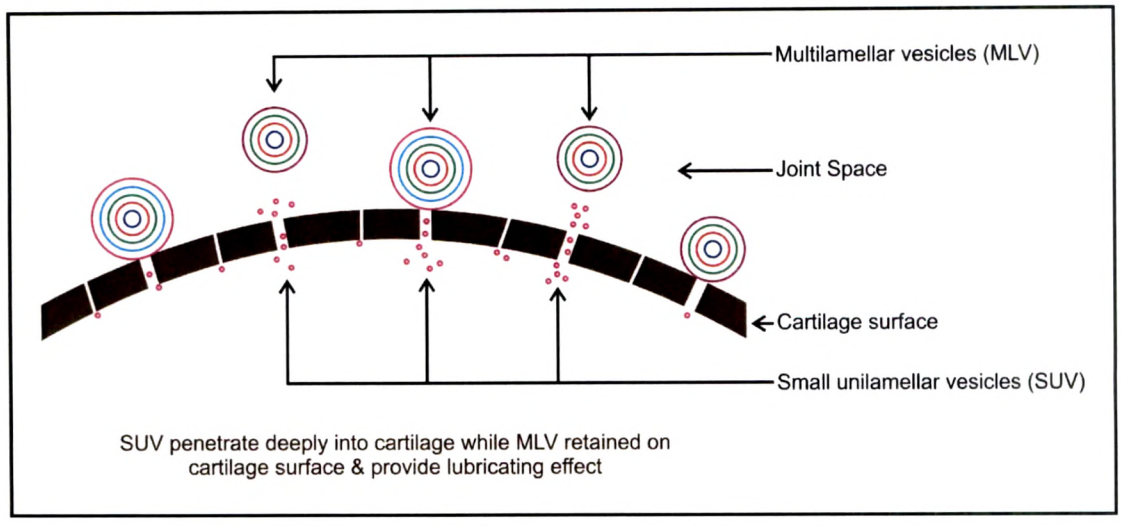

Fig. 3.30: Retention and penetration of liposomes having different sizes

B) Morphology

As discussed in detail in Section-I, not only the size but also the shape of the particles injected into the joint is important for triggering an immune response. Irregularly shaped microparticles have been demonstrated to promote tissue inflammation in comparison to the round shaped drug delivery systems. Hence shape is also important for drug delivery system for IA drug delivery.

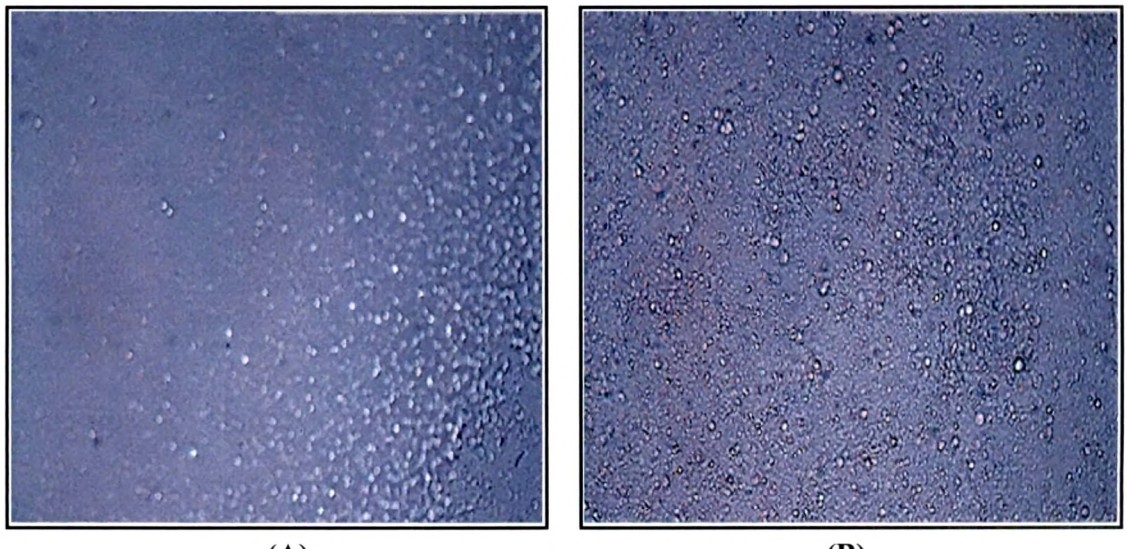

(A) **(B)**

Fig. 3.31: Photograph of liposomes in Olympus microscopy **(A-B)**

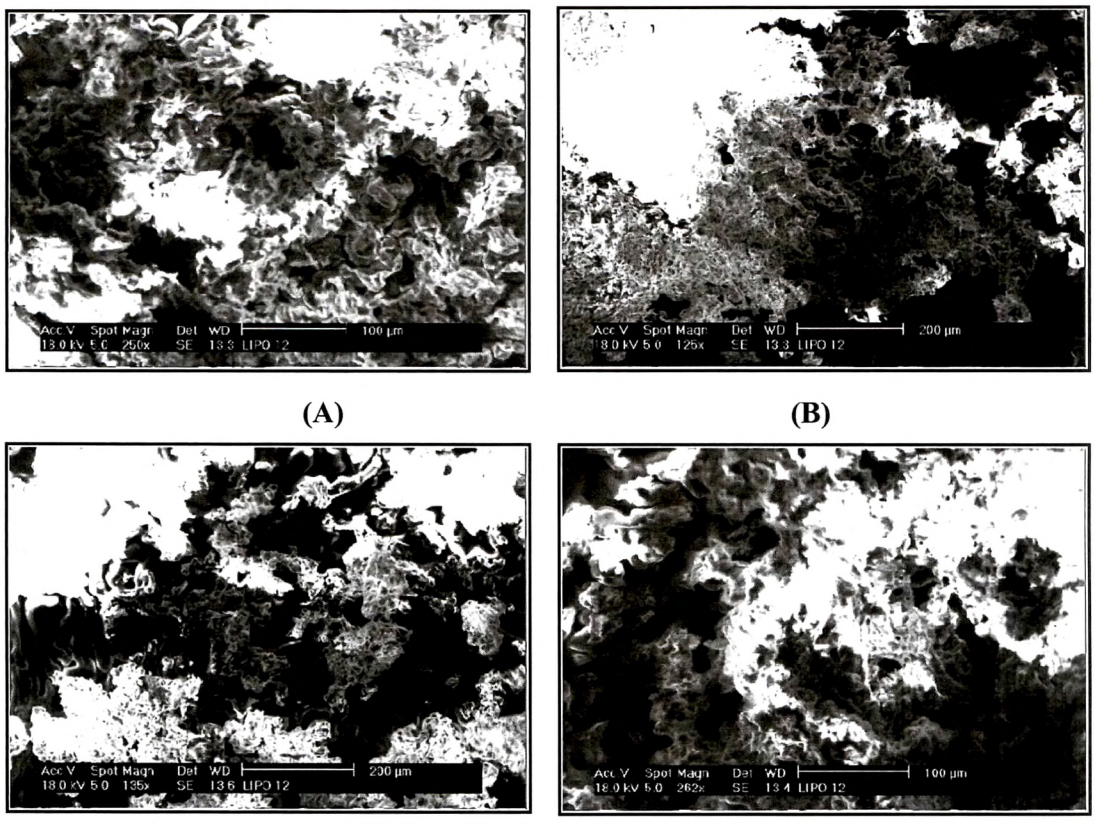

Fig. 3.32: Scanning electron microscope images of lyophilized liposomes.

Morphological evaluation was conducted using Optical microscopy, SEM and Cryo TEM. Photographs showed that all the liposomes (SUV/LUV/MLV) were round in shape with combination of MLV, LUV and SUVs as shown in **Fig. 3.31-3.34**

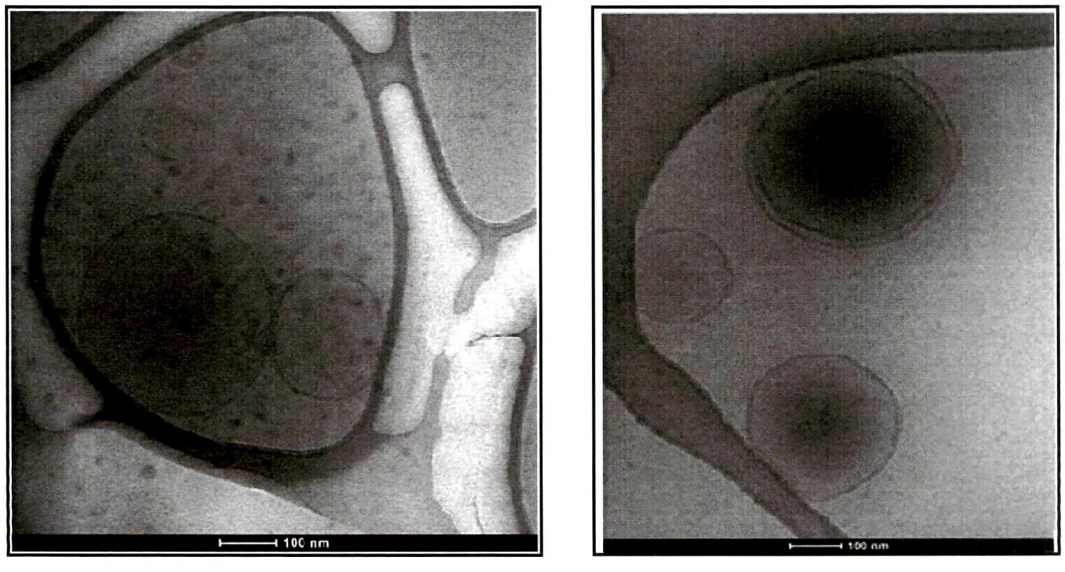

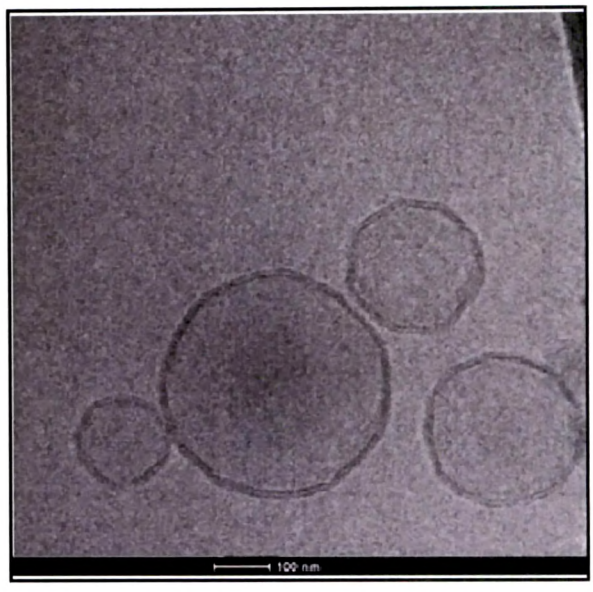

(C) **(D)**

Fig. 3.33: Cryo-TEM images of liposomes **(A-E)**

C) Zeta (ς) potential analysis

Literature suggests that positively charged molecules interact with negatively charged sugars present in cartilage and may improve drug residence time within the joint cavity.[18-21]. Due to this aspect it is essential to prepare liposomes having positive zeta potential. The zeta potential (ς potential) of the prepared liposome suspensions was measured and was found to be dependent on concentration of DOTAP used in formulation. The obtained zeta potential was found to be around 30 mV as shown in **Fig 3.34 A-D**.

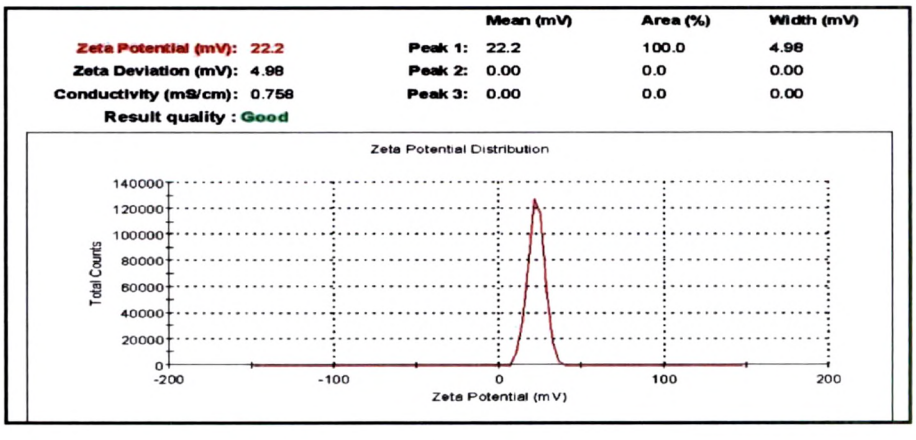

(A)

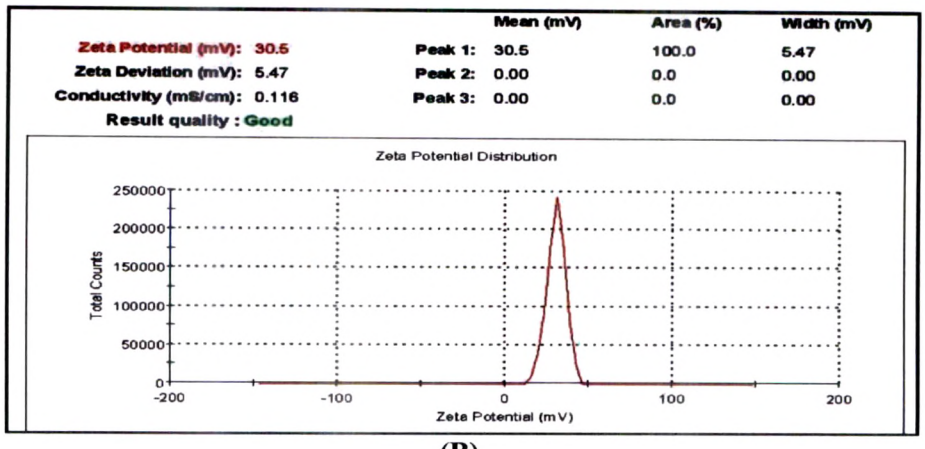

(B)

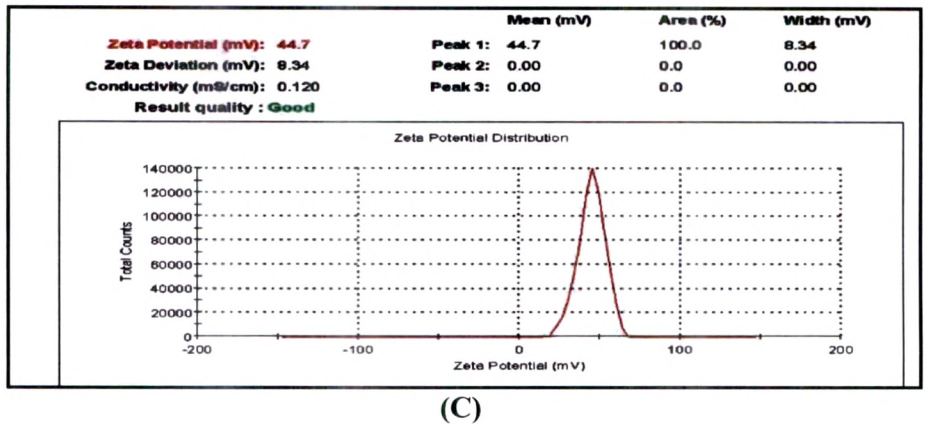

(C)

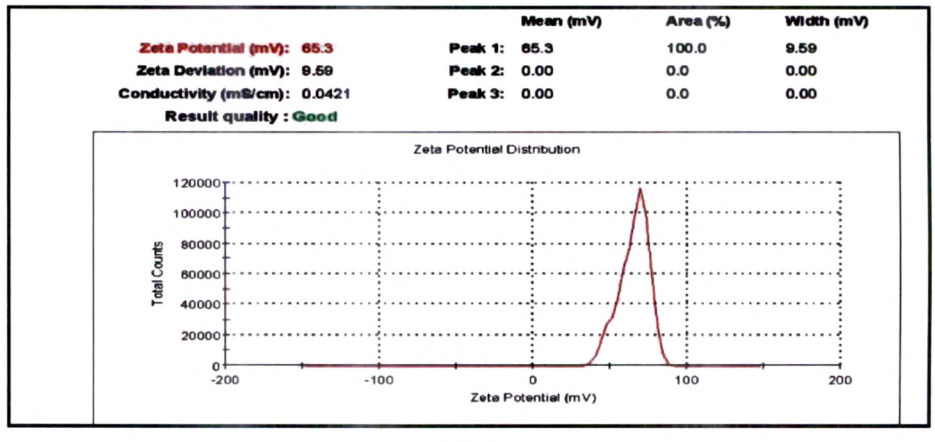

(D)

Figure 3.34: Zeta potential analysis data of the liposomes (samples **A-D)**

4.4.6 *In vitro* diffusion studies of liposomes

In vitro diffusion studies were performed on liposomal formulations and on plain MNA. Results of the release studies show **(Fig. 3.35)** that liposomes prepared with 6-MNA plus 6-MNA-DSPE salt in 8:2 ratio offered the slowest release (<45 %) over 12 h as compared to liposomal formulation containing 6-MNA in free form (~60 %). Studies

further showed that plain 6-MNA gave >85 % release within 30 min indicating that incorporation of drug into liposomal formulation coupled with salt retard drug release over a long period of time. The data of *in vitro* release studies is shown in **Table 3.9**

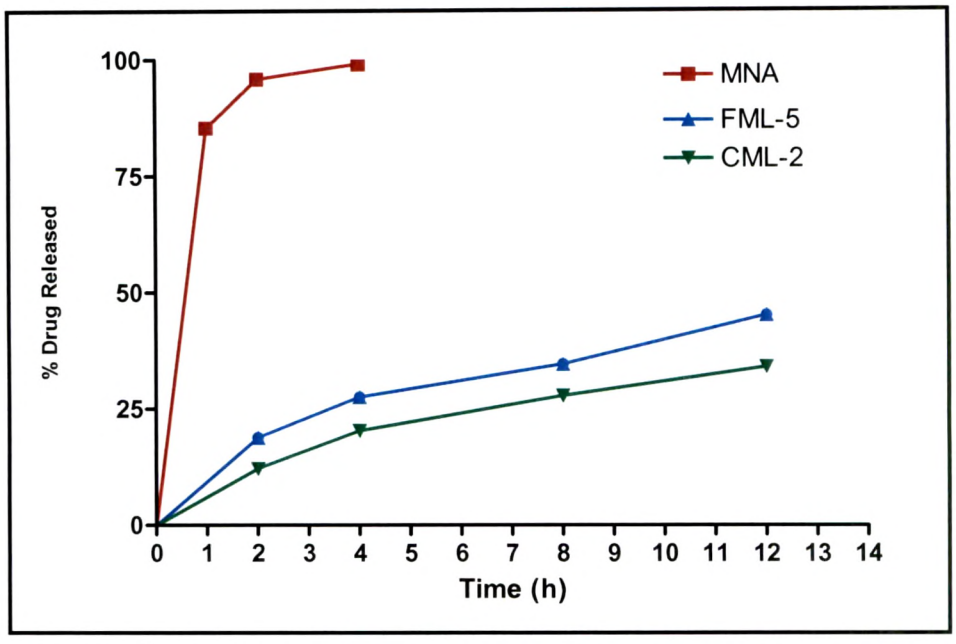

Fig. 3.35: *In vitro* release studies of GEM at *p*H 7.4 buffer (FML-5=Liposomes having MNA; CML-2=Liposomes having MNA and MNA-DSPE)

Table 3.9: *In vitro* release of **6-MNA** from liposomes at *p*H 7.4

Time (h)	% Cumulative Release at *p*H 7.4		
	6-MNA	**FML-5**	**CML-2**
30 min	85.41±0.38	--	--
1	95.88±0.75	18.89±0.68	12.22±0.78
2	99.08±0.49	27.55±0.54	20.33±0.94
4	--	34.62±0.94	27.88±0.55
8	--	45.18±0.43	34.08±0.81
12	--	58.74±0.87	42.77±0.56

3.5 Stability testing of liposomes

3.5.1 Introduction

The physical and chemical properties of the formulation must be maintained during storage and distribution, therefore stability studies of formulations are required to be performed. Physical and chemical data are generated as a function of time and storage conditions [e.g., temperature and relative humidity (RH)]. Stability testing provides

evidence whether the quality of a drug substance or drug product under the influence of various environmental factors gets altered with time or not.

3.5.2 Stability of liposomes

The stability of liposomes depends upon conditions like temperature/humidity and is affected by processes like oxidation/hydrolysis etc. which lead to aggregation and leakage of the entrapped material from the vesicles affecting the shelf life of liposomes greatly. Liposomal formulations have been known to show poor stability and do not meet the required standards for long term stability of pharmaceutical preparations when stored as aqueous dispersions. Decrease in the entrapment efficiency, fusion and aggregation are the major stability problems associated with liposomal preparations. Lyophilization is considered as a promising means of extending the shelf-life of liposomes. However, both freezing and drying can induce structural and functional damage into the liposomes. Sugars are frequently used as the cryoprotectants in lyophilization for stability of liposomes[22]

The liposomal aqueous dispersions were evaluated for the effect of temperature on the particle size, zeta potential and percent entrapment efficiency of the drugs and for stability over a period of 2 months at refrigeration (2-8 °C) and room (30±5 °C) temperatures.

Table 3.10: Stability data of liposomal dispersion

Duration of storage	Particle Size (nm)	Zeta potential (mV)	% Entrapment Efficiency (EE)
0 Day	695±10.89	33.4±5.3	72.55±4.25
2-8 °C (Refrigerator conditions)			
15 Day	715±13.45	31.6±4.2	71.12±5.02
1M	704±11.66	34.2±3.8	70.33±4.14
2M	738±16.87	35.2±5.4	67.44±3.82
30 ± 5 °C (Room temperature)			
15 Day	708±09.27	32.1±4.4	71.88±4.97
1M	752±12.71	34.8±5.2	65.11±5.07
2M	795±14.56	33.1±6.7	61.08±6.07

Liposomal formulations were found to be stable when stored at 2-8 °C as aqueous dispersions, whereas when stored at 30±5 °C they showed increase in particle size after 2 months, compared to the initial samples **(Table 3.10)**, Saturated phospholipid (HSPC) was used in the preparation of liposomes. Higher positive zeta potential decreases vander

Waals interactions (which is a major contributor to aggregation of electrostatically neutral complexes) in the liposomes, ultimately preventing liposomes from fusion and aggregation[23]. The entrapment efficiency of liposomal dispersions got lowered with time at all the storage conditions but maximum decrease in entrapment efficiency was observed for aqueous dispersions at 30±5 °C **(Table 3.10)**.

Hence, it can be concluded that these liposomal dispersions can be stored at 2-8 °C as aqueous dispersions for 2 months. Liposomal dispersion stored at 30±5 °C shows a decrease in entrapment efficiency and increase in particle size.

3.6 Biodistribution and gamma imaging studies

The aim of the current study was to assess the residence time of the liposomes in the joint cavity upon IA administration. Little information is available in the literature on the effect of charge on residence time of drugs in joint cavity but our previous study has indicated that positively charged CDS possess improved drug residence time. To know the effect of positively charged liposomes, radiolabeling of the liposomes was required to be done for their localization/quantification in the joint cavity. To study these aspects, parent NSAID and the liposomes were labeled using ^{99m}Tc as per the details mentioned in **Section-I**. Radiolabeling parameters were optimized for liposomes and are shown in **Table 3.11**.

IA residence times of prepared liposomes and parent drug were studied in inflammatory condition. Animals were divided into three groups, Group-A (standard) was administered by IA the parent NSAID i.e 6-MNA **(1)**. Group-B (Test) was administered by IA the liposomes, 3 h after induction of inflammation in the rat paw. And the third group was kept as control. Inflammation was induced in the right hind paw of the rats by injecting carrageenan (0.1 ml, 1 % w/v in normal saline) into the subplantar region of the paw. The animals were anaesthetized, fixed on a board and images were taken 1 h, 2 h, 6 h and 24 h after the administration of the radiolabeled complexes by IA route. Percentage radioactivity was calculated as given in **Table 3.12.**

Table 3.11: Optimization of radiolabeling of liposomes

No	Drug/Formulation	*p*H	Incubation Time (min)	$SnCl_2.2H_2O$ (µg)	% Radiolabe-ling	% Stability (saline) 24 h
1	6-MNA	7.0	30	150	95.06±2.0	86.75±4.55
2	CML-2 (Liposome)	7.0	15	150	96.05±4.5	82.46±5.87

Table 3.12: Percentage of radioactivity in knee after IA administration

Time (h)	% Radioactivity in ROI*		
	6-MNA	Liposome	Q-CDS (7aI)
1	100±4.0	100±3.1	100±3.0
2	58.47±3.1	91.44±3.0	76.54±3.1
6	42.06±4.3	84.97±3.7	60.78±3.0
24	13.44±3.0	69.81±4.2	40.96±4.1

*Radioactivity counts converted in to percentage and initial counts taken as 100%

*ROI=Region of interest

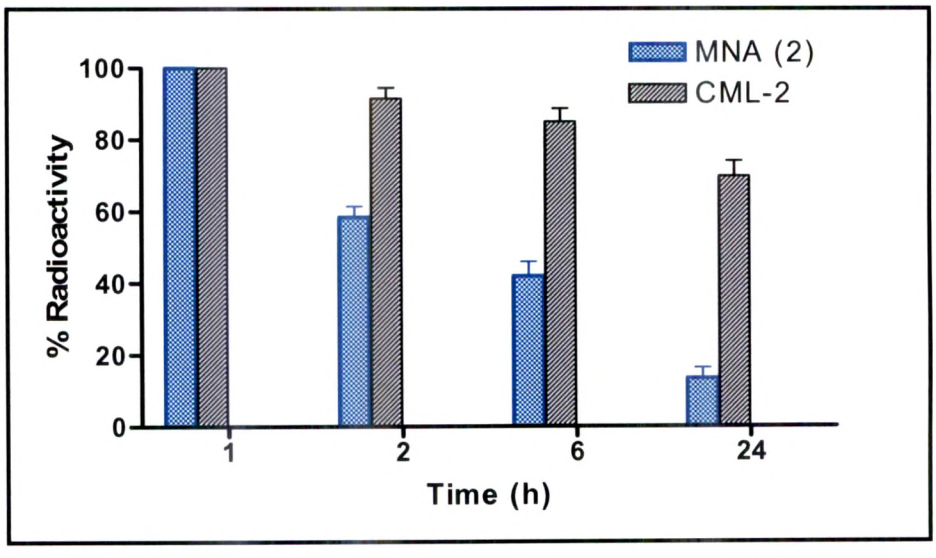

Fig. 3.36: % Radioactivity retained in rat knee after IA injection of 6-MNA **(1)** and liposomal formulation CML-2 after 1, 2, 6, 24 h

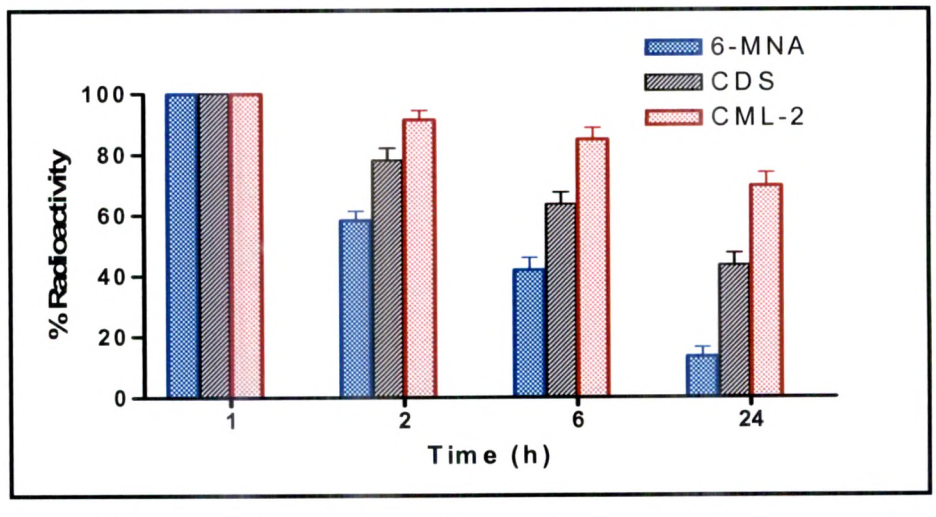

Fig. 3.37: % Radioactivity retained in rat knee ROI after IA injection of 6-MNA (1), Liposomal formulation CML-2, and quaternized CDS [(7aI) from section-I)] after 1, 2, 6 and 24 h (ROI=Region of interest)

From the obtained data and figures it is clear that liposomes showed higher retention in joints after IA administration as compared to parent drug **(2)** and quaternary ammonium chemical delivery system [(7aI) from section-I). Further, radioactivity obtained for the prepared liposomes after 24 h was about 5 times higher in ROI compared to the parent drug. So it could be concluded that liposomal drug delivery having cationic charge are retained for a longer period of time in joint cavity by ionic interaction. Hence it is clear that we can extend residence time of the drug by these drug delivery systems. Moreover, sustained release of the drug will give anti-inflammatory effect for a longer duration.

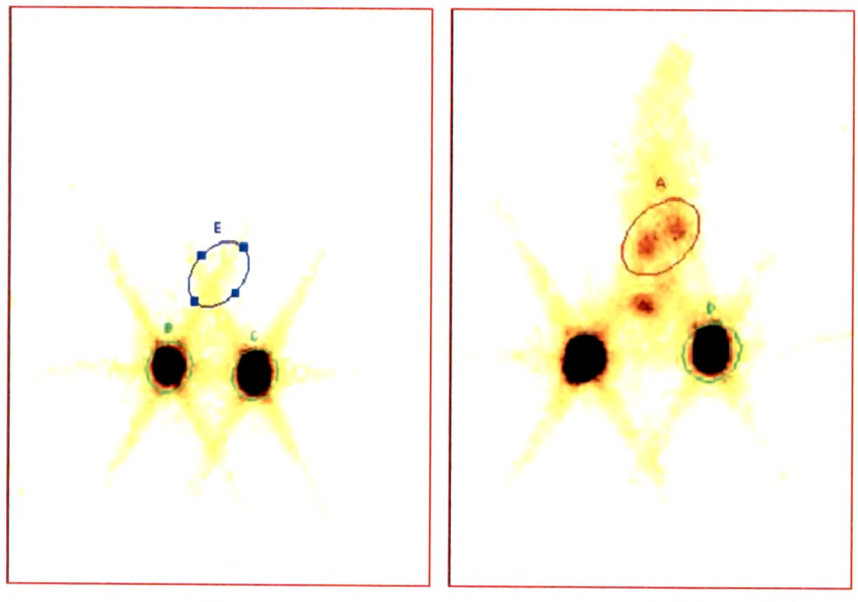

(A) **(B)**

Fig. 3.38: Gamma camera image of rats after IA injection of **1** after 1 h **(A)** and 6 h **(B)**

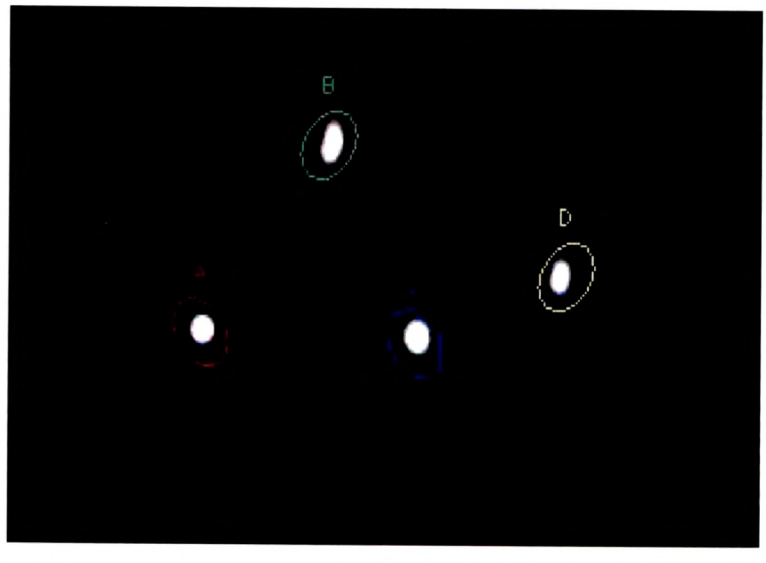

Fig. 3.39: Gamma camera image of rats after IA injection of **CML-2** after 1 h

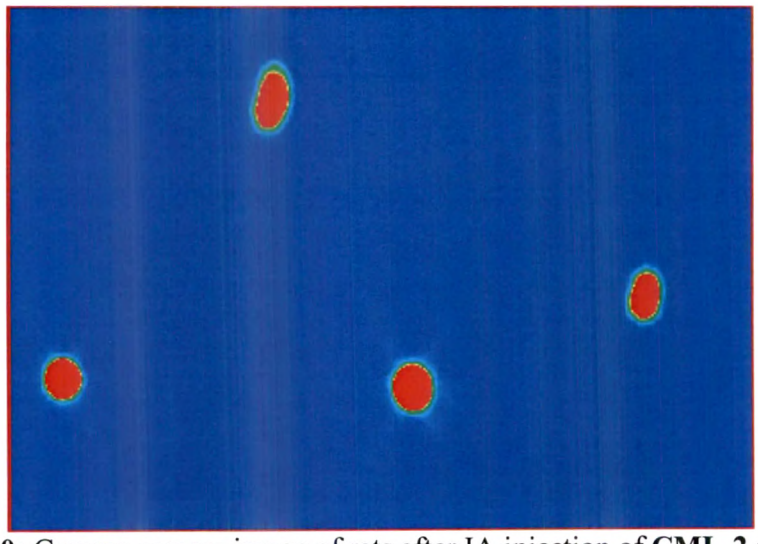

Fig. 3.40: Gamma camera image of rats after IA injection of **CML-2** after 6 h

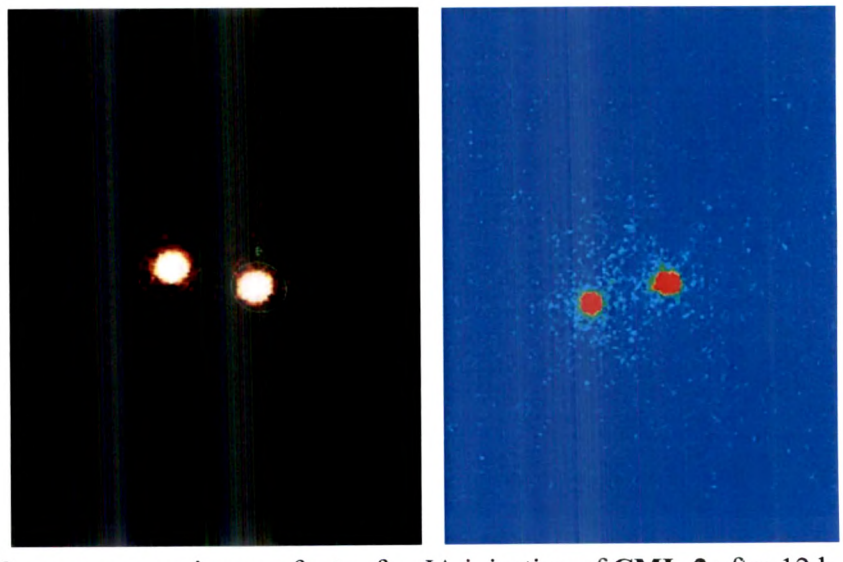

Fig. 3.41: Gamma camera image of rats after IA injection of **CML-2** after 12 h

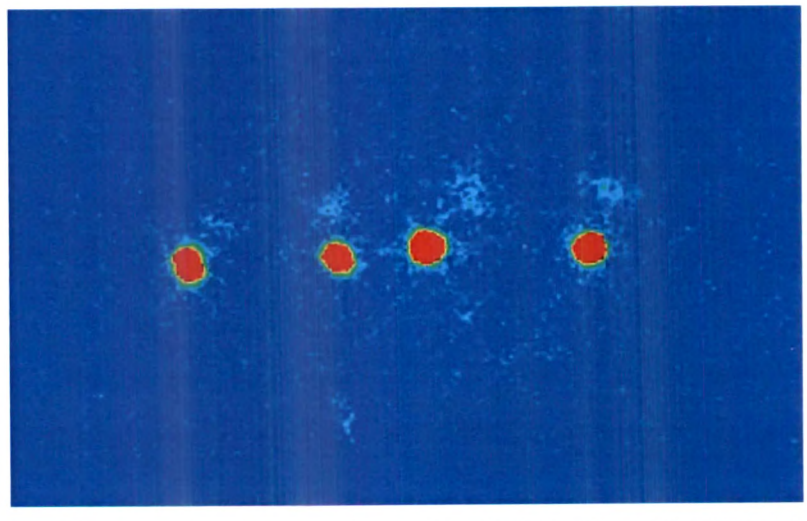

Fig. 3.42: Gamma camera image of rats after IA injection of **CML-2** after 24 h

3.7 *In vivo* studies in arthritis model

Adjuvant arthritis, an accepted and well established standard model was chosen for this purpose.[24-25] The parent NSAID 6-MNA **(1)** was used as standard for comparing the anti-inflammatory activity of the prepared liposomal formulation **(CML-2)**, which was administered on equivalent molar doses (4.27 mg/kg). Animals were dosed on day 1 with parent drug **(1)** and the liposomal formulation **(CML-2)** by IA route.

The phlogistic agent (Mycobacterium butyricum) suspended in heavy paraffin oil was injected into the subplantar region of the hind paws of the rats only on day 1. Paw volumes of all the test animals and controls were measured on days 0, 3, 7, 14 and 21. On day 21, liposome formulation exhibited significantly higher anti-inflammatory activity than the parent drug **(Table 3.9)**. The percent inhibition of inflammation exhibited by the parent drugs **(1)** declined on 21st day whereas, the percent inhibition of inflammation by the liposomal formulation increased on 21st day in comparison to that observed on 14th day. This could be due to the sustained release of 6-MNA from liposomal formulation in the body, which exhibited its normal anti-inflammatory activity over longer duration.

Table 3.9: Percent anti-inflammatory activity of liposomal formulation

Treatment with	Dose mg/kg	% Inhibition of paw edema (days)†			
		3rd	7th	14th	21st
6-MNA	4.27	32±2.33	41±2.98	45±3.60	40±2.88
CML-2	4.27	28±2.78	44±3.45	56±3.14	74±4.25

† mean±SD (n=6), $p<0.05$

The data obtained from the experiments was subjected to statistical analysis using the Student's t test and the chosen level of significance was $p < 0.05$

In vivo studies further indicate that there is decreased erythrocyte sedimentation rate (ESR), and C-reactive protein level (CRP) in test group administered IA with liposomal formulation compared to the control and standard group **(Table 3.10-3.13)**.

Table 3.10: Estimation of ESR and CRP levels in normal Rats.

No	Normal Group	Day 0		Day 21	
		ESR mm/hr*	CRP Quantitative†	ESR mm/hr*	CRP Quantitative†
1	N1	1	3.5	1	3.5
2	N2	7	2.2	5	2.0
3	N3	4	4.0	6	3.2
4	N4	3	3.2	2	4.2
5	N5	2	4.5	3	1.5

*Westergreen method, Normal range 1-15; †Normal range 1-10mg/L

Table 3.11: Estimation of ESR and CRP level in Control group rats

No	Control Group	Day 0		Day 21	
		ESR mm/hr*	CRP Quantitative†	ESR mm/hr*	CRP Quantitative†
1	C1	2	11	11	06
2	C2	2	2	14	17
3	C3	4	4	16	19
4	C4	3	3	11	22
5	C5	6	4	18	10

*Westergreen method, *Normal range 1-15; †Normal range 1-10mg/L

Table 3.12: Estimation of ESR and CRP level in test group rats

No	Test Group	Day 0		Day 21	
		ESR mm/hr*	CRP Quantitative†	ESR mm/hr*	CRP Quantitative†
1	T1	9	13	2	14
2	T2	2	26	5	09
3	T3	8	11	4	05
4	T4	10	14	6	06
5	T5	9	12	2	08

*Westergreen method, Normal range 1-15; †Normal range 1-10mg/L

Table 3.13: Estimation of ESR and CRP level in standard group rats

No	Standard Group	Day 0		Day 21	
		ESR mm/hr*	CRP Quantitative†	ESR mm/hr*	CRP Quantitative†
1	S1	8	9	2	08
2	S2	6	3	8	10
3	S3	4	7	3	12
4	S4	9	8	9	09
5	S5	3	6	2	14

*Westergreen method, Normal range 1-15; †Normal range 1-10mg/L

Histological studies: Histopathological studies of cartilage tissue indicated less tissue damage in the test group than the control and standard groups. 21 Days after single IA injection of test and standard drug/delivery system, the joint capsule of the arthritic knee was removed, fixed in 10 % formalin and processed through routine paraffin embedding and sectioning to carry out histological studies. After staining by haematoxylin-eosin (HE), and Safranin-O, the sections were examined.[26-28]

Safranin-O and hematoxylin eosin (HE) stain articular cartilage and bone respectively as shown in **Fig. 3.43-3.47.** From this study it is concluded that IA

administration of anti-inflammatory drugs encapsulated in cationic liposomes provides better therapeutic effect in arthritic animal model.

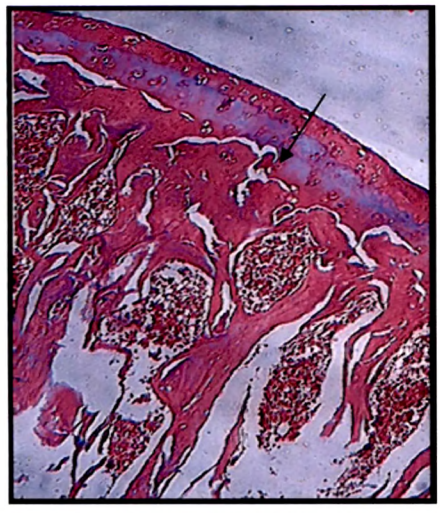

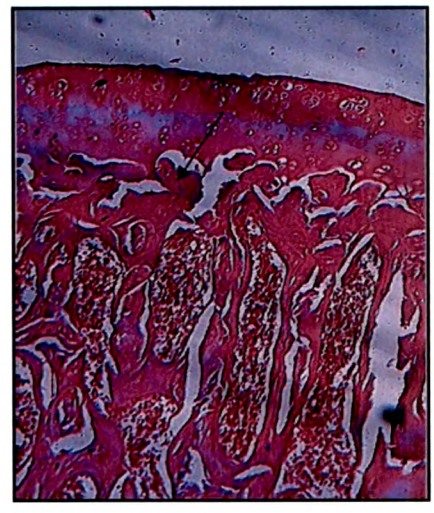

(A) 10x (B)

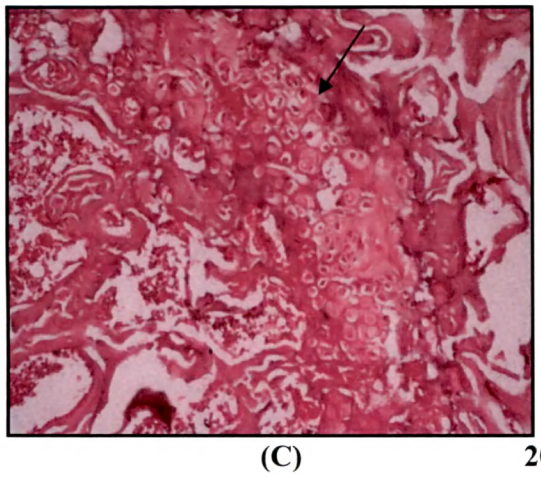

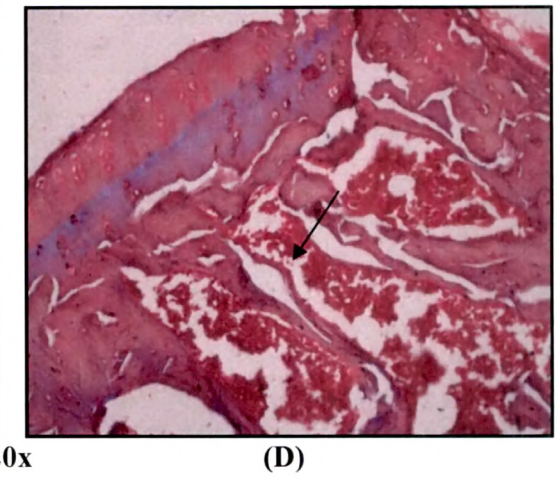

(C) 20x (D)

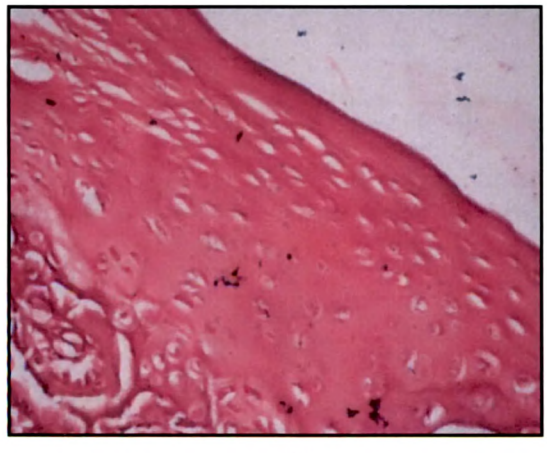

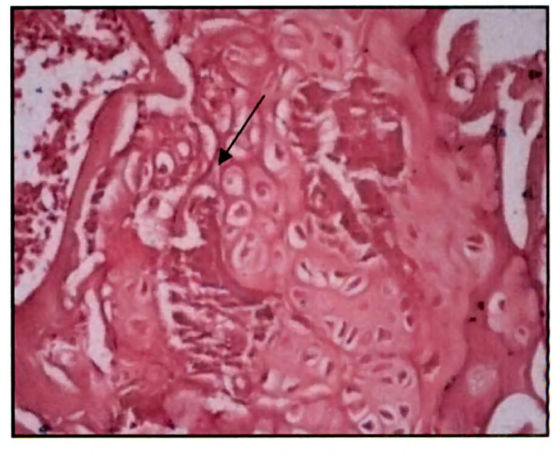

(E) 40x (F)

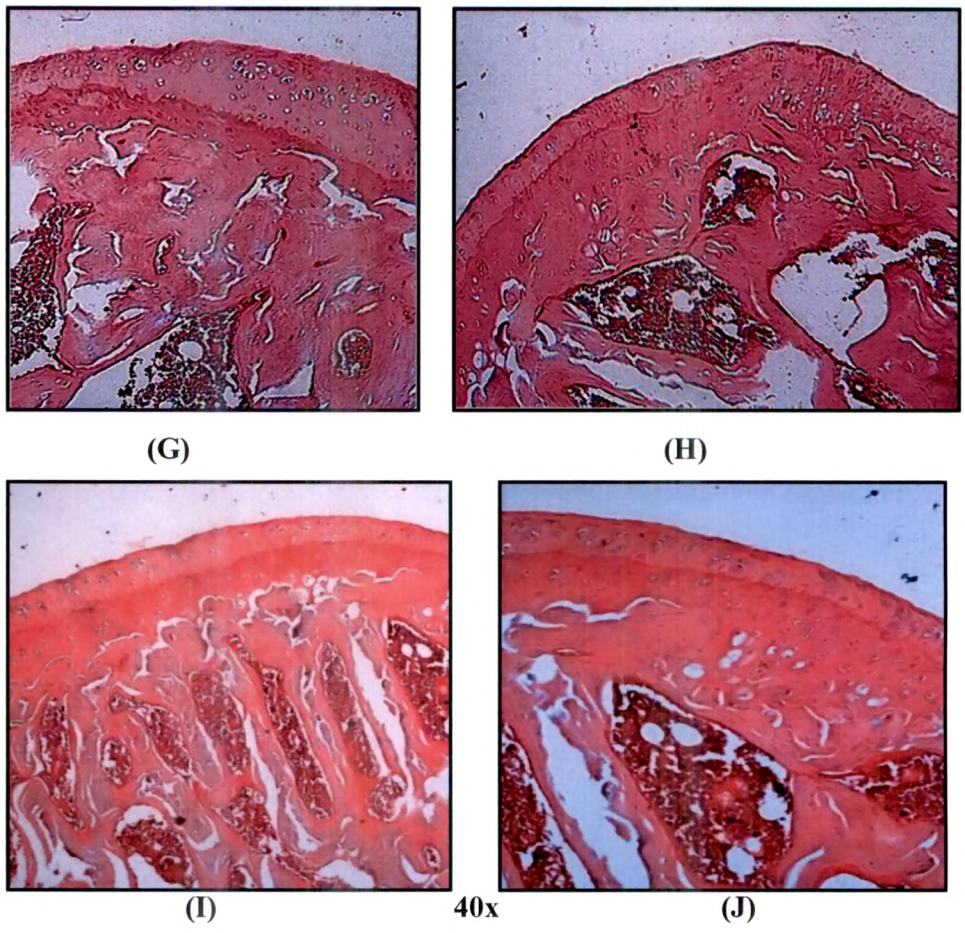

Fig. 3.43: A-F: Histopathological examination of normal knee haematoxylin and eosin Staining (H/E). **A-B**: Normal cartilage; **C-F**: Chondrocytes; **D**: Bone **G-J:** Safranin-O staining.

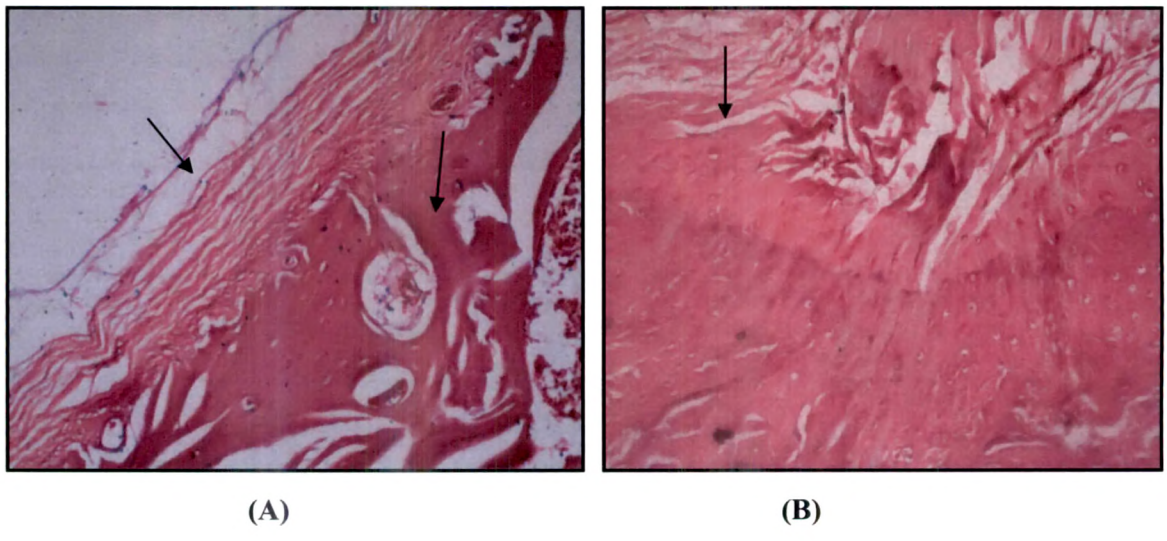

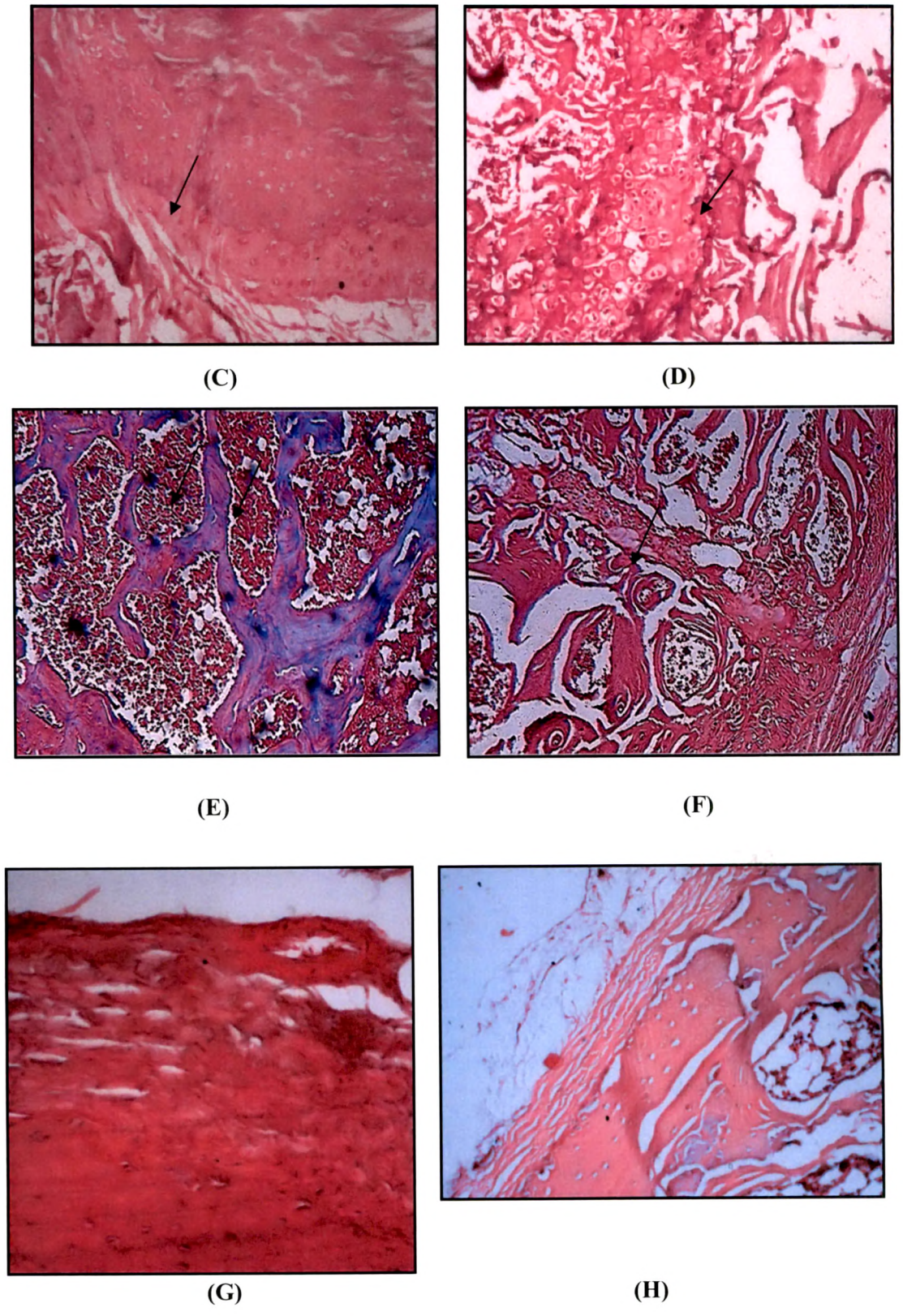

Fig. 3.44: **A-F**: Histopathological examination of knee treated with 6-MNA **(2)** haematoxylin and eosin staining (H/E). **A-D**: Cartilage and bone damage; **E**:Lymphocyte group; **F**: Polymorphonuclear leukocytes. **G-H:** Safranin-O staining.

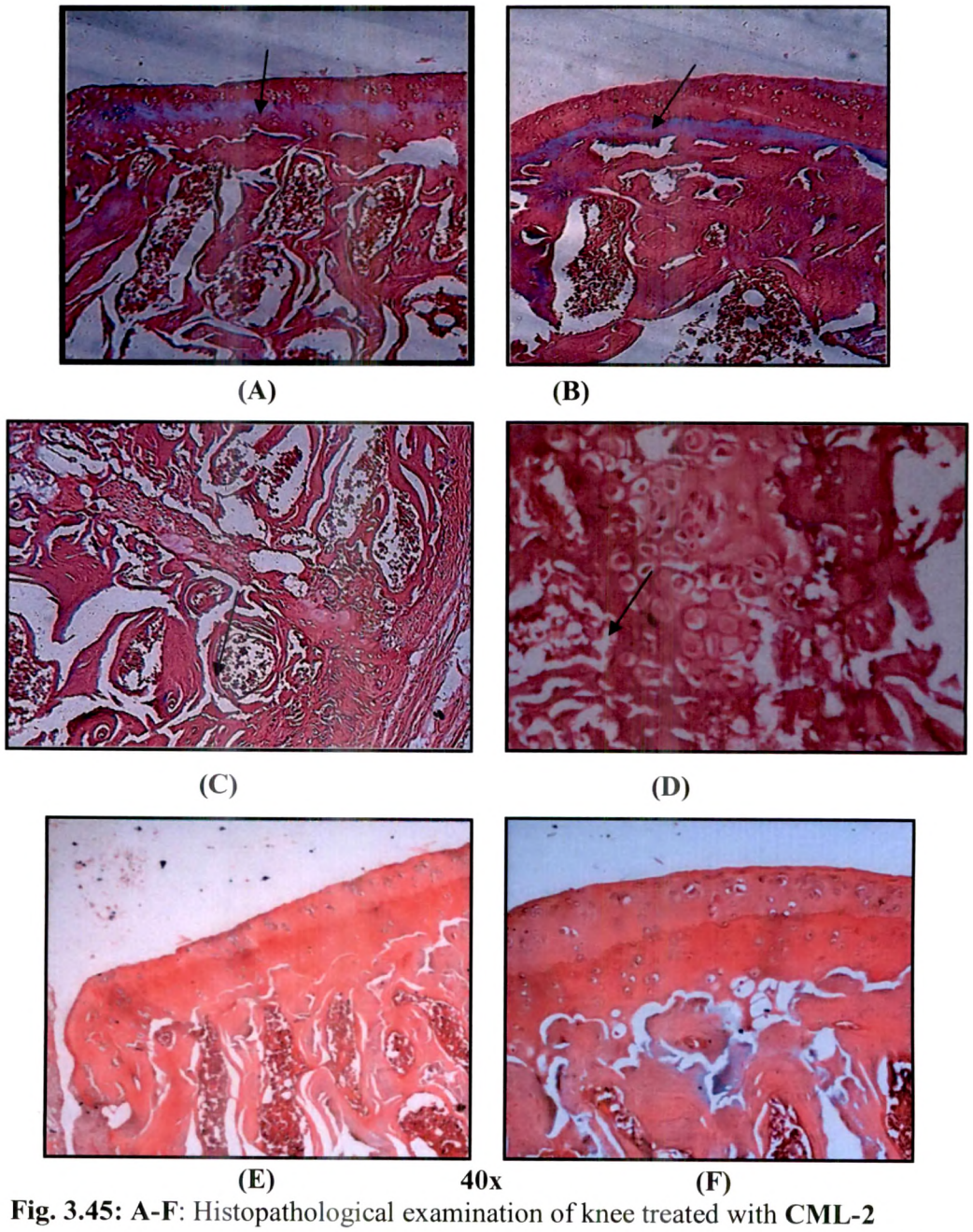

Fig. 3.45: A-F: Histopathological examination of knee treated with **CML-2** haematoxylin and eosin staining (H/E). **A-B:** Normal cartilage; **C**: Bone; **D**: Chondrocytes. **E-F:** Safranin-O staining.

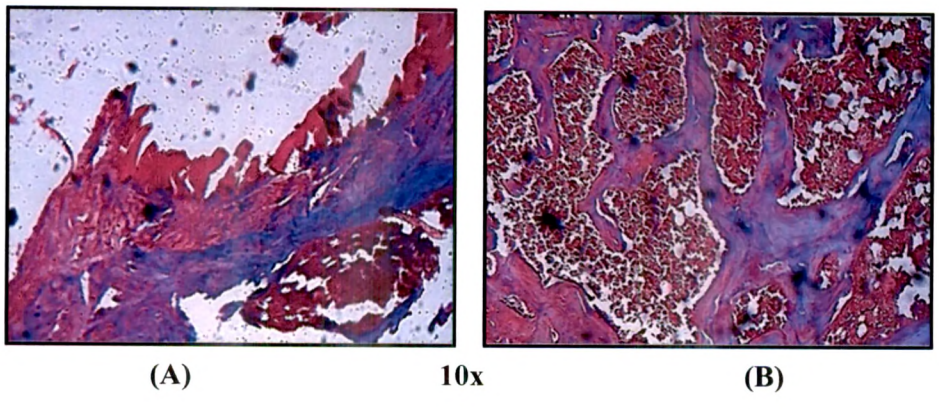

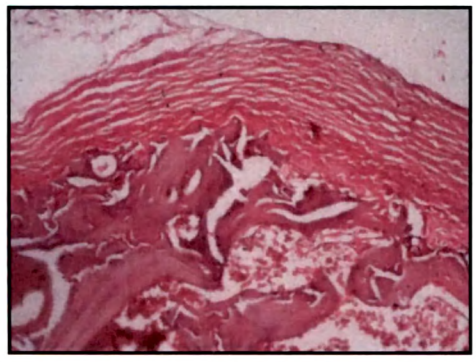

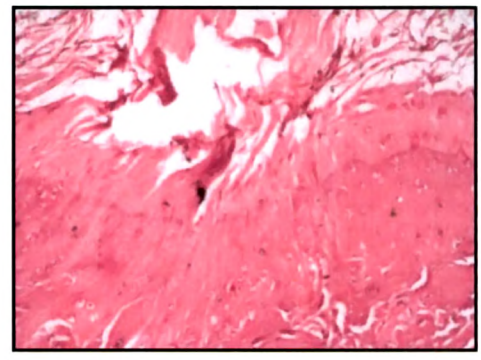

(C) **20x** **(D)**

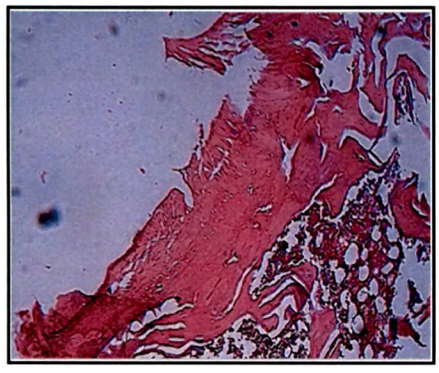

(E) **(F)**

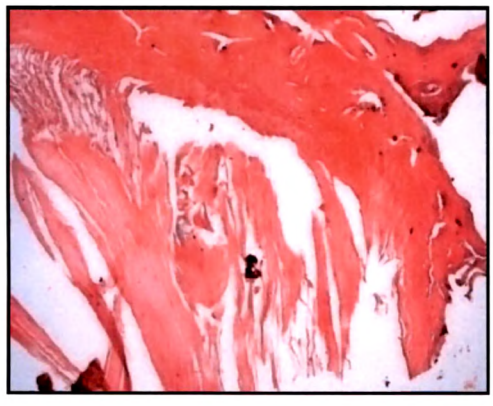

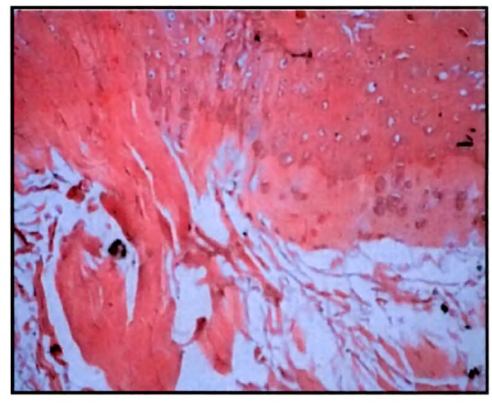

(G) **(H)**

Fig. 3.46: A-D: Histopathological examination of knee **control group** haematoxylin and eosin staining (H/E). **E-H:** Safranin-O staining

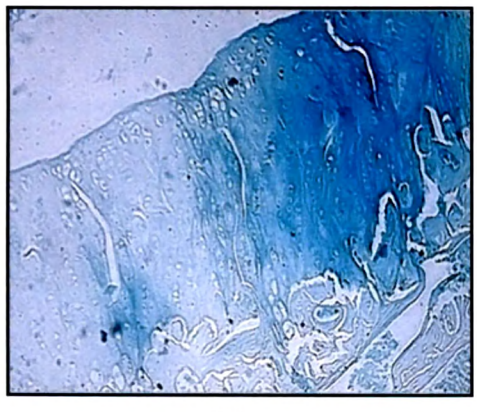

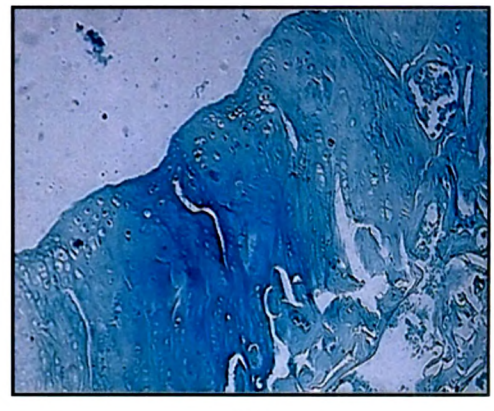

(A) **(B)**

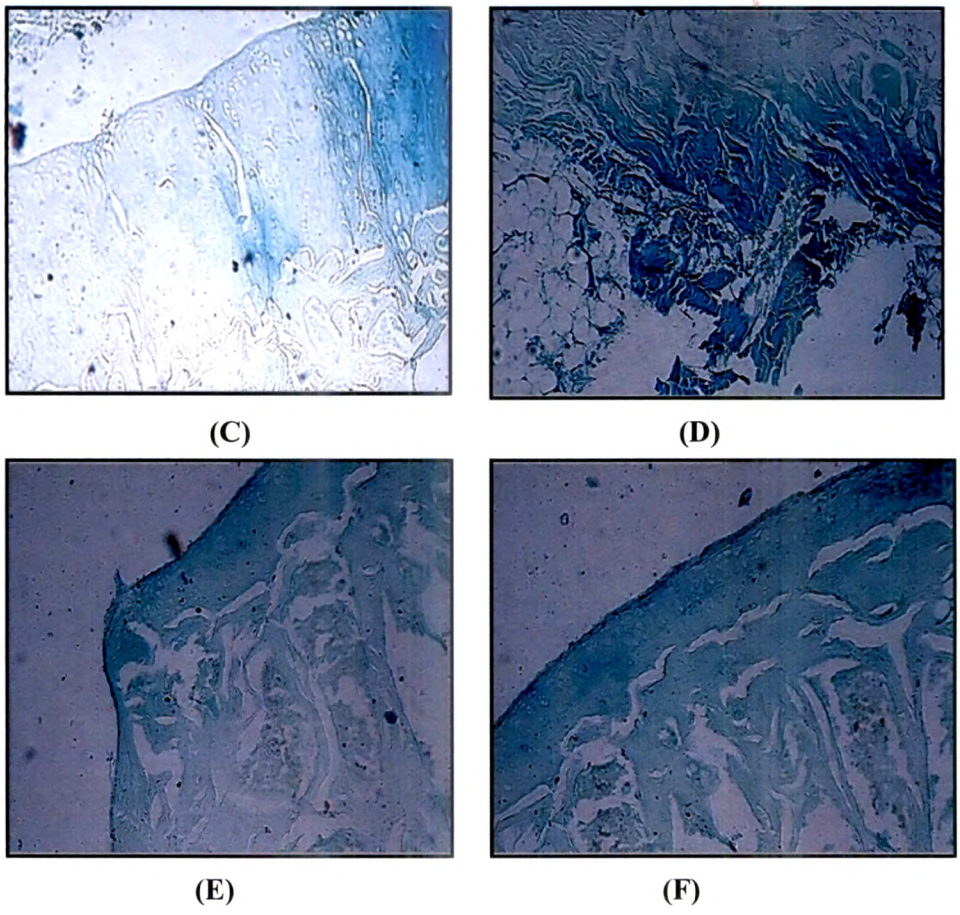

Fig. 3.47: A-F: Histopathological examination of knee toluidine blue staining;
A-B: Normal group; **C-D**: Control group; **E** and **F** Test and standard group.

It is concluded that retention time of a liposomal drug delivery system containing 6-MNA administered IA got extended significantly in this study. A drug carrier with a long half-life has great potential for the IA delivery of drugs used in the treatment of knee arthritis. The liposome dose was well tolerated by all animals indicating good biocompatibility. Additionally the liposomal formulation may provide lubricating effect due to presence of MLVs in liposome formulation along with SUV and LUVs.

A Coupled effect of positive charge and sustained release of drug from liposome formulation on retention time in joint cavity is responsible for the highest efficacy of liposomal formulation. *In vivo* studies further indicated that there is a decreased ESR, and CRP level, in test group administered with liposomal formulation compared to the control and standard groups. From this study it is concluded that IA administration of NSAIDs (having long half life) encapsulated in cationic liposomes prolong the residence time in the joint cavity. This type of drug delivery system will decrease frequency of IA drug administration and could provide good therapeutic option for the treatment of arthritis.

4. Experimental

All the reagents and solvents required for synthesis were purified by general laboratory techniques before use. Purity of the compounds and completion of reactions were monitored by thin layer chromatography (TLC) on silica gel plates (60 F_{254}; Merck). Melting points were determined using a Veego make silicon oil bath-type melting point apparatus and are uncorrected. The IR spectra were recorded using KBr disc method in cm^{-1} on a Bruker FT-IR, Model 8300. The PMR and ^{13}C-NMR (ppm) spectra were recorded in $CDCl_3$ or $CDCl_3$ plus one drop of glacial acetic acid-d_4 on a Bruker 400 MHz spectrometer (chemical shifts in δ ppm, coupling constant *J* in Hz). λ_{max} was determined on Shimadzu 1800 UV spectrophotometer.

HPLC analysis was performed by using Shimadzu prominence UV/VIS (pump LC-20AT, detector SPD 20 A), column purospher 5 μ (e) C-18, 5 X 250 mm (Merck), Column temperature was 25-28 °C. Chromatography was performed under isocratic conditions, at a flow-rate of 1.0 ml/min. The mobile phase consisted of acetonitrile-phosphate buffer (PB, 15 mM) in 3:1 ratio. Dialysis membrane-70 was procured from Himedia (Mumbai) with average diameter 17.5 mm and width 29.31 mm (Batch No: 0000116060), Confocal microscopy was performed on Carlzeiss LSM-710 model, made in Germany with 10x, 20x and 40x magnification. For optical microscopy Optical microscope with polarizer BX 40, Olympus Optical Co. Ltd., at a magnification of 40X was used. DSC was performed on Shimadzu DSC-60 model with thermal analyser TA 60WS. Mass of the compounds was determined in LC-MS or GC-MS using various ionization methods such as EI, ESI and ESCI (ESI+APCI). Scanning electron microscope (SEM) model ESEM-EDAX XL-30, Philips (Netherlands) was used for surface morphology study. TEM was performed on Holand Tecnai-20 model of Philips with operating accelerating voltage of 200 KV, line resolution 2.0 nm, and magnification of 25x to 750000x.

The work carried out has been discussed under the following heads:

4.1. Syntheses of NSAIDs

4.2. Salt formation and its characterization

4.3. Formulation of liposomes

4.4. Characterization of liposomes

4.5. Stability testing of liposomes

4.6. Biodistribution and gamma imaging studies

4.7. *In vivo* studies in arthritis model

4.1. Syntheses of NSAIDs

4.1.1.2-Methoxynapthene (nerolin) (5)

β-Naphthol **(4)** (3.6 g) was dissolved in an aqueous solution of sodium hydroxide (100 ml, 1.5%) and filtered. Dimethyl sulphate (2.35 ml) was added gradually to the above solution of β-naphthol with constant stirring at 10 °C. The reaction mixture was heated on water bath for two hours, cooled and poured into ice-cold water (200 ml). Precipitates so obtained were filtered, dried and the crude product crystallized from methanol to obtain white crystalline product[4] **(5)** (4.20 g, 76.55 %) m.p. 72-74 ^{0}C (lit.[4] 72-73°C).

Anal.:

TLC : R_f 0. 74 (Chloroform: methanol, 1:0.3)

UV (MeOH) : 270 nm

IR (KBr, cm^{-1}) : 1627, 1258, 1024 and 837

4.1.2. 2-Acetyl-6-methoxynaphthalene (6)

Anhydrous aluminium trichloride (4.30 g, 32 mM) was dissolved in nitrobenzene (20 ml) and the solution was cooled to 5 °C. Powdered nerolin **(5)** (3.95 g) was added to the above cooled solution with stirring. Acetyl chloride (2.3 ml, 32 mM) was added to it dropwise maintaining the temperature of the reaction mixture between 10.5 to 13 °C. The reaction mixture was stirred further in an ice-bath for two hours and left overnight at room temperature. The stored reaction mixture was poured into a mixture of ice (100 g) and conc. hydrochloric acid (10 ml) and extracted with chloroform (4 x 10 ml). The organic layer was washed with water (50 ml), dried and chloroform removed on rota evaporator. The solution so obtained was steam-distilled for about 3-4 h and the residue in the flask was allowed to cool. Residual water in the flask was decanted and the solid material extracted with chloroform and dried over sodium sulphate. The solvent was removed on rota evaporator yielding a solid mass which was vacuum-distilled at 140-60 °C/10 mm of Hg. The yellow distillate so obtained was crystallized from methanol to offer the white crystalline 2-acetyl-6-methoxynaphthalene[5] **(6)**. (2.1 g, 41.79 %) m.p. 106-108 ^{0}C (lit.[5] 104-105°C).

Anal.:

TLC : R_f 0.80 (Chloroform)

UV (MeOH) : 241 nm

IR (KBr, cm^{-1}): 1666, 1260, 855 and 666

Mass (m/z) : 199.91 (M^+)

4.1.3. 2-(6-Methoxy-2-naphthyl)-1-(4-morpholino)ethanethione (7)

A mixture of 2-acetyl-6-methoxynaphthalene **(6)** (5.0 g, 25 mM), and sulphur (2.40 g, 75 mM) in morpholine (6.52 ml, 75 mM) was refluxed for 18 h. The hot reaction mixture was poured into hot methanol and left overnight in a refrigerator. The precipitated material was filtered and washed with cold methanol (2 x 5 ml) to afford **7** as a brownish solid.[6] (5.5 g, 73.08 %) m.p. 130-132 ^{0}C (lit.[6] 131-133°C).

Anal.:

TLC : R_f 0.71 (Chloroform)

UV (MeOH) : 230 nm

IR (KBr, cm^{-1}): 1601, 1492, 1103 and 854

Mass (m/z) : 300.92 (M^+)

4.1.4. 6-Methoxy-2-naphthylacetic acid (MNA) (1)

The thiomorpholide **(7)** was dissolved in methanol (20 ml) and aqueous sodium hydroxide (50 ml, 3.5%). The reaction mixture was refluxed for eighteen hours, excess of methanol recovered and the thick solution diluted further with water (100 ml), cooled and filtered. The clear filtrate was acidified with conc. hydrochloride acid (5 %) in cold and the precipitate so obtained was filtered, washed with water and dried. The dried residue was crystallized from methanol to afford the acid **(1)** as white solid[6] (2 g, 55.86 %) m.p.171-173 ^{0}C (lit.[6] 172-173°C).

Anal.:

TLC : R_f 0.89 (Chloroform: Methanol; 1:0.5)

UV (MeOH) : 230 nm

IR (KBr, cm^{-1}): 1693, 1634, 1265 and 1216.

NMR (DMSO-d_6): δ 7.67-7.07 (m, 6H, naphthalene-*H*), 3.87 (s, 3H, O-C*H*$_3$) and 3.68 (s, 2H, -C*H*$_2$)

Mass (m/z) : 215.91 (M^+)

HPLC Purity : 99.6 %

4.1.5. 4-Phenylacetophenone (10)

In a 100 ml two necked round bottom flask provided with a dropping funnel and a reflux condenser with guard tube, biphenyl **(9)** (5.0 g, 32.46 mM), anhydrous aluminium trichloride (9.7 g, 72.40 mM) and anhydrous carbon disulphide (30 ml) were charged. The mixture was refluxed on a water bath for 20 minutes. Acetic anhydride (3.31 g/3.0 ml, 32.46 mM) in carbon disulphide (5 ml) was added dropwise over a period of 30 minutes

with efficient stirring at 30-35 °C. The reaction mixture was further refluxed for 3 hours and poured into crushed ice (100 g) containing concentrated hydrochloric acid (15 ml) and the residual carbon disulphide removed by air bubbling. The precipitate so obtained was filtered, dried and recrystallized from methanol to give[9] **10**, (4.30 g, 67.57 %), m.p. 118-120 °C. (lit.[9] 120-21°C).

Anal. :

TLC : R_f 0.74 (Benzene)

UV (MeOH) : 283 nm

IR (KBr, cm^{-1}) : 1677, 1262 and 763

Mass (m/z) : 195.84 (M^+)

4.1.6. 2-(4-Biphenyl)-1-(4-morpholino)ethanethione (11)

4-Phenylacetophenone (5.0 g, 25.5 mM), morpholine (6.7 ml, 76.5 mM) and sulphur (2.5 g) were refluxed for 18 h. The hot reaction mixture was poured into hot methanol (15 ml) and refrigerated overnight. The precipitated matter so obtained was filtered and washed with ice-cold methanol (5 ml) to get yellow colored thiomorpholide **(11)**.[9] (5.4 g, 71.27 %), m.p.138-140 °C (lit.[9] 137-139 °C).

Anal. :

TLC : R_f 0.74 (Benzene)

UV(MeOH) : 279 nm

IR (KBr, cm^{-1}) : 1677, 1262 and 763

Mass (m/z) : 296.93 (M^+)

4.1.7. 4-Biphenylacetic acid (BPA) (2)

The thiomorpholide **(11)** (7.6 g, 25.5 mM) was dissolved in a mixture of methanol (10 ml) and sodium hydroxide solution (50 ml, 6 %). The reaction mixture was refluxed for 16-18 h. Excess of the solvent was removed and the residue was dissolved in water and filtered. The filtrate so obtained was chilled and acidified with dilute hydrochloric acid to yield a buff colored precipitate which was filtered, dried and crystallized from methanol to yield 4-biphenylacetic acid **(2)**[9] (3.4 g, 62.67 %), m.p. 163-165 °C (lit.[9] 164-165°C).

Anal. :

TLC : R_f: 0.61 (Chloroform: Methanol; 1:0.5)

UV (MeOH) : 253 nm

IR (KBr, cm^{-1}) : 1685, 1413, 1249 and 924

PMR ($CDCl_3$) : 8.84 (bs, 1H, -COO*H*), 7.88-7.28 (m, 9H, biphenyl-*H*) and 3.58 (s, 2H, Ar-CH_2)

Mass (m/z) : 211.93 (M^+)

HPLC Purity : 99.7 %

4.2. Synthesis of salts

4.2.1. Synthesis of DSPE-Na (14)

1,2-Distearoyl-*sn*-glycero-3-phosphoethanolamine (DSPE) was dissolved in cold chloroform-methanol (20 ml, 3:1). Cold methanol containing sodium hydroxide (equimolar ratio) was added slowly into above solution containing DSPE and the reaction was continued for 30 min. Then solvent was removed and the product so obtained was characterized.

Anal.:

IR (KBr, cm^{-1}) : 3430, 1741 and 1081

PMR ($CDCl_3$) : 5.34 (bs, 2H, NH_2), 4.28-4.25 (m, 2H, O-CH_2), 3.59-3.56 (m, 4H, $(CH_2)_2$), 3.15-3.05 (m, 1H, C*H*), 2.25-2.15 (m, 4H, $(CH_2)_2$), 1.99-1.98 (m, 2H, N-CH_2), 1.55-1.52 (m, 4H, $(CH_2)_2$), 1.17-1.15 (m, 56H, $(CH_2)_{14}$) and 0.81-0.78 (m, 6H, $(CH_3)_2$),

Mass (m/z) : 771 (M+Na)

4.2.2. Synthesis of MNA-DSPE salt (15a)

Equimolar amounts of MNA **(1)** and DSPE-Na **(14)** were dissolved in dichloromethane (25 ml) under stirring and the stirring was continued for 2-4 h till the salts precipitated out. Solvent was removed in *vacuo* and the residue was crystallized from methanol or ethyl acetate to get pure solid of the salt.

Anal.:

IR (KBr, cm^{-1}) : 1741, 1698 and 1080

PMR ($CDCl_3$) : 7.69-7.09 (m, 6H, Ar-*H*), 4.30-3.97 (m, 6H, (CH_2) NH_2), 3.88 (s, 2H, Ar-CH_2), 3.22 (s, 2H, CH_2), 2.31-2.25 (q, 4H, $(CH_2)_2$), 2.05-2.02 (m, 1H, C*H*), 1.56-1.52 (m, 4H, $(CH_2)_2$), 1.22-1.18 (m, 56H, $(CH_2)_{14}$) and 0.86-0.82 (m, 6H, $(CH_3)_2$)

Mass (m/z) : 217.22 (MNA) and 750.62 (DSPE)

4.2.3 BPA-DSPE salt (15b)

Equimolar amounts of BPA **(2)** and DSPE-Na **(14)** were dissolved in dichloromethane (25 ml) under stirring and the stirring was continued for 2-4 hour till the salts precipitated out. The solvent was removed in *vacuo* and the residue was crystallized from methanol or ethyl acetate to get pure solid of the salt.

Anal.:

IR (KBr, cm^{-1}) : 1741, 1689 and 1080

PMR ($CDCl_3$) : 7.66-7.32 (m, 9H, Ar-*H*), 5.23-5.20 (m, 1H, C*H*), 4.37-4.02 (m, 6H, $(CH_2)_2$, NH_2), 3.27 (s, 2H, Ar-CH_2), 2.35-2.29 (m, 4H, $(CH_2)_2$), 1.59-1.56 (m, 4H, $(CH_2)_2$), 1.26-1.20 (m, 56H, $(CH_2)_{14}$) and 0.89-0.86 (m, 6H, $(CH_3)_2$)

Mass (m/z) : 212.32 (BPA) and 748.81 (DSPE)

4.3 Formulation of liposomes

4.3.1 Formation of film: Thin film hydration method was used for the preparation of liposomes. All the lipids and the drug were mixed with cholesterol in different molar ratios separately in a 250 ml of round bottom flask (RBF) and dissolved in chloroform: methanol (3:1) mixture (40 ml). The organic solvent was evaporated using rotary flask evaporator under vacuum on a thermostatic water bath at 50±2 °C at a speed of 60 rotations per minutes (RPM) of the rotor. This was continued till the complete evaporation of organic solvents leaving behind a dry thin lipid film deposited on the walls of the flask. This flask was further dried under vacuum in order to remove traces of organic solvent.[13]

4.3.2 Hydration of thin film: The film was hydrated using purified water (8 ml) in rotary flask evaporator under thermostatic water bath at 55±2 °C at a speed of 60 RPM of the rotor. The multilamellar vesicles (MLVs) formed after hydration was kept at room temperature for 2 h for annealing. The liposomes were characterized for microscopic observation using Olympus microscope (BX40F4, Tokyo, Japan) at 40X magnification and photographed using digital camera.

Hydration Time

The film was hydrated with the hydration media for different time intervals from 30 min to 80 min and evaluated to optimize hydration time, for complete hydration of the lipid film. The above procedure was repeated three times. The effect of hydration time was shown in **Table 4.2.**

4.3.3 Size reduction (production of small unilamellar vesicles)

In order to get average liposome size below 1.5 μ, size reduction of the MLVs were carried out using probe sonicator (Labsonic, Sartoris, Germany) at 60 % amplitude 0.6 cycles for 15-20 sec. To convert large (>1.5 μ) MLVs into a mixture of MLV and SUVs, sonication of liposomal suspension was optimized by altering time, cycle and amplitude according to the size requirements. The procedure was repeated three times. The effect of sonication on liposomal formulation was shown in **Table 4.3.**

Table 4.2: Optimization of hydration time

Hydration time	Effect on Hydration of Lipid
20 min	Not properly hydrated leaves film behind.
30 min	**Complete hydration**
60 min	Complete hydration but loss of liposomal suspension

Table 4.3: Parameters for optimization of sonication

Sr.No.	Time (sec)	Cycle	Size (nm) *
1	10	60% Amplitude, 0.4 cycles ×2	1570±16.3
2	20	60% Amplitude, 0.4 cycles ×2	942±12.5
3	30	60% Amplitude, 0.4 cycles ×2	508±10.9
4	40	60% Amplitude, 0.4 cycles ×2	321±08.4
5	**50**	60% Amplitude, 0.4 cycles ×2	146±05.8
6	10	80% Amplitude, 0.6 cycles ×2	1290 ±24.1
7	20	80% Amplitude, 0.6 cycles ×2	859±18.1
8	30	80% Amplitude, 0.6 cycles ×2	498±14.5
9	40	80% Amplitude, 0.6 cycles ×2	275 ±10.6
10	**50**	80% Amplitude, 0.6 cycles ×2	110±6.50

* Mean±SD (n=3)

4.3.4 Determination of entrapment efficiency

The percent of drug entrapment in liposomes was calculated by estimating the entrapped drug in the liposomes after centrifugation at 8,000 RPM for 15 min at 4 °C (Sigma 3K30). The supernatant was removed and discarded. The sedimented liposomes (0.2 ml) were diluted up to 1.0 ml with methanol and the supernatant was estimated for drug content after suitable dilution using HPLC. Liposomal batches were prepared by

varying the process parameters like applying vacuum, changing of rotation per minute (rpm) and time. The films were prepared by keeping the lipid to cholesterol ratio constant. The films formation time was found to be dependent on applied vacuum and speed of rotation. Vacuum was kept constant at 300 mmHg and speed of rotation was varied between 50 to 120 rpm. The above procedure was repeated three times. The entrapment efficiency of the drug in liposomes was determined for each batch.

4.4 Characterization of liposomes

4.4.1 Size

The particle size (z-average) and polydispersability index (PDI) of the liposomes was analyzed by photon correlation spectroscopy (PCS) using a Malvern Zetasizer Nano (Malvern Instruments; UK). Liposome suspension (0.2 ml) was diluted to 1.0 ml with distilled water (DW) and the size distribution was measured after an equilibration time of 1 minute. The Zetasizer Nano is operating with a 4 mW He-Ne-Laser at 633 nm using non invasive back-scatter technique (NIBS) at a constant temperature of 25 °C. The measurements were conducted in the manual mode.

The size distribution by intensity and volume was calculated from the correlation function using the multiple narrow mode of the Dispersion Technology Software version 4.00 (Malvern, Herrenberg, Germany). The resulting size distribution shows the hydrodynamic diameter. The average particle size and PDI was calculated after performing the experiment in triplicate. PDI of 0.0 represents a homogenous particle population while 1.0 indicates a heterogeneous size distribution in the liposomes.

4.4.2 Morphology

Olympus microscopy

Morphological evaluation was conducted using optical microscope with polarizer BX 40, Olympus Optical Co. Ltd., at a magnification of 40X. On the basis of morphological evaluation it was concluded that the liposomes prepared by TFH method were spherical in nature.

TEM:

TEM is a microscopic technique wherein a beam of electrons is transmitted through an ultra thin specimen, interacting with the specimen as it passes through it. An image is formed from the interaction of the electrons transmitted through the specimen. The image is magnified and focused onto an imaging device. To prevent charge build-up at the sample surface samples need to be coated with a thin layer of a conducting material, such as carbon, where the coating thickness is several nanometers. For negative-staining 5

μl of dilute liposome dispersion was placed on a 200 mesh copper grid (TAAB Laboratories Equipment, Berks, UK). The surplus dispersion was removed by filter paper and the suspension was, stained with 5 μl of 2.5 % uranyl acetate for 30 seconds. The surplus uranyl acetate was removed, and the sample was dried at room conditions before imaging the liposome with a transmission electron microscope operating at an acceleration voltage of 200 KV.

4.4.3 Zeta (ς) potential analysis

The zeta potential (ς potential) of prepared liposome suspension was measured by micro-electrophoresis using Malvern Zetasizer Nano ZS (Malvern, Instrument, U.K.). Zeta potential of the liposome was measured after separation of the free drug from the liposome. Liposomes (0.2 ml) were diluted to 1 ml with distilled water. The determination of the zeta potential was realized at 25 °C after injecting 1 ml of the sample into a standard sample cell.

4.4.4 *In vitro* diffusion studies of liposomes

The release studies were performed at 25±2.0 °C using the rotating dialysis cell model.[18] In this model, the donor compartment is separated from the acceptor compartment by a dialysis membrane (interfacial area: 22 cm^2, MW cut-off: 15000 Da). Experiments were conducted by applying the formulations to the donor compartment containing the phosphate buffer of *p*H 7.4 and tween 80 (1 %). At time zero, the dialysis cell containing the liposomes (2 ml) was placed inside a round-bottomed vessel containing 100 ml of preheated release medium (PBS). The revolution speed of the magnetic stirrer was 50 rpm. At appropriate times (1, 2, 4, 8, 12 h), samples were withdrawn (1 ml) from the acceptor phase and analyzed by HPLC. All release experiments were followed for a period of 10-12 h and repeated in triplicate. The cumulative amount of 6-MNA released was calculated.

4.5 Stability testing of liposomes

Stability studies of liposome were carried out to evaluate the change in particle size, zeta potential, percent drug loading, chemical stability of phospholipids and the drug over the period at different storage conditions. Change in the size of liposomes can take place over a period of time and these changes can be the result of aggregation and fusion. Drug molecules can leak from the liposomes reducing the entrapment efficiency. The leakage of the drug form the liposome depends upon liposome composition and physicochemical nature of the drug. Various methods have been used in improving the stability of liposome, like incorporating saturated phospholipids to avoid oxidation process which is generally

observed with unsaturated phospholipids, using charged phospholipids to reduce the possibility of aggregation and fusion, freeze drying of liposomes in presence of cryoprotectant to increase shelf life of the liposomes.[22-23]

The optimized formulations were studied for their stability and their potentials to withstand the atmospheric/environmental changes. These formulations were subjected to stability testing by evaluating parameters like particle size, zeta potential and percent entrapment efficiency.

4.6 Biodistribution and gamma imaging studies

6-MNA and the liposomal formulations were labeled using ^{99m}Tc as per the method mentioned in **Section-I**. Radiolabeling parameters such as *p*H, incubation time, stannous chloride concentration, and percentage of radiolabeling were optimized.

IA residence time of prepared liposomes and the parent drug were studied in inflammatory condition by injecting liposomal preparation IA in to rat knee. Animals were divided into two groups, Group-A (standard) was administered by IA the parent NSAID i.e 6-MNA **(1)**. Another group, Group-B (Test) was administered by IA the liposomal formulation, 3 h after induction of inflammation in the rat paw. Inflammation was induced in the right hind paw of the rats by injecting carrageenan (0.1 ml, 1 % w/v in normal saline) into the subplantar region of the paw. The animals were anaesthetized, fixed on a board and images were taken 1 h, 2 h, 6 h and 24 h after the administration of the radiolabeled complexes by IA route.

4.7 *In vivo* studies in arthritis model

For anti-inflammatory activity (arthritis model) Sprague-Dawley male rats with an initial body weight of 150-200 g were used. Rats were divided into groups of six each for test formulation, standard compound, control and normal group. On day 1, the animals were injected into the sub-plantar region of the left hind paw with 0.1 ml of complete Freund's adjuvant (6 mg/ml Mycobacterium butyricum suspended in heavy paraffin oil) except in the normal group.[24-25] On day 1 IA dose of 6-MNA and liposomal formulation **(CML-2)** were injected (4.27 mg/kg) on equivalent molar doses. Paw volumes of both sides were measured plethysmographically. The paw volumes were measured on days 0, 3, 7, 14 and 21. Parent NSAID **(1)** dissolved in aqueous-DMSO as 'standard' was administered to the animals through IA route. Results are expressed as percentage inhibition of edema formation, calculated by the formula,

% Inhibition of paw edema = [1 – Ed (test)/Ed (control)] X 100

Where, Ed (test) and Ed (control) are the edema volumes in liposome/compound-treated and control groups, respectively.

On day 21 animals were sacrificed and cartilage tissue was removed and histological evaluation done. Blood samples were also tested on day 1 and 21 for the measurement of ESR and CRP levels.

4.7.1 Histology and haematology

Histological study of cartilage tissue was done by using three dyes namely Hematoxylin-Eosin (HE), Safranin-O and Toluidine blue.[26-28] Immature and mature bone show different staining characteristics; immature bone stains more with Hematoxylin and mature bone more with Eosin. Toluidine blue and Safranin-O are cationic stains (basic dyes) that stain acidic proteoglycan present in cartilage tissues. Toluidine blue, also called metachromasia dye, shows subtle color changes depending on the tertiary structure of the sample. Cytoplasm stains light blue, nuclear region dark blue and mast cell purple. Safranin-O, which binds to glucosaminoglycans and shows an orange color, is often used to stain articular cartilage. Fast green, the contrast stain of Safranin-O, is a sulfate-group containing acidic substrate, which binds strongly to the amino group in proteins and thereby strongly stains the non-collagen sites.

References

1. Goudie A.C., Gaster L.M., Lake A.W., Rose C.J., Freeman P.C., Hughes B.O. and Miller D., 4-(6-Methoxy-2-naphthyl)butan-2-one and related analogs, a novel structural class of antiinflammatory compounds. *J. Med. Chem.* **1978**, 21, 1260-64.
2. Friedel H.A., Langtry H.D. and Buckley M.M., Nabumetone: A reappraisal of its pharmacology and therapeutic use in rheumatic diseases. *Drugs* **1993**, 45, 131-56.
3. Davies N.M., Clinical Pharmacokinetics of Nabumetone. *Clin. Pharmacokinet.* **1997**, 33, 403-16.
4. Furniss B. S., Hannaford J. H., Smith P. W. G. and Tachell A. R., In: Vogel's Text book of Practical Organic Chemistry, 5th edition, Longman, Singapore, **1996**, 987
5. Arsenijevic L. Synthesis of 2-acetyl-6-methoxynaphthalene Organic synthesis Vol-6, 34
6. Furniss B. S., Hannaford J. H., Smith P. W. G. and Tachell A. R. In: Vogel's Text book of Practical Organic Chemistry, 5th edition, Longman, Singapore. **1996**, 1054.
7. Chalmers I. M., Bell M. A. and Bychanan W. W. Effect of flurbiprofen on the metabolism of antipyrine in man. *Ann. Rheum. Dis.* **1973**, 32, 58-61
8. Takase K., Masumoto S. and Okumura F. Anti-inflammatory studies of 2-(2-fluoro-4-biphenylyl) propionic acid (Flurbiprofen), *Folia Pharamcol.* **1975**, 71, 573
9. Schwenk E. and Papa D. Preparation of aryl aliphatic acids by the modified willgerodt reaction. *J. Org. Chem.*, **1946**, 11, 798
10. Puglia C., Bonina F., Rizza L., Cortesi R., Merlotti E., Drechsler M., Mariani P., Contado C., Ravani L. and Esposito E., Evaluation of Percutaneous Absorption of Naproxen from Different Liposomal Formulations. *J. Pharm. Sci.* **2010**, 99, 2819
11. Srinath P.P., Vyas S.P. and Diwan P.V., Preparation and Pharmacodynamic Evaluation of Liposomes of Indomethacin. *Drug. Dev. Ind. Pharm.* **2000**, 26, 313
12. Ruozi B., Tosi G., Forni F. and Angela V. M., Ketorolac Tromethamine Liposomes: Encapsulation and Release Studies. *J. lipo. Res.* **2005**, 15, 175
13. New RRC. Preparation of liposomes : A practical approach, New RRC ed. Oxford University Press, Oxford, **1990**, 33-104
14. Bonanomi M.H., Velvart M., Stimpel M., Roos K.M., Fehr K. and Weder H.G., Studies of pharmacokinetics and therapeutic effects of glucocorticoids entrapped in liposomes after intraarticular application in healthy rabbits and in rabbits with antigen-induced arthritis. *Rheumatol. Int.* **1987**, 7, 203-12.

15. Bonanomi M.H., Velvart M. and Weder H.G., Fate of different kinds of liposomes containing dexamethasone palmitate after intra-articular injection into rabbit joints. *J. Microencapsul.* **1987**, 4, 189-200
16. Williams A.S., Camilleri J.P., Goodfellow R.M. and Williams B.D., A single intraarticular injection of liposomally conjugated methotrexate suppresses joint inflammation in rat antigen-induced arthritis. *Br. J. Rheumatol.* **1996**, 35, 719-724.
17. Butoescu N., Jordan O. and Doelker E., Intra-articular drug delivery systems for the treatment of rheumatic diseases: A review of the factors influencing their performance. *Eur. J. Pharm. Biopharm.* **2009**, 73, 205-18
18. Larsen C., Ostergaard J., Larsen S.W., Jensen H., Jacobsen S., Lindegaard C. and Andersen P.H., Intra-Articular Depot Formulation Principles: Role in the Management of Postoperative Pain and Arthritic Disorders. *J. Pharm. Sci.* **2008**, 97, 4622-54.
19. Simkin P.A. and Pizzorno J.E. Transsynovial exchange of small molecules in normal human subjects. *J. Appl. Physiol.* **1974**, 36, 581-87
20. Nicolas C., Verny M., Giraud I., Ollier M., Rapp M., Maurizis J.C. and Madelmont J.C., New quaternary ammonium oxicam derivatives targeted toward cartilage: synthesis, pharmacokinetic studies, and anti-inflammatory potency. *J. Med Chem.* **1999**, 42, 5235-40.
21. De. Silva M., Hazleman B.L., Thomas D.P. and Wraight P., Liposomes in arthritis: a new approach. *Lancet.* **1979**, 1, 1320-22.
22. Lu D. and Hickey A.J., Liposomal Dry Powders as Aerosols for Pulmonary Delivery of Proteins. *AAPS Pharm Sci Tech.* **2005**, 6, E641-E648.
23. Maitani Y., Aso Y., Yamada A. and Yoshioka S. Effect of sugars on storage stability of lyophilized liposome/DNA complexes with high transfection efficiency. *Int. J. Pharm.* **2008,** 356, 69-75.
24. Saha, G. B. In Physics and Radiobiology of Nuclear Medicine; Saha, G. B., Ed., 5th ed.; Springer-Verlag: New York, **1993**, 100-106
25. Yadav M.R., Pawar V.A., Marvaniya S.M., Halen P.K., Giridhar R., Mishra A.K., Site specific chemical delivery of NSAIDs to inflamed joints: synthesis, biological activity and gamma-imaging studies of quaternary ammonium salts of tropinol esters of some NSAIDs or their active metabolites. *Bioorg. Med. Chem.* **2008**, 16, 9443-9.

26. Butoescu N., Seemayer C.A., Palmer G., Guerne P.A., Gabay C., Doelker E. and Jordan O., Magnetically retainable microparticles for drug delivery to the joint: efficacy studies in an antigen-induced arthritis model in mice. *Arthritis Res. Ther.* **2009**,11, R72
27. Butoescu N., Seemayer C.A., Foti M., Jordan O. and Doelker E., Dexamethasone-containing PLGA superparamagnetic microparticles as carriers for the local treatment of arthritis. *Biomaterials.* **2009**, 30, 1772-80
28. Türker S., Erdoğan S., Ozer A.Y., Ergün E.L., Tuncel M., Bilgili H. and Deveci S., Scintigraphic imaging of radiolabeled drug delivery systems in rabbits with arthritis. *Int. J. Pharm.* **2005**, 296, 34-43